Binocular Inhibition: Using MEG and EEG to measure Binocular Integration in the Occipital Cortex.

by

Michael Craig

Submitted in partial fulfillment of the requirements
for the degree of Master of Science

at

Dalhousie University
Halifax, Nova Scotia
March 2019

TABLE OF CONTENTS

LIST OF TABLES

LIST OF FIGURES

ABSTRACT

Purpose: To determine if Binocular Inhibition and Binocular Summation are measurable using MEG, and explore their origins in the brain.

Methods: Binocular Inhibition was induced in 8 normal, healthy subjects using a neutral density filter in front of one eye. Visual evoked field Magnetoencephalography recordings were compared to visual evoked potential Electroencephalography recordings. Dynamic statistical parametric maps were generated to map brain activity under different viewing conditions.

Results: Binocular inhibition was measured at the occipital pole in both EEG and MEG using pattern reversal checkerboard stimuli for early components, MEG is less sensitive to late components. Flash stimuli did not induce binocular inhibition in either EEG or MEG sensors. The distribution of activity between binocular inhibition and binocular summation suggests that these are independent processes. Source estimation techniques produced limited interpretation for contributions of brain areas for inhibitory mechanisms but are able to capture generalized distributions in visual cortices.

LIST OF ABBREVIATIONS AND SYMBOLS USED

ANOVA	Analysis of variance
BI	Binocular Inhibition
BM	Binocular Monocular Ratio
BS	Binocular Summation
BSV	Binocular Single Vision
cd	Candela
cGMP	Cyclic Guanosine Monophosphate
dSPM	Dynamic Statistical Parametric Mapping
EEG	Electroencephalography
ETDRS	Early Treatment Diabetic Retinopathy Study
FM	Filter Monocular Ratio
fMRI	Functional Magnetic Resonance Imaging
fT	Femtotesla
GRADS	Gradiometer
HPI	Head Position Indicator
Hz	Hertz
ICA	Independent Component Analysis
IT	Implicit Time
LGN	Lateral Geniculate Nucleus
MAG	Magnetometer
MEG	Magnetoencephalography
MNE	Minimum Norm Estimation
MRI	Magnetic Resonance Imaging
MSR	Magnetically Shielded Room
ND	Neutral Density
ON	Optic Neuritis
PE	Pulfrich Effect
PR	Pattern Reversal
PR-VEF	Pattern Reversal Visual Evoked Field
PR-VEP	Pattern Reversal Visual Evoked Potential
PSD	Power Spectral Density
PSP	Post Synaptic Potential
RSM	Root Squared Mean
SR	Summation Ratio
µV	Microvolt
VEF	Visual Evoked Field
VEP	Visual Evoked Potential
‘	Minute of Arc
“	Second of Arc

CHAPTER 1: INTRODUCTION

1.1 Background

Having two eyes carries with it numerous advantages when we are able to combine images from both eyes to create binocular single vision. Our ability to combine images from both eyes to create binocular single vision allows us to perceive objects in depth (Steinman, Steinman, & Garzia, 2000). Other advantages include superior performance on tasks such as resolvable acuity and contrast detection with two eyes as compared to one eye. This increase in binocular performance is referred to as binocular summation (BS) and is defined as an increase in visual performance when using two eyes together as compared to our monocular visual performance. However, under some conditions the use of two eyes can actually be detrimental to performance. This commonly occurs in ophthalmological pathologies that are characterized by a difference in the visual acuity of the two eyes such as: optic neuritis, amblyopia, and cataracts (Donzis, Rappazzo, & Burde, 1983; Macmillan, Grey, & Heron, 2007). These conditions lead to a decrease in binocular vision when compared to the monocular performance and often people subject to these pathologies will resort to closing, or occluding one eye and report an improved visual experience. This decrease in binocular visual performance compared to monocular visual performance is called binocular inhibition (BI) and it has been previously studied by comparing the amplitudes of visual evoked potentials (VEP), a diagnostic form of electroencephalography (EEG) brain monitoring (Adachi & Chiba, 1979,; Katsumi, Tanino, & Hirose, 1985; Pardhan & Gilchrist 1990, Di Summa, Polo, & Tinazz, 1997; Smith, 2013). In normal healthy eyes with normal binocularity, the binocular VEP amplitude is approximately 1.4x larger than the monocular VEP amplitude. A decrease in binocular performance on VEP can be induced in

normal eyes with the placement of a neutral density filter in front of one eye. This effect can be modified by a number of means. Neutral density filters of increasing strength will increase the amount of inhibition until returning to monocular levels in a u-shaped response curve (Katsumi et al. 1985; Pardhan & Gilchrist 1990; Smith, 2013).

While this phenomenon has been extensively studied using VEP, the brain areas that give rise to this activity are not sufficiently localized using the conventional diagnostic setup for VEPs. Magnetoencephalography (MEG) is a non-invasive functional brain imaging technique that captures the magnetic fields evoked from the same brain activity that produces the VEP. MEG is frequently used to explore the exact timing of neural processes and multiple data processing suites are available for signal processing and source localization efforts (Baillett, 2001; Gramfort, Luessi, & Larson, 2014). It is of particular interest to determine how EEG and MEG record BS & BI differently and if the combination of these two techniques can provide any insight into where and how the brain generates these two types of phenomena.

1.2 Purpose Of The Study

The purpose of this study was to take the well-established parameters used to invoke BI in previous research and measure this phenomenon using MEG. There is little literature investigating BI/BS with MEG, such studies could produce results that may reveal the processing mechanisms in the brain that create these changes in activity which could lead to further clinical implications.

1.3 Hypothesis & Research Questions

Driving Hypothesis: Binocular inhibition is the result of temporal interference occurring between areas of the visual cortex.

Research question 1: Will binocular summation and inhibition be captured by MEG signal analysis similarly to the traditional EEG measurements (i.e., significantly increased/decreased activity during binocular symmetric/asymmetric input, as compared to monocular input in one eye) ?

Research question 2: Can the EEG and MEG multi-sensors approach be used to quantify regional cortical activation, to determine if the magnitude of binocular summation and inhibition differs between cortical areas ?

Research question 3: Is the strength of the binocular summation and inhibition dependent on the nature of the stimulus (pattern vs diffuse) ?

CHAPTER 2: LITERATURE REVIEW

2.1 The Physiology Of The Visual System

Our visual system is a fascinating set of specialized tissues dedicated to the transduction of light into neural signals. In order for this to occur every structure & physiological process must be intact and properly transmitting their inputs for further downstream processing. At the onset, light reflected off of a target first strikes the cornea, which is the principal refracting element of the eye consisting of five transparent avascular layers made up of dense connective tissue and non-keratinized epithelium. The eye provides approximately 60 Diopters of refractive power, 43 of these diopters are provided by the cornea despite being only 0.53 mm in thickness on average. Once light passes through the cornea it may be refracted further by the aqueous humor of the anterior chamber before striking the crystalline lens, an avascular, transparent, elliptic structure. The crystalline lens provides the remaining bulk of the refractive power of the eye at approximately 20 diopters. The lens is suspended by zonular fibers originating from the ciliary body, and upon retinal blur the ciliary muscle contracts leading to a decrease in the diameter of the ciliary ring. This leads to a loosening of the zonule fibers tension on the lens allowing it to conform to a more spherical shape. This is known as accommodation. Once an image has been refracted by the crystalline lens, its light rays then pass through the vitreous chamber before interacting with the retina at the back of the eye (Remington, 2011).

The retina is a thin transparent membrane that houses photoreceptors, bipolar cells, and ganglion cells. Photoreceptors can be separated into two subtypes based on of their structure and physiology: 1.) the low spatially resolving, exquisitely light sensitive rods, 2.) the high spatially resolving, higher threshold light sensitive cones. When light is captured by the photopigment

inside the outer segment of the photoreceptors it causes a graded hyperpolarization in membrane potential transmitted to postsynaptic bipolar cells via a reduction in the release of neurotransmitter. This begins when light strikes the photopigment in the receptor disks opsin (rhodopsin in rods). This induces a change in the chromophore 11-cis-retinal to all-trans-retinal which leads to an interaction with the G protein transducin. Transducin dissociates into several subunits, The alpha-subunit binds to phosphodiesterase, freeing a catalytic site and allowing the transformation of cGMP to 5'GMP in an act of signal cascade. 5'GMP is necessary as without it cation channels embedded within the plasma membrane will close reducing the amount of net Na+ outflow resulting in a more positive membrane potential. Potentials are inverted (or not depending on the nature of the glutamate receptors on the bipolar cells, resulting in two streams for bipolar cell responses, giving rise to ON and OFF subsystems at the junction with bipolar cells modulated by glutamate before making connections with ganglion cells. Bipolar cells are an important level of signal processing as they make direct connections with photoreceptors but also are connected to nearby photoreceptors via horizontal and amacrine cells. This networking allows bipolar cells to have a central and peripheral activation field that is either characterized by an Off center, On surround (hyperpolarizing signal is conserved from the direct connection to photoreceptors) or vice versa. Graded membrane potential activity elicited from the bipolar cells is then carried by the retinal ganglion cells in the form of action potentials. Ganglion cell axons converge into a bundle and exit the retina via the optic nerve (Purves, Augustine, & Fitzpatrick, 1997).

The optic nerves pass through the optic canal until they reach the circle of Willis where fibers decussate at the optic chiasm. The fibers representing the nasal portion of retina that serves the temporal portion of the visual field cross over to the opposite hemisphere resulting in

total separation of the left and right visual fields in their opposing brain hemispheres. Axons originating from the retinal ganglion cells in the optic tract terminate in the lateral geniculate nucleus (LGN), the major visual relay center where inputs are divided by cell type. The LGN is a 6 layered structure, the more ventral layers 1 & 2 contain only magnocellular cells, layers 3,4,5, & 6 contain only parvocellular cells, with koniocellular inter-layers between each of these division (6 in total). Each of these cell types have distinct spatial, temporal, luminance, and chromatic preferences and these divisions have been speculated to allow for parallel processing in the brain (Denison, Vu, Yacoub, Feinberg, & Silva, 2014). The LGN is also the target of reciprocal innervation from downstream areas, allowing it to regulate flow of information. The final destination of the optic radiations departing the LGN is the primary visual cortex (V1) or Brodman's area 17.

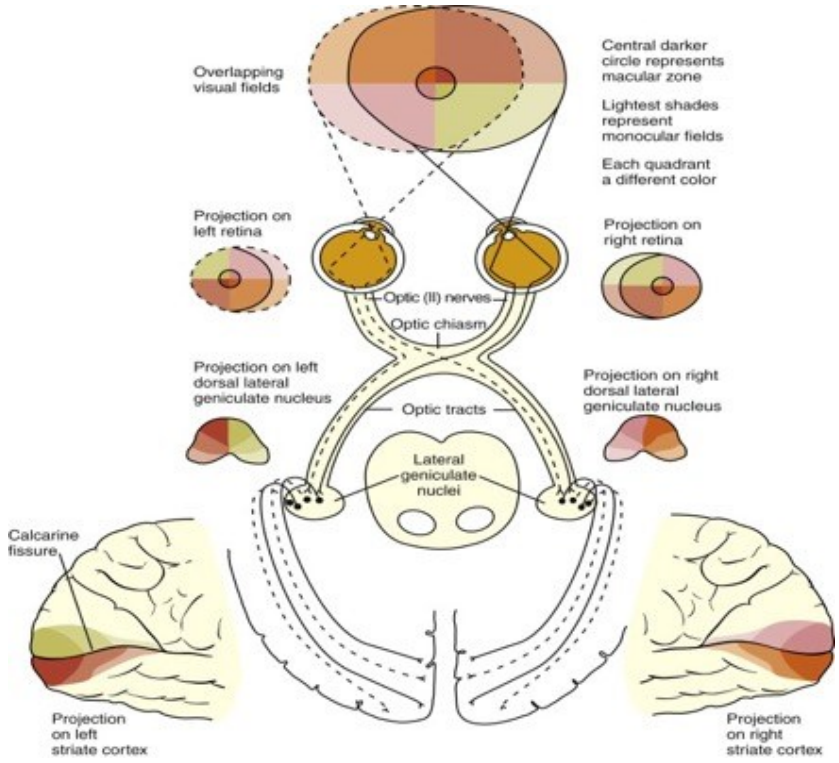

Figure 1: The visual pathway. Axons carrying information from the right visual field travel to the left visual cortex, while axons carrying information from the left visual field travel to the right visual cortex (Adapted from Remington. 2011).

V1 is made up of 6 layers, LGN axons terminate in layer IVc where spiny stellate neurons convey carried information to pyramidal neurons which make contact with extrastriate areas involved in downstream processing. It is at V1 that cells combine inputs from either eye to create binocular cells that respond to either eye and preferentially to stimuli that was received by both eyes. Neurons at the visual cortex are discretely organized into columns with similar receptive field properties (edge orientation, motion direction, color) and also exhibit retinotopy, where regions in visual space correspond to a map like representation of the visual field in the cortex (Purves et al. 1997). Specialized binocular cells have receptive fields from the left and right eyes that are slightly offset such that these cells are activated by retinal disparity. Cells that respond to disparity are either maximally affected to phase shifts away from fixation (far tuned), near fixation (near tuned) or at the plane of fixation (zero tuned) (Tsao, Conway & Livingstone 2003). Outputs from V1 to the associative visual cortices V2 & V3 continue to be segregated by cell type and stimulus properties. Paracellular cells in layer IVca travel through layer IVb of V1 before continuing on to V3 and V5, in what is called the Dorsal stream or the Occipitoparietal pathway. The dorsal stream is characterized by a sensitivity to the entire visual field and processes movement detection. Magnocellular cells & koniocellular cells in layer IVcb travel through layer IVa blobs to V2 then V4 in a different path known as the ventral stream or Occipitotemporal "what" pathway. This pathway is responsible for responding to certain classes of shapes and are independent of location (Purves, 1997).

2.2 Binocularity

Having two eyes allows for a number of advantages. For these advantages to be present, critical components of the visual system that provide binocularity must be intact. This includes not only the brain, visual pathways and resulting sensory and motor reflexes but also the anatomy of the eye and its adnexa. The eyes must be properly aligned with functioning extra ocular muscles, ligaments and connective tissues to allow for motor fusion of images. Any exceptions to this can cause an abnormal binocular interaction that can lead to a change in experience. For example, the reduction in strength of one extraocular muscle in one eye may result in the fovea's of the two eyes to have misaligned. This condition can cause visual confusion (superimposition of two dissimilar objects) or double vision (diplopia). Binocular single vision (BSV) depends on an element known as retinal correspondence. Retinal correspondence requires the retinal images related to an object in space fall onto corresponding areas of the retina of either eye such that the localization of these visual sensations is in one visual direction. These corresponding retinal points have a fixed position that is relative to the principal visual direction and it is the unification of these images that gives rise to a single perceptible visual image. This process is known as sensory fusion (Von Noorden & Campos, 1985; Barlow, Blakemore & Pettigrew, 1967). BSV lends us additional information in the form of stereopsis. Stereopsis is a high grade of BSV, which can be defined as our visual system's ability to order images in our visual field in terms of depth (Von Noorden & Campos, 1985). To understand stereopsis, we must first address the horopter; a geometric distribution of corresponding retinal elements where binocular single vision occurs. All objects lying on the empirical horopter stimulate corresponding retinal elements and are thus seen singly. Any objects falling outside the horopter stimulate disparate retinal elements and theoretically produce

diplopia. However, this is a conditional rule as a theoretical area around the horopter exists in which retinal images that lie outside the horopter can still be fused (Panum's fusional area). In the horizontal plane stereopsis is produced when objects exist within this space despite retinal disparities of up to 3 degrees (Von Noorden & Campos, 1985).

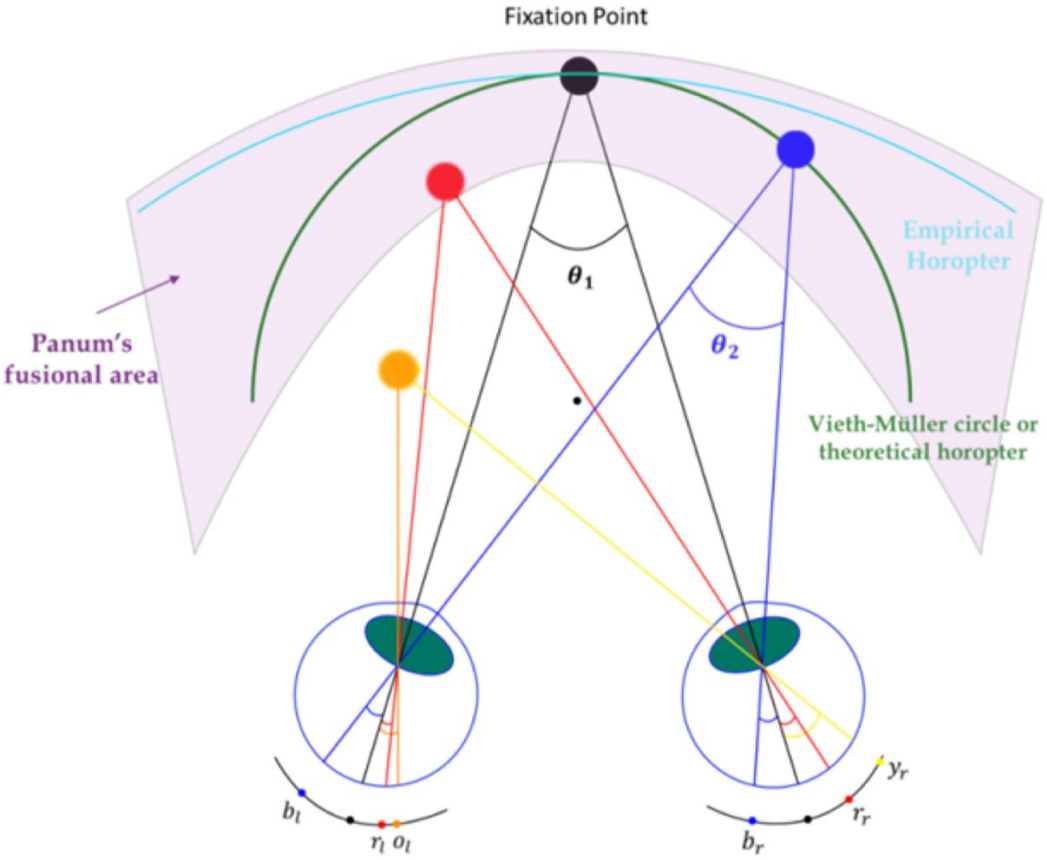

Figure 2: The Horopter. When fixating straight ahead, points $b_{r/l}$ on the horopter stimulate corresponding retinal elements and are seen singly. Points $r_{r/l}$ exist within Panums fusional area and slight disparities cause them to be seen with depth. Points y_r and o_l stimulate disparate retinal elements outside of Panums fusional area and are seen as double images (Adapted from Cutolo & Ferrari, 2018).

Despite many monocular cues for depth, true stereopsis is impossible without disparate retinal elements. The monocular contour and form input alone does not provide enough information for the brain to compose depth information even at a foundational level as demonstrated by random

dot stereograms which suggest that form perception must occur following stereopsis (Von Noorden & Campos, 1985).

Apart from the sensory characteristics that are gained from having two eyes, it also serves numerous other functions. One obvious advantage of having a second eye is that it serves as a backup in the case one is damaged or lost to disease. It also provides a larger visual field of view. A single eye only provides 160º of visual field, but with the addition of a second eye under conditions of BSV, the total visual field amounts to 200 º, 120 º of which are overlapping and the remaining 80 º is split between the two on each temporal side (Von Noorden & Campos, 1985). Perhaps most importantly having a second eye seems to facilitate visual function in the form of binocular summation (BS). Pattern detection and luminance sensitivity is significantly higher in binocular viewing conditions attributed to the brain's facilitated ability to detect a visual signal in a noisy environment (Simpson, Manahilov, & Shahani 2009).

The degree of binocularity is directly linked to the state of the visual system. Amblyopia is defined as a decrease of visual acuity in one or both eyes as a result of pattern form deprivation during visual immaturity, for which no cause can be detected during physical examination of the eye(s) and which in appropriate cases is reversible by therapeutic measures (Von Noorden & Campos, 1985). Amblyopia affects up to 4% of the world's population (Levi, Knill, & Bavelier, 2014), and can come about due to a variety of different reasons. These reasons include: strabismic amblyopia (ocular misalignment), anisometropic amblyopia (uncorrected difference in refractive error between the two eyes), meridional amblyopia (due to uncorrected astigmatic refractive error), and ametropic amblyopia (due to general uncorrected refractive error). Organic amblyopia refers to vision loss as a result of ocular pathology, though it is named amblyopia, there is a physical cause present. This decrease in vision during visual

immaturity, regardless of the means, results in a reduction in binocular function, most frequently measured via stereopsis (Levi et al. 2014). Generally speaking, worse visual acuity (or increasing differences between eyes) correlates with worse stereoacuity. This decrease in stereoacuity can be replicated in normal subjects simply by degrading vision (i.e., blurring) with neutral density filters or reducing contrast. This effect is achieved more effectively by blurring the vision of one eye rather than both.

Amblyopia is not the only case where binocular processing is interrupted. Other cases of asymmetric ocular inputs such as the presence of a significant cataract that causes image distortion can lead to issues with BSV. Similarly damage to the optic nerve or fovea disrupt the integration of binocular inputs. Perhaps most interestingly are cases of optic neuritis (ON) an inflammatory condition of the optic nerve that occurs in patients suffering from multiple sclerosis. The condition is characterized by the inflammation and subsequent destruction of the myelin sheath that insulates the optic nerve resulting in a transient decrease in vision in the affected eye (Osinga, Van Oosten, & de Vries-Knoppert, 2017). This produces an interocular difference in signal latency that produces an altered sense of depth. This effect is known as the Pulfrich Effect (PE). Traditionally it is tested by swinging a pendulum in the frontal plane in front of the subject. Patients experiencing this effect as a result of optic neuritis experience the swinging pendulum to be moving elliptically. The reduced latency of the effected eye produces a spatial disparity which stimulates the disparity sensitive neurons to create the sensation that the pendulum is moving in depth (Heng & Dutton, 2011).

2.3 Early Models Of Binocular Interaction

It has long been established that under conditions of normal binocularity, having two eyes causes an increase in the ability to detect inputs. This ability to detect inputs is best described by probability theory put forth by Pirenne (1943) who noted that the detection threshold for vision was lower under binocular conditions compared to monocular conditions. He put forth the following expression to quantify this finding following an experiment wherein he recorded the number of times stimuli of different intensities were detected monocularly vs. binocularly:

$$P_{binocular} = P_{right} + P_{left} - (P_{right} \times P_{left}) = 0.6 + 0.6 - (0.6 \times 0.6) = 0.84$$

What he found is that for a set of stimulus conditions, each eye produced a 0.6 probability of detecting the stimulus. With the addition of a second eye the chances of detecting a stimulus climbed to 0.84. Thus, being binocular allows us a 1.4x increase in probability of detecting a stimulus (Blake & Fox, 1973). Now there are several potential results of binocular processing. The interaction can yield a summation effect (in which the resulting input is larger than the independent value of the monocular input), or inhibitory (in which the resulting input is processed to be smaller than that of the monocular input). Summation can be divided into complete (where the resulting output is the sum of both inputs) or partial (where the output is greater than the monocular input but less than the total sum of both monocular inputs). Finally there can be no summation where the output is equal to the monocular input (Blake & Fox, 1973). To refer momentarily back to Pirenne for a quick example, if his experiment were to indicate that complete summation occurred then both eyes stimulated at the same time would behave as a single unit and the same result would be achieved by exposing both eyes to a certain brightness or exposing one eye to double that brightness (Pirenne, 1943). Similarly, if such

information underwent no summation then the lowest possible stimulus that could be detected with both eyes, would also be the least detectable with one eye. This was translated into a theory of neural summation as the presentation of identical stimuli slightly offset to one another at the same visual angle and typically produces a summation neural signal in the visual cortex that is larger than if either eye was stimulated independently (Apkarian, Nakayama & Tyler, 1981). This is further supported by the fact that low luminance stimuli that are below the monocular threshold are able to be seen under binocular conditions, and that the overall superiority of detecting a stimulus binocularly is greater than what can solely be attributed to probability (Blake & Fox, 1973).

2.4 Fechner's Paradox And Clinical Manifestation Of Binocular Processing

One of the earliest descriptions of cortical brightness processing was provided by Fechner (1860) who described a psychophysical paradox in which a stimulus brightness is perceived as the average of two inputs. This can be induced with the use of a neutral density filter placed in front of one eye when viewing a bright stimulus binocularly as seen in Figure 3.

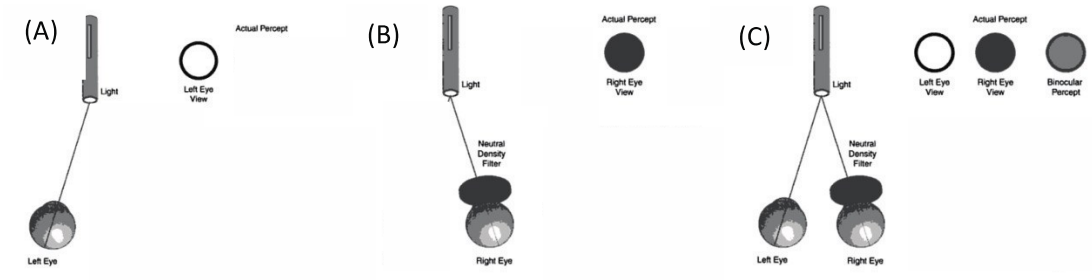

Figure 3: Fechner's paradox, (A) light viewed with LE and its corresponding brightness perception. (B) RE viewing light through a ND filter reducing the brightness perceived proportional to the ND strength. (C) Under binocular conditions with the ND in front of the RE the perceived brightness is less than if viewed with the LE alone (Adapted from Steinman et al. 2000).

It is referred to as a paradox as the closing of the eye with the filter in front of it under these conditions reduces the luminance while the closing of the other increases luminance. Despite the increased total retinal stimulation present the perceived brightness is decreased due to the blending of perceptions under conditions of BSV.

From a clinical perspective, having asymmetric visual inputs can lead to a decrease in performance on standardized binocularity tests (Donzis et al, 1983). Pathologies such as amblyopia, cataracts and optic nerve disease can cause a large enough disparity between the eyes to disrupt binocular processing on clinical examination, but such changes do not always conform to convention. For example, a unilateral cataract will cause a decrease in BSV, but the reduced light to the retina of the affected eye will not cause a relative afferent pupillary defect despite a significant decrease in light reaching the eye (Sadun, 1990). These patients also do not report any differences in perceived luminance, indicating that the brain is capable of compensating for differences in retinal illumination (Macmillan et al. 2007). Despite this, cases of interocular input differences as a result of cataract have demonstrated that inhibitory processes under binocular conditions occur at higher spatial frequencies than 2 cycles/degree. In some cases, these patients are aware of the decreased binocular performance and may prefer to close or patch the affected eye (Pardhan & Gilchrist 1991). Monocular contrast sensitivities in amblyopes have been shown to depend on the cause of amblyopia (Bradley & Freeman, 1981; Hess & Howell, 1977; Hess, Campbell & Zimmerman, 1980), interocular ratios estimated as a function of contrast sensitivity at changing spatial frequencies demonstrated that anisometropes experience lower sensitivities at higher spatial frequencies and strabismic amblyopes have reduced sensitivities at both low and high spatial frequencies. This produces a larger binocular ratio for

anisometropic amblyopes at lower spatial frequencies, while strabismic amblyopes have a more generalized depression of summation across the spectrum (Pardhan & Gilchrist, 1992).

2.5 Electroencephalography (EEG)

The use of electrophysiology to observe the electrical activity of human tissues and structures dates back to as early as Galvani's first publication in 1741 detailing the movement of a frogs legs when a wire with current was applied to the muscle tissue (reported in: Olmsted, 1955). Since then electrophysiological techniques have become a standard clinical practice for many modalities from brain function, to heart health. While the majority of the techniques may have been established many decades ago, use of electrophysiology to view the evoked language of the brain in instruments such as EEG (electroencephalography) are still making important progress today. Following the surge of galvanism, many scientists looked to discover just how the brain responded to different stimuli, in hopes to aid in classification of the anatomy of the brain in functional terms. Caton was the first to describe the changes evoked by visual stimulation in 1875 and by 1940 a standard EEG neurological testing routine had been developed by a scientist by the name of Hans Berger (reported in: Millett, 2001). Clinically significant findings related to Berger's research efforts surfaced during the first part of the 1900's (Adrian & Matthews, 1934) and by 1970 Halliday published the first use of pattern reversal visual evoked potentials to diagnose optic neuritis (Halliday, 1973).

Visual evoked potential can be best described as electrical potential differences recorded between electrodes from the scalp relative to a ground electrode following visual stimuli (Celesia, Bodis-Wollner, & Chatrian, 1993). The produced waveform is believed to be derived from cortical pyramidal cells firing in synchrony. This synchronous activation of neurons

creates a fluctuating electrical field known as an electrical current dipole, which describes a pair of electrical charges of equal magnitude but opposite sign. The mechanism behind this is the extracellular currents evoked during a post synaptic potential (PSP). As an action potential reaches the apical dendrite of a neuron it propagates down the neuron causing it to become electronegative with respect to the soma and basal dendrites. The cell acts as a volume conductor and current flows from the electronegative apical dendrite through to the electropositive basal dendrites as illustrated in Figure 4 (Gloor, 1985).

The current density drops off as the distance from the source of the PSP increases as demonstrated by the isopotential lines in Figure 4. The electromotive force for the continuation of the current is the difference in membrane potential between the excited and resting state potentials of the cell. These currents are collectively known as extracellular currents and are the currents responsible for the generation of the electrical dipole, in which a flat zero isopotential line is present at the midway point between the positive and negative poles of the cell surrounded by curved ellipsoid isopotential lines. One may note in Figure 4 that the electrical gradient at the point nearest the zero isopotential is much smaller as the isopotential lines are very crowded here in comparison to either poles demonstrating the large effect distance has on potential differences (Gloor, 1985).

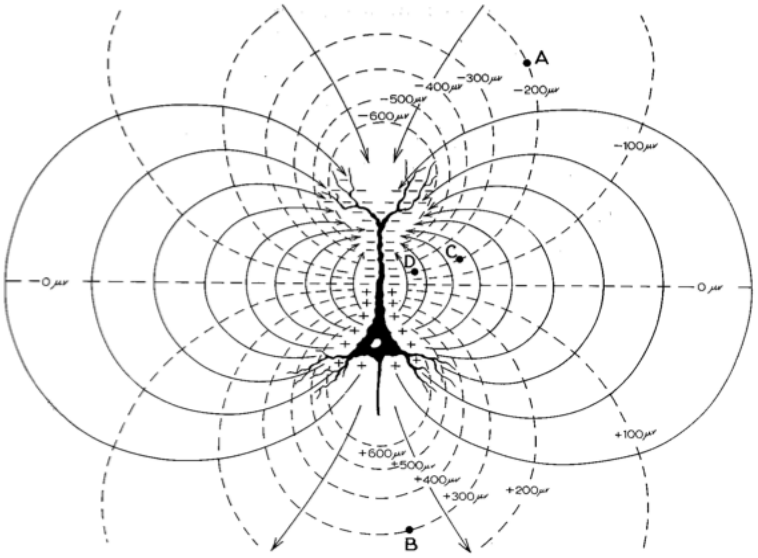

Figure 4: Dipolar electrical field evoked from an excited pyramidal neuron. Depolarization of the apical dendrite causes this segment to become electronegative with respect to the soma which in turn become electropositive. Solid lines depict extracellular current flow, dashed lines depict the potential distribution on the form of isopotential surfaces which represent the same potential at any point along their course. A & B have a significant potential difference compared to C & D despite their distance from the source (Adapted from Gloor, 1985).

The end result in EEG analysis is that the current dipole model is used as an equivalent source for a unidirectional primary current extending over a small area of cortex of usually a few cm^2 (Hämäläinen, 1993).

2.5.1 Volume Conductor Theory

Solid angle concept of volume conductor theory measures potential *P* at any point in a volume conductor to be equal to the solid angle subtended by the dipole at its position of measure. It is expressed by the following formula as seen in Gloor, 1985:

$$P = \frac{\pm e}{4\Pi}\Omega$$

The expression described above refers to potential P being equal to e, the potential across the dipole layer of the neuron were multiplied by Ω, the solid angle subtended by said dipole. A good analogy for solid angle concept is that of visual angles. Objects in our environment that are closer and larger subtend a larger visual angle than those that are smaller and further from us, but for the purpose of this analogy it is important to consider the point at which the object is seen. Some objects are easily identifiable when seen straight on but more difficult to discern when viewed from the rear or below. Similarly a potential captured by an electrode is modified by such, as the potential seen depends on what side of the surface dipole is facing the measuring electrode. A neuron undergoing a change from resting potential to excited will possess portions of the cell membrane that are undergoing membrane potential change and those that are not. If we assume that this change in potential is sudden then in a simple scenario in which the neuron is located in a plane parallel to the electrode, the solid angle captures three possibilities: 1.) a potential in where the membrane is not yet activated and still at rest; 2.) a potential where the membrane has already undergone depolarization; 3.) a potential where depolarization is occurring. Now the first two potentials effectively cancel one another out, however the remaining site undergoing depolarization is flanked by membrane that is both negative and positive in a sense. It is this angle that is proportional to the Potential at P captured by our electrode. When taking these concepts at a more macroscopic level it is easier to see how potential is measured for different areas of the head. Cortical pyramidal neurons are closely assembled in parallel fashion in the brain and positioned at right angles to the cortical surface. Cortical pyramidal cells also fire in synchrony creating a volley of identical dipolar electric fields. The resulting macroscopic patch of synchronized pyramidal neurons need only to reach a

solid angle size estimating approximately 6 cm^2 to be measured at the scalp with an electrode (Gloor, 1985).

2.5.2 Effects Of Cortical Organization On EEG

The intricate organization of the brains cortical surface involves much folding of brain tissue resulting in an increase in the total surface area. The grey matter of the cortex is roughly 2-4mm in thickness and the convolutions allow for almost 2500 cm^2 to fit into the skull without complication (Hämäläinen, 1993). As a result of this the pyramidal cells within the sulci and gyri produce dipoles that are positioned in a multitude of ways. As briefly mentioned previously, the simplest encounter of a dipole generator is when pyramidal neurons are oriented parallel to the scalp. The top-down orientation of the dipole as seen in Figure 4 is a good indication that determines that the highest potential would be near the midpoint of the patch of cells of interest. However due to the folding of the cortex, this type of distribution is very sparse. The more common scenario is that the patch of activated cells is arranged in a curved sulcus or gyri. The result of this is that the angle seen by the electrode may capture the parallel oriented cortex electrical structure well, but the tangential areas of cortex that make up the sulcus wall only expose the most superficial charges resulting in a net charge that is primarily driven by the parallel tissue. However, if the electrode is slightly offset to allow the angle to 'view' more of the deeper sections of the sulcus this allows for the more positive side of the dipole layer to be seen resulting in a more positive net charge. If the electrode is positioned such that it only is able to capture the active area of cortex within the sulcus then the position has a much larger effect on the potential recorded. This is because depending on what side the electrode is positioned it will

either capture solely the positive or negative or as mentioned previously, a combination of the two (Gloor, 1985).

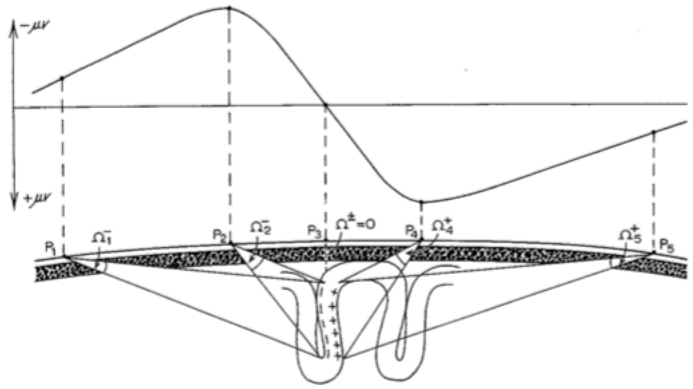

Figure 5: Potential distribution captured by electrodes at different positions. Electrodes positioned at P1 and P2 see only the negative side of the dipole layer corresponding to the pial surface cortex of the sulcus wall. Where electrodes at P4 and P5 see only the positive side of the dipole layer corresponding to the white matter surface of the sulcal cortex. Electrode at P3 record no potential as it looks at the dipole such that the positive and negative components cancel each other out (Adapted from Gloor ,1985).

Figure 5 demonstrates this very clearly. To combine this into a clinical example, imagine the case of a whole head EEG recording as seen in Figure 6. In this case, the dipolar regions of the activity take place in the front and back of the left hemisphere with the phase reversal in the center of the head.

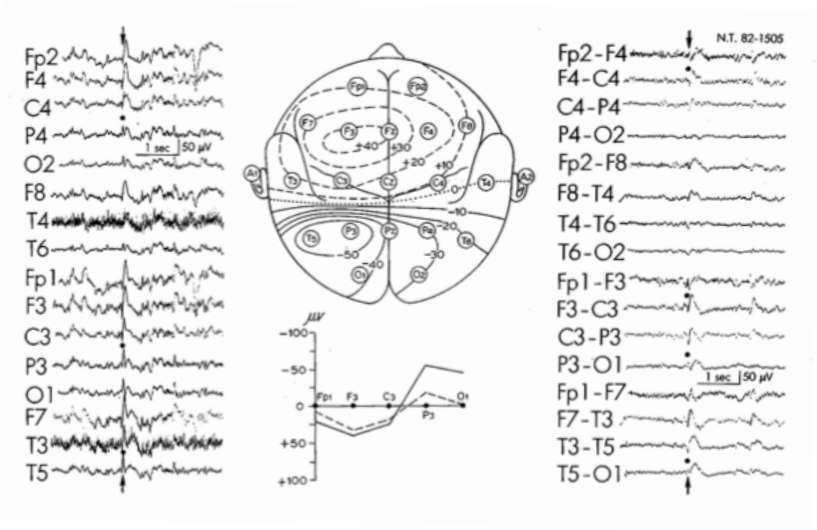

Figure 6: Sample Recordings from a scalp EEG on a 2 dimensional topographical representation of the head. Dipolar potential distribution depicts the largest positive response emanating from F3 in the left frontal hemisphere, and maximum negative activity in the left parietal hemisphere (Adapted from Gloor 1985).

The waveform at the bottom denotes the change in potential as the electrodes cross the midline demonstrating that the activity must be originating from a horizontal dipole and thus the wall of a sulcus (Gloor, 1985).

2.6 Visual Evoked Potentials (VEP)

EEG recordings are filled with potential differences due to activity in many brain regions that are unrelated to the specific waveform that one may be interested in studying. This noise may be magnitudes larger than the signal one wishes to examine. To combat this, stimulus triggers are time locked to the acquisition of EEG data and averaged in a small time window to increase the signal to noise ratio. This evoked activity can be elicited by many types of activity, but for our purposes, we will refer to the VEP recorded from the occipital lobe as a function of contrast stimulation. The VEP is an extremely useful clinical tool that can confirm visual function in the context of unreliable clinical testing. Furthermore, VEPs are able to detect

organic causes for subjective symptoms that may appear normal on other clinical testing scenarios. A VEP is able to diagnose a patient suffering from optic neuritis in the absence of visual acuity, visual field, or color vision deficits (Kothari, Bokariya, & Singh, 2016). Two forms of VEP are the flash and pattern reversal (PR) VEP. PR VEP is induced using reversing checkerboard stimuli and is the most optimal for clinical use as the test produces consistent morphology, timing with little interindividual variability and minimal variation with repeated recordings. Flash VEP are useful in cases where clear PR VEP results are not possible or ideal, such as in cases with media opacities or with young infants who will not properly fixate (Kothari et al. 2016).

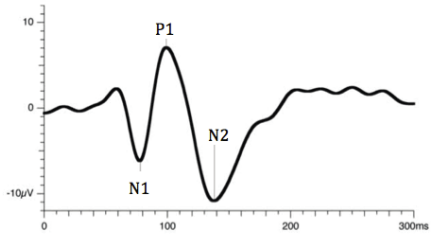

Figure 7: Typical PR VEP waveform morphology (Adapted from Creel, 2011).

The normal morphology of the PR VEP as seen in Figure 7 is composed of three primary components. A small negative component at 75ms known as N1, followed by P1 a positive component at 100 ms, which is then followed by N2 a second negative inflection at 135 ms.

There has been much debate and research into the origin of the components of the VEP waveform. The first component N75 is the most agreed upon, it is speculated that this component arises from the striate cortex (Di Russo, Pitzalis, & Spitoni, 2005) and more specifically the calcarine fissure. This has been supported by the finding that this component will reverse in

polarity when only stimulating the top or bottom visual field corresponding with the retinotopic organization of the primary visual cortex, a feature less adamant in associate visual cortices (Jeffrey's & Axford, 1972). There is less agreement with the neural origin of the second component P1. Unlike N75, P1 does not show polarity reversal with manipulation of visual field stimulation so many speculate that it may be generated from extrastriate areas, whereas others maintain that V1 is still the origin (Onofrj, Fulgente, Thomas, 1995a&b; Di Russo et al. 2005). The N2 component at 135 ms has been studied less extensively but has been speculated to arise from extra striate areas. The evidence for this is not conclusive as many speculate that the primary receiving areas of the brain such as V1 are responsible for processing signals and subsequently producing VEPs for up to 250 ms post stimulus though it could be that downstream processing could be more spatially widespread and the signal relatively weak in comparison (Noachtar, Hashimoto, & Lüders, 1993).

2.6.1 VEPs And Binocular Parameters

Electrical potentials measured via VEP are a good indicator of visual cortical processing since it is recorded from the striate cortex where inputs from both eyes are combined at the cellular level. Modifications to binocular inputs have determined that a number of factors can influence the amount of binocular summation (BS) of the neural signal received at the striate cortex, even to the point of producing an inhibitory interaction, resulting in a lower binocular VEP amplitude (Smith, 2013). Previous work (Adachi & Chiba, 1979; Katsumi et al. 1985; Pardhan & Gilchrist 1990; Di Summa et al. 1997; Smith 2013) on the topic have used the ratio of the binocular response (amplitude obtained with both eyes viewing the stimulus) divided by the monocular response (amplitude obtained with one eye occluded).

At lower contrast thresholds (20%, 40%), binocular summation is largest, but as contrast increases the difference between binocular and monocular evoked responses decreases, with the smallest amount of BS occurring at 95% contrast (Katsumi et al. 1985a). This comes as both a decrease to the binocular amplitude as well as relative increase in the monocular amplitude. At the lower levels of contrast where the binocular evoked response was highest, the highest expected value of BS was found at 1.4, which decreased to 1.1 at 95% contrast where the evoked responses between conditions were the closest in amplitude (Katsumi et al. 1985a). Other studies have not shown any significant difference between BS/BI using different contrasts (Smith, 2013).

Katsumi et al. (1986) performed a second part in their BS study to investigate changing luminosity effects on BS/BI using neutral density filters ranging from 0.2 to 3.0 log units, when viewing a 3 Hz PR checkerboard at 30% contrast viewed in 50 cd/m^2 conditions. As luminosity was steadily decreased, binocular and monocular amplitudes decreased producing BS at all levels. When the luminance was adjusted such that it was constant for one eye to create an interocular difference (IOD), BS was found at small IOD, but the BS steadily decreased with increasing IOD until no summation occurred at 0.6 log units and maximum BI occurred at 2.0 log units (Katsumi et al. 1986). At higher IODs induced, BI was reverted back to just below no summation or the monocular amplitude value. Authors speculate that there could be a multiphase structure to this response in which at small IOD the response is driven by both eyes, but as the IOD increases this puts further burden on combining inputs. This is supported by the interference they recorded upon introducing 0.8 log units and above as the dissimilar inputs may be becoming to disparate to properly integrate. The final phase suggested by the authors at which the IOD becomes too large to integrate and total suppression occurs, as seen at ND

strengths above 2.0 where amplitudes returned to monocular values (Katsumi 1986a). This finding was corroborated by Pardhan & Gilchrist 1990, who used ND filters ranging from 0.4 to 3.2 log units. They too observed a maximal BS response with no ND used, but a steadily decreasing BS with weak ND filters becoming equal to the monocular response at 0.6 log units. Similarly, they observed BI at 1.0 log units and a maximum amount of BI from 1.6-2.0 log units before a return to monocular response level at 3.0 log units. Smith (2013) documented similar results with a maximal BS with binocular viewing and minimal ND filter strength of 0.3 log unit. A range of 1.2 to 1.8 log units was found to induce the strongest BI, with a strength of 3.0 log units returning the response to monocular values.

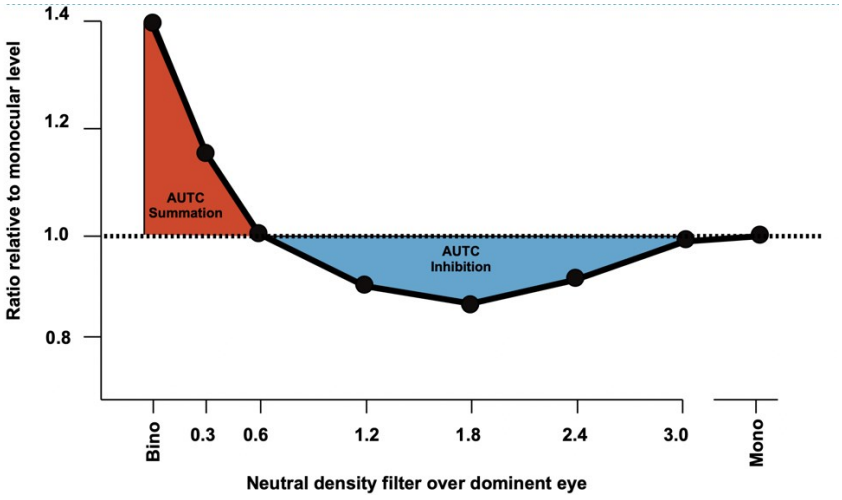

Figure 8: Relationship between neutral density strength and binocular evoked activity as a ratio over monocular levels, a seen with VEP represented by area under the curve (AUTC) (Adapted from Smith, 2013).

Check size has been determined to be an important factor on the amount of BS/BI induced in PR VEP. Katsumi et al. (1988) tested optimal check sizes and pattern reversal rates. The check sizes ranged from 7.5' to 100', with reversal rates ranging from 1.5 to 24 Hz. What they found in regards to check size was that binocular responses were larger than monocular responses, the largest binocular amplitudes at 25'and 12.5'. The largest responses evoked for the

monocular viewing condition were also at 25'. The amplitudes obtained during binocular recordings were significantly larger than the monocular ones, in which the biggest difference yielding the highest level of BS was at 7.5'. Results from this study suggest that as check size decreases, BS increases. BS measured as a change of temporal frequency resulted in an inverted u-shaped graph peaking at 12 Hz (Katsumi et al. 1988). Smith (2013) used check sizes varying from 115' to 6', results also indicated maximum BS occurred at the smallest check sizes of 6', maximal BI occurred at the largest size of 115' but still occurred at all check sizes in the range of 1.2-1.8 ND log units.

The location of pattern elements has also been tested to determine if either of these parameters have any effect on the magnitude of BS. Katsumi et al. (1986) used decreasing full field and peripheral field PR VEP at the aforementioned luminance and contrast levels beginning at 8.9x7.1° (320 elements) dwindling to 0.8x0.8° (4 elements) for central field stimulation. For peripheral field stimulation an increasing portion of the central field was masked ranging from 0.4x0.4° (1 check) to 4.0x4.0° (100 checks). They reported that increasing the size of the central field stimuli led to increases in both the binocular and monocular evoked responses. Monocular responses increased significantly at 3.2x3.2° and leveled off at 5.0x5.0°. Binocular responses increased significantly starting at 2.4x2.4°, but again leveled off at 5.0x5.0°. These amplitudes when converted to ratios demonstrate BS at positions above 0.8x0.8° with the maximum BS occurring at 4.0x4.0°. For peripheral fields the monocular and binocular amplitudes were changed little below 1.6x1.6° but larger occlusion produced significantly reduced amplitudes for both viewing conditions. When converted to ratios, BS was maximal at the lowest levels of occlusion and becoming equal to the monocular amplitude at 3.2° of occlusion. BI was induced at the largest amount of occlusion of 4.0° (Katsumi et al. 1986). Many other researchers have

replicated these results (Adachi & Chiba, 1979; Di Summa et al. 1997) further confirming that using a smaller visual angle for individual check sizes produces more BS. Pardhan 1997 performed a similar task using eccentric retinal illumination via a Humphrey Field Analyser on old and young participants (ages:18-68 yrs). It was found that younger participants had a higher retinal sensitivity in all locations. Foveal ratios produced BS of 1.54 (sd ±0.35) for the younger group and 1.27 (sd ±0.33) for the older group. Furthermore, the amount of BS decreased with increasing eccentricity. Smith (2013) found a significant difference in components affected by location of stimuli. N1 component was found to be significantly affected with central stimulation (central 10°) while the N2 component was only significantly affected by peripheral stimulation (10° mask). The P1 component was significantly affected between filters with both central and peripheral stimulation.

2.6.2 Binocular Ratios With Ganzfeld Stimulation

Ganzfeld flash stimuli has been an important proponent to studies involving Fechner's Paradox since they have been shown to produce different results than PR VEPs. Dichoptically viewed Ganzfelds of different luminance still produce BS (Bolanowski, 1987). Grossberg & Kelly (1999) posited that models involving homogenous areas of luminance will elicit only positive activity, as once an eye is adapted to the Ganzfeld the remaining perceived brightness is considered to be greater than the "non-zero" brightness that is associated with the lack of light of a dark scenario. This may suggest that the presence of boundaries and contours inhibits the summation of brightness signals, as Ganzfelds of widening areas result in further increases in summation (Leibowitz & Walker, 1956). Similar experiments involving full field Ganzfeld stimulation as well as smaller targets with graded decreases in spatial frequency (sharp contours)

also produce large amounts of summation without ever reducing to monocular levels (Bourassa & Rule, 1994). Smith (2013) found slight inhibition only at N2 when using ND filters between 1.2-2.4 log units, these values were not statistically significant and no ratios were found to be inhibitory at N1 or P1 on all subjects.

In summary, the research reported above suggests that BS at its peak approaches a value of 1.4x the monocular amplitude. This is facilitated by low contrast, small check size, centrally located PR stimuli at similar inter ocular luminance levels. BI is strongest at inter ocular luminance differences between 1.6-2.0 ND log units and can be facilitated by masking the central visual field. Ganzfeld stimulation produces BS with changing spatial frequency and minimal BI with inter ocular luminance differences.

2.7 Magnetoencephalography (MEG)

The first documented study of magnetic fields emanating from living tissue was found on a functioning human heart in the 1960's. The discovery that the change in ionic potential produced a measurable magnetic response that was distinct from the currents captured on traditional electrophysiology naturally led researchers such as David Cohen to investigate the brain in this new endeavor. One of the first studies involving a magnetic field recording of the human brain was done by David Cohen using an early analog to a modern MEG to capture the evoked magnetic fields produced during simultaneous recording of alpha waves via EEG in a sleeping subject (Cohen, 1968). Magnetic fields are a by-product of synchronous neuronal activity. The same cortical pyramidal cells that generate EEG signals are responsible for producing the magnetic fields evoked during stimulus presentation. The extracellular currents evoked during an PSP travel from the apical dendrite propagate down the neuron causing it to

become electronegative with respect to the soma and basal dendrites. As mentioned earlier, the extracellular currents flow from the electronegative apical dendrite through to the electropositive basal dendrites, however it is the intracellular currents which flow more directly from the apical dendrite through the dendritic trunk that carries the highest density of current which is of importance in MEG (Gloor, 1985; Baillett, 2001; Hämäläinen, 1993).

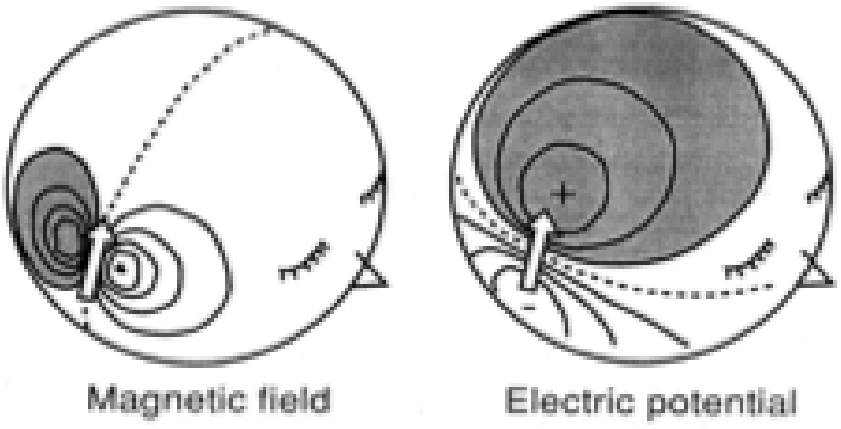

Figure 9: Idealized magnetic field & electrical potential elicited from a tangential dipole (white arrow). Electrical fields are always 90 ° perpendicular from magnetic fields (Adapted from Hämäläinen, 1993).

The intracellular current is more dense and concentrated and it is the combined activation of thousands of orthogonally oriented pyramidal cells that make up the MEG signal. These intracellular currents are also known in MEG science as primary currents, whereas extracellular currents are referred to as secondary or volume currents. Magnetic fields generated by this activity behave similarly to those seen on EEG to an extent. Magnetic fields captured are always positioned orthogonally from electrical fields captured by EEG, or perpendicularly to the current flow as induced magnetic fields follow the right hand rule as seen in Figure 9 (Hansen, Kringelbach & Salmelin, 2010).

2.7.1 MEG Instrumentation

It was not until recently that the magnetic fields evoked by the brain were able to be captured. Neuromagnetic signals are incredibly small in magnitude, in the range of 50-500 fT (femtotesla 10^{-15}) or roughly 1 part in 10^9 of the earth's magnetic field (Hämäläinen, 1993). Due to the small magnitude in signal, precautions must be taken to ensure that the signal is not compromised by any external noise from the environment as well as internal noise caused by the body from things such as the heart. To combat this problem a magnetically shielded room (MSR) is used to reduce the amount of noise from the outside environment. The rooms walls consist of 3 nested main layers made of a pure aluminum layer with a high permeability ferromagnetic layer. The magnetic continuity between layers is permitted by the addition of aluminum overlay strips, insulated washers and junctions electroplated with silver or gold (Cohen, Schläper, & Ahlfors, 2002). There is also active shielding available which consists of a subset of low flux-gate magnetometer mounted onto the sensor array helmet. The amplifier connected to these magnetometer connects to two coils arranged in series which encircle the entirety of the room around the ceiling and floor. Shaking and degaussing wires are built into the inner layer of the room. The active shielding component adds a signal shielding factor of 6-10 at 0.10 Hz which decreases at higher frequencies (Cohen et al. 2002).

Fluctuating magnetic fields are detected using SQUIDs (Super Conducting Quantum Interference Devices). SQUIDs are formed by interrupting a superconducting ring by one or more Josephson junctions (a nonsuperconducting material positioned tightly between two layers of superconducting material)(Vrba & Robinson, 2001). When kept at a very cold temperature these junctions produce practically no resistance to the flow of direct electrical current and produce no magnetic field (Ryhänen, Seppä, & Ilmoniemi, 1989). The design of flux

transformer connected to the SQUID determines the specificity of the orientation of activity captured.

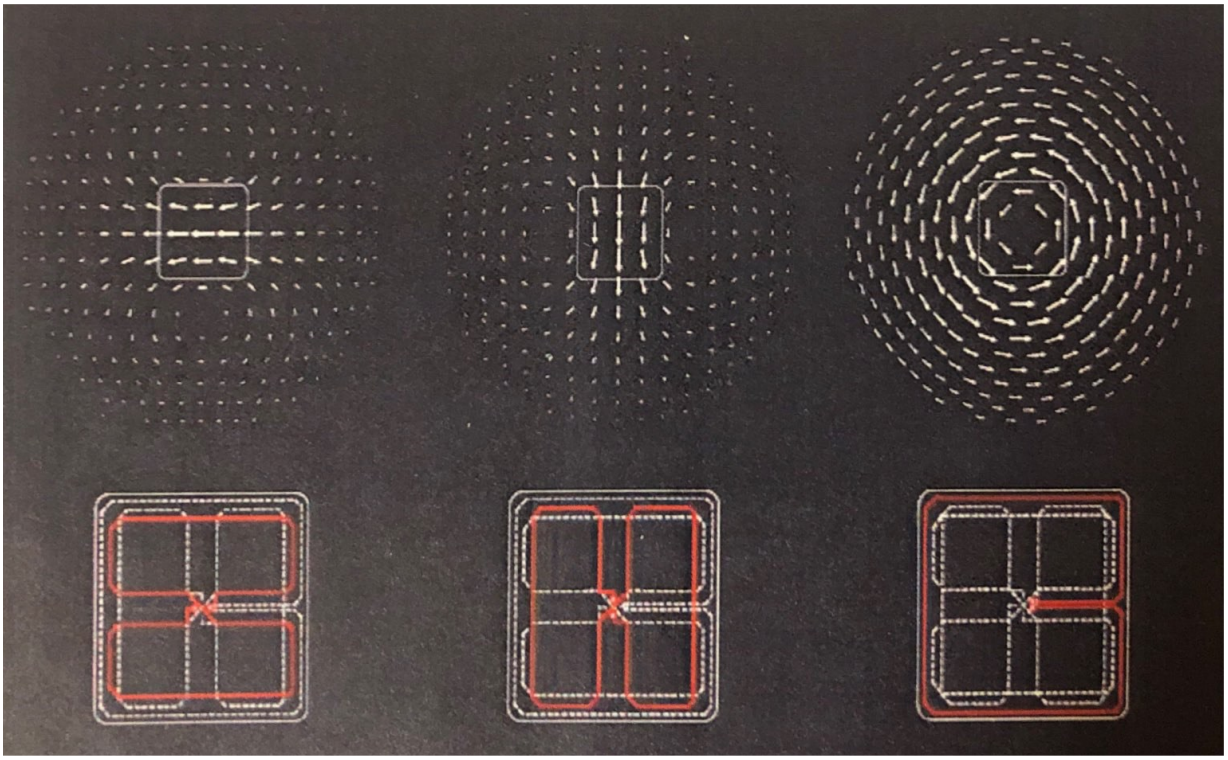

Figure 10: MEG sensor coil configuration, on the left and middle are two planar gradiometers highlighted in red, on the right is the coil configuration for the magnetometer. Above are the 2 dimensional projections of the lead fields being measured (adapted from Elekta Neuromag, Oy 2017).

Figure 10 demonstrates the different arrangement of coils for gradiometers as well as the sensitivity to a tangential current dipole for a magnetometer and planar gradiometer (Hämäläinen, 1993). To put it simply, magnetometers are used to measure magnetic fields located perpendicularly to their coils. They are the simplest configuration of a pickup coil and measure the components perpendicular to their surface, and thus are able to view deeper sources (Hansen, Kringelbach, & Salmelin, 2010). Planar gradiometers are used to establish a magnetic gradient at the location of their coils by measuring the spatial derivative in two orthogonal directions perpendicular to the sensor. The idea behind this is that interference originating from

far sources is captured as a homogenous entity and side by side wound planar gradiometers that are wound in the opposite direction create no net shielding and are blind to distant sources such as homogenous fields (Hansen et al. 2010). As a result, planar gradiometers are less sensitive to distant sources making them ideal for reducing environmental noise and most sensitive to sources directly beneath them (Garces, 2017). Though it is suggested that equivalent information can be gathered by both sensor types to a degree (Garces, 2017) many MEG systems contain both types of sensors in hopes to capture a combination of focal and widespread sensitivities (Elekta Neuromag Oy, 2017). These sensors are then placed into a helmet array under which the subject sits.

Due to the numerous tools needed to digitally modify raw MEG & EEG data to produce brain signals that reflect specific activity, many analysis pipelines and packages have been developed. MNE-Python is an open source academic software package that provides a complete set of algorithms for use in various analysis pipelines. It allows data to be transformed between multiple data containers from raw data to evoked (averaged) objects and offers above average readability. MNE-Python provides a high level of reproducibility, allowing researchers to reproduce results on data using different machines while running an equivalent task. This coupled with its peer reviewed open source contribution process makes it a powerful analysis tool that will continue to develop new and improved methods of source analysis (Gramfort et al. 2014).

Spatial filtering methods via noise removal software are frequently provided by MEG manufacturers as well as source estimation software such as MNE-Python. High pass, low pass, or band pass filters are commonly used to remove artifacts and signals in unwanted frequency ranges (Taulu & Hari, 2009, Gramfort et al. 2014). Temporal Signal Space Separation or TSSS,

is another tool used to reduce environmental noise. TSSS works by separating magnetic sources from inside the sensor helmet array, and those originating from outside of it. The temporal patterns of internal and external signals are compared to remove artifacts that may contribute to both magnetic fields (Taulu & Hari, 2009).

Independent Component Analysis (ICA) is also used to denoise the MEG signals. ICA works by separating artefacts that are embedded in the data and simultaneously reconfiguring the signals of interest once removed. By setting specific thresholds, ICA is able to remove signals outside of expected brain activity strength. Artefacts arising from saccadic eye movements, blinks and heartbeats are large enough to interfere with temporal, frontal, and occipital sources so removal ensures accuracy of localization (Bardouille, Picton, & Ross, 2006; Fatima, Quraan, & Kovacecic, 2013; Gramfort et al. 2014).

A set of source localization algorithms have been developed to find anatomical correlates of brain activity. One popular method is a form of spatial filtering known as beamforming. Beamformer's are able to localize an area of cortex as the source generator by applying a weighted sum of the data at each site based on minimizing output constrained in a linear manner. This prevents regions that generate large neural power from exhibiting too much noise. The result is a minimizing of activity at all other areas without the need for prior source information (Van Drongelen, Yuchtman, & Van Veen, 1996; Van Veen et al. 1997, Brookes, Gibson, & Hall 2004).

Dynamic Statistical Parametric Mapping (dSPM) is an analysis technique used to combine information from other neuroimaging technologies such as fMRI and PET that contain subject specific anatomical and physiological information to produce better spatiotemporal estimations of source activity. This was achieved by normalizing noise sensitivity of activity

estimates in each area to produce statistical measures regarding the accuracy of the brain signal at the area of interest over time (Dale, Liu, & Fischl, 2000).

Further developments that anatomically separate the brain into discrete areas via a sulco-gyral parcellation have added further depth to localizing to functional brain areas (Fischl, Van Der Kouwe, & Destriuex, 2004). More recently a database for the parcellation of the entire cortex based on sulcal and gyral cortices which depend on the values of the local average curvature reconstructed from the cortical surface output of several subjects has granted researchers an easily adaptable cortical based model that surpasses surface-based inflations in regards to accuracy (Destrieux, Fischl, & Dale, 2010).

The result of the amalgamation of all of these scientific instruments is a technique that allows clinicians and researchers to obtain brain activity recorded in its natural state. The temporal resolution of an MEG/EEG recording is in the millisecond range, and while it does not possess the spatial resolution of MRI techniques it is free from the haemodynamic changes undergone during blood oxygenation level dependent changes as what is typically measured in the latter method (Baillett, 2001). MEG's advantage over the cheaper and less convoluted methodology of EEG is that the electrical currents produced by the cortex during EEG are more difficult to localize. Magnetic fields emitted by brain activity are not changed when passing through biological tissues, as the magnetic permeability of these tissues is virtually identical to empty space (Singh, 2014). Electrical currents measured on EEG must account for the conductive properties of the brain, cerebrospinal fluid, skull and scalp distorting the electrical potentials. The estimation of the head's conductive properties in attempt to localize a source of electrical currents in the brain is known as the "forward problem", in which we are estimating the results in the context of specific parameters (Gencer & Acar, 2004). Studies involving

planting electrodes directly onto the surface of the brain produce an electrical potential with higher amplitude, more rapid decay, and a more accurately localized dipole but are too invasive for the average research endeavor (Van Der Broek, Reinders, & Donderwinkel, 1998). This exemplifies the conductivity hurtle EEG must overcome as these cases allow for fewer assumptions regarding homogeneity of conductive layers and a more accurate representation of the head shape. The presence of ventricles and other significant anatomical landmarks can produce errors on EEG dipole localization up to 1.5 cm, while these differences are reduced in MEG recordings (Van Der Broek et al. 1998). While the magnetic fields measured by MEG are not affected by tissue conductance, we must instead primarily compensate for the "inverse problem" which is in this case, the estimation of the properties of the neuronal currents that generated the signals in the brain (Baillett, 2001). This is oft described as an ill posed question as the number of sources that could produce electromagnetic fields outside a volume conductor ie 'head' has an infinite number of possible solutions (Baillett, 2001). Orientation of sources also has an effect as to how they are represented on MEG & EEG. Radial dipole sources, as well as sources that are located near the center of a sphere model emit no magnetic field and are unable to be captured by MEG (Cohen & Cuffin, 1983). Thus MEG is only able to see sources located in sulci and not gyri. Further, MEG and EEG have a preferred orientation of localization that is approximately 90 degrees apart and while MEG is able to localize its source in its most sensitive direction better than EEG, it is only by a minuscule amount (Cohen & Cuffin, 1983).

While both methods have their limitations they are commonly used as complementary techniques. When used simultaneously each modality provides information that the other lacks making them a useful complement in both scientific and clinical settings.

2.7.2 Vision & Neuroimaging

Vision-based MEG research is relatively scarce in the literature compared to other sensory modalities and studies on epilepsy or attention, but has nevertheless built upon the foundational knowledge primarily by supplementing other neuroimaging findings. Invasive studies on primates and other animal models have outlined the functional boundaries of visual system processing (Tsao, Conway, & Livingstone, 2003; Hubel & Wiesel 1959), while MRI and other neuroimaging methods have assisted in the mapping of human visual centers in the presence of dynamic visual parameters (Avidan, Harel, & Hendler, 2002). Studies have moved beyond linking visual areas delineated by preferred stimulus and have accomplished outlining maps of higher order visual attentional centers such as the posterior parietal cortex, frontal eye fields, and dorsolateral prefrontal cortex (Hagler, Rieke, & Sereno 2007). These endeavors are improved by the use of MEG due to its advantage in temporal resolution over fMRI. The retinotopic organization of V1 has been previously confirmed using multiple equivalent dipole analysis in several EEG studies (Di Russo et al. 2005), MEG allowed the specificity of source areas to be reduced to a smaller patch of cortex. Ahlfors, Ilmoniemi, & Hämäläinen (1992) used pattern onset checkerboard stimuli presented at a foveal angle in quadrants then analysed using two source estimates; an equivalent current dipole model, and the minimum norm estimate (MNE). MNEs calculated showed a distinct symmetry between left and right visual fields with current direction changing in a retinotopic manner, with parafoveal responses localizing superiorly. Since then retinotopically-constrained source estimation methods which allow for multiple source estimations for time courses affected by more than one visual area have been developed. This model is able to determine source areas by fixing MEG source areas and orientations based on subjects MRI retinotopy and surface tessellations. This allows for solving

of multiple visual field locations simultaneously so long as amplitude does not vary significantly across the field. Such a technique reduces the amount of error caused by closely located dipoles interfering with one another from neighboring cortical areas (Hagler et al. 2009). Source localization of visually evoked magnetic fields (VEFs) have produced sources similar to those found using EEG. The N75, P100, N145 responses have been found to localize in V1 around the Calcarine fissure using quadrant PR stimuli (Shigeto, Tobimatsu, & Yamamoto, 1998; Nakamura, Kakigi, & Hoshiyama,1997). Other studies have demonstrated extra striate origins suggesting that pattern onset evoked potentials may arise from multiple visual generators (Hall, Holliday, & Hilllebrand, 2005; Matsumoto, Nagamine, & Matsuhashi, 2004).

Visual paradigms for MEG have demonstrated that changes to the psychophysical parameters produce changes similar to those found on EEG. Changing check size of PR VEP stimuli produces increases in P100 amplitude when increasing from 15' to 120', further increases attenuate amplitude. Changes in inter-stimulus interval (ISI) indicate that shorter reversal times such as 0.16 & 0.18 seconds produce the largest P100 amplitude, with attenuation at longer ISI's (Chen et al. 2005).

Ophthalmological considerations have determined that PR VEP P100 amplitudes are diminished and latency is increased with the introduction of +1 to +4 diopter lenses, with the strongest lenses having the most significant effect (Suzuki, Nagae, & Nagata, 2015). Likewise EEG studies report a reduced PR VEP amplitude with the introduction of both minus and plus lenses attributed to retinal blur (Collins, Carroll, & Black, 1979; Sokol & Moskowitz, 1981). Studies involving amblyopia and MEG have shown that amblyopes have reduced bilateral activity in the occipital cortex as well as modulated parietal activity at 250 ms after stimulus onset compared to normal. Beamforming revealed a different pattern of activation between

striate and extra striate areas in amblyopes compared to normals (Cortese, Wong, Goltz, Cheyne, & Wong 2009). Amblyopic eyes have lower Global Field Powers (spatial standard deviation that quantifies the amount of activity by time) when exposed to isoluminant sinusoidal gratings. Due to previous work indicating that the parvocellular pathway is more affected than the magnocellular projections in amblyopia in animal studies (Horton & Hocking, 1997), this could lend support to a processing issue in the parvocellular pathway in extra striate areas (Anderson, Holliday, & Harding 1996). Earlier fMRI studies imaging ocular dominance columns support this as amblyopes have reliable if not reduced V1 activation but lower activity in V2, V3, V5 compared to normal subjects (Anderson & Swettenham, 2005). A study performed in 1999 by Anderson, Holliday & Harding using equivalent current dipole modeling on strabismic amblyopes presented with isoluminant sinusoidal gratings again demonstrated that amblyopes have longer latencies and reduced amplitudes with dipole localization at the V1/V2 border. The authors speculated that it could be that the dipole fit only represents the "center" of the surrounding activity which could involve other visual processing areas, nonetheless it implies that there may be dysfunction at the level of V1.

Chapter 3: Methods

3.1 Research Design*:*

This project employed a quasi-experimental design using Electroencephalography and Magnetoencephalography investigations in normal adult subjects. Two visual stimuli were used under 3 different conditions. The stimuli used included a 25 x 25 degrees pattern reversal checkerboard with individual checks subtending 32 minutes of arc, reversing at a rate of 1 Hz at 50% contrast and overall luminance of 30 cd/m^2, as well as a diffuse unpatterned white field (60 cd/m^2) in alternation with a black one at a rate of 1 Hz. Both stimuli were presented at 1 meter. The three viewing conditions used in this experiment were: binocular, monocular and asymmetric (1.8 log unit neutral density filter placed in front of the dominant eye). Inclusion/exclusion criteria for the participants can be found in table 1.

Table 1: Participant inclusion and exclusion criteria

	Inclusion Criteria	Exclusion Criteria
General	• Between the ages of 18-65. • Cognitively and physically able to perform the Orthoptic screening and MEG data collection, and able to remain in MEG magnetically shielded room for duration of collection. • Physically healthy.	• Presence of metallic foreign bodies (dental fillings, piercings, metallic implants, or medical devices) , inducing significant noise on sensors. • Lack of consent. • Inattentive behavior during data acquisition.
Eye Health	• Normal Binocular status, 40" stereoacuity, with uncorrected visual acuity better than or equal to 6/7.5 OU	• Presence of ocular misalignment. • Manifest or latent nystagmus.

3.2 The Sample*:*

3.2.1 Study Population

A total of 13 subjects were screened for participating in the study. Of these, 2 were deemed unfit based off of subpar uncorrected visual acuity and the presence of magnetic noise outside of normal range. The initial first 3 participants were pilot subjects, 2 of which underwent stimulus paradigms that differed from the final project's methodology (reversal rate & check size were adjusted) and as such were not included in the final analysis. The third pilot subject had EEG recordings included, and this led to the EEG protocol adoption for all the subsequent subjects (n=8) who were investigated with the final protocol; the reversal rate used was slightly different then the reversal rate used for the remainder of the study, however, results were directly comparable and these results were deemed fit to be included in the final analysis.

3.2.2 Statistical Power:

Using results generated by the Smith (2013) pilot study, variability and mean PR VEP's using a 1.8 log unit ND filter produced an average amplitude of 0.743 ± 0.153μV (mean and SD) in normal subjects. An effect can thus be demonstrated with a statistical power of 0.90 with the use of as few as 6 subjects.

3.2.3 Recruitment of Participants:

Participants were gathered for this study by word of mouth between the months of June 2018 and August 2018. Several participants were recruited from a pool of members within BIOTIC (Biomedical Translational Imaging Centre) at IWK Health Centre who had previously

taken part in Magnetic Resonance Imaging research studies. Interested members were contacted by email by the investigator.

3.2.4 Risk & Benefit Analysis:

Subjects were informed that all forms of EEG and MEG recordings are non-invasive and do not pose any threat of harm. The only potential risks in taking part of this project would be a slight skin irritation from the electrode placement and preparation, or irritation from the adhesive patch applied during the monocular stimulus viewing portion of the paradigm. Any results that were obtained and deemed abnormal were to result in that participant being referred to the Ophthalmology fellow at the IWK Health Centre. No such measures were required to be taken.

3.2.5 Ethical Considerations:

Ethics approval was obtained from the IWK Health Centre Research Ethics Board. As mandated by the board, all participants were fully briefed of the studies purpose and methods and informed consent was obtained by the principal investigator himself. Copies of provided information & consent forms can be found in Appendix B & C.

3.3 Experimental Procedure

3.3.1 General Protocol

Once participants confirmed their interest in taking part in the study, information on the purpose and methodology of the study was dispensed before consent was obtained. From here, a general orthoptic workup was performed while confirming that the subject did not have any metallic foreign bodies in their head or abdomen. A 2 minute noise evaluation was done by

having the subject sit in the MEG to ensure that there were no additional sources of noise present before the subject was prepped for the scan and to ensure the subject was comfortable in the enclosed environment of the MEG apparatus.

3.3.2 Orthoptic Assessment

During the orthoptic assessment, participant's age & sex were recorded. All testing was done without the use of corrective lenses as no metal can enter the MSR without causing significant distortion on the MEG signal. Distance visual acuity was obtained using an Early Treatment Diabetic Retinopathy Study (ETDRS) chart (Precision Vision, La Salle, Illinois, USA) calibrated for 2.43 m (8 ft). Visual acuity was scored monocularly as well as with both eyes open. Binocularity was assessed using a Titmus stereoacuity test (Stereo Optical Co., Inc. Chicago, Illinois, USA) performed at 38 cm. Ocular alignment was determined by having the subject fixate on a 6/12 sized letter at near (1/3m) and distance (6m) and an alternate prism cover test was performed. Dominant eye was identified by having the subject line up his thumb with a letter on the vision chart with both eyes open as well as making a circle with his hands around an object in the testing room and seeing which eye was on the principle visual axis when either eye was closed.

3.3.3 Electroencephalography:

EEG was recorded simultaneously during MEG data acquisition. Electrode placement followed the 10/20 system convention. Head circumference was first measured to determine proper cap size. The distance from each pre-auricular point was measured with the midpoint landmarked, then the distance from nasion to inion was measured and the midpoint landmarked.

At the intersect of these two distances the Cz channel was placed, and remeasured after EEG cap (EasyCap Med. 52-58, Herrsching Germany) placement as seen in Figure 11. After cap placement, Oz was also measured to ensure that it was approximately 2 mm above the subject's inion. Twenty-five of the 64 electrodes in the parietal and occipital regions from TP9 to Oz, as well as a reference electrode placed on the nose were then filled with electrode gel (ECI Electro-Gel, Electro-Cap International Inc. Eaton, Ohio). A blunt syringe (16G$^{3/4}$ Blunt Square Grind, Becton Dickinson, Franklin Lakes, NJ) was used to move hair out of the way and lightly scratch the scalps surface to ensure proper impedance would be attained (<5MΩ). Finally, a surgical elastic (Surgilast, Glenwood Lab. Oakville Ontario) was then placed around the EEG cap to ensure that electrodes remained in place and in close contact with the scalp.

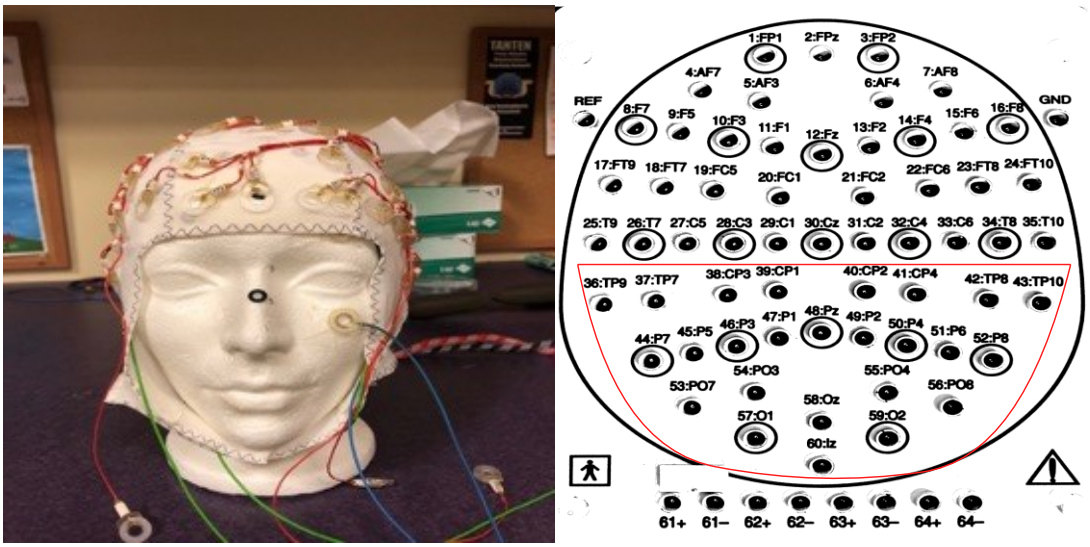

Figure 11: On the left electrode placement example. EEG cap placement with EOG's for horizontal eye movement detection are hidden under the cap, vertical EOG can be seen above and below the left eye. On the right is an EEG channel schematic, the posterior channels circled in red, were used in this study.

3.3.4 Magnetoencephalography:

Electrooculograms (EOG) and electrocardiograms (ECG) are also recorded for the purpose of noise removal from the acquired brain signal. Two horizontal electrodes were placed next to the lateral canthi of either eye to detect and remove eye movements. One electrode was placed above the left eye and one below the left eye to detect and remove blinks and vertical eye movements. For the removal of heart beat artefacts, one electrode was placed on the inner bicep just above the elbow near the brachial artery of each arm. Finally, a grounding electrode was placed on the left clavicle. Places on the skin where the electrodes were to be placed were first cleaned with Nuprep (Weaver & Company, Aurora, CO) and rubbing alcohol before applying the electrode filled with electrode cream (Elefix EEG paste, Nihon Kohden America Inc. Irvine, CA) and taping them down using Tegaderm Film (3M, St. Paul, MN). Once electrodes were in position, four HPI (head position indicator) coils were used to determine the subjects head placement and movement throughout the scan. These coils were placed behind either ear and at the left and right temples of the face. The subjects head shape was then digitized using the Polhemus Isotrak system (Polhemus Inc., Colchester, USA) to provide a head model for source localization. Approximately 200 points were obtained to ensure an accurate representation for co-registration including the two pre-auriculars and the nasion for easy identification. MEG data was recorded using a 306 channel MEG system (Elekta Neuromag Oy, FL).

3.3.5 Stimulus Presentation:

Stimuli were presented at a distance of 1 meter from the participant using a projector (Panasonic PT 7700, Osaka, Japan) located outside the MSR, which projected through a glass covered hole reflected onto a screen via two angled mirrors. Luminance was controlled via a

light dimmer to ensure the proper conditions before closing the subject in the MSR and beginning recording. To ensure strict timing of the stimuli for event-related analysis, the timing and order of the stimuli were recorded continuously with the MEG data using Presentation software (Neurobehavioural Systems Inc., Berkeley, CA, USA).

Stimuli consisted of a PR checkerboard with a 32' check size, as calculated using:

$$a=\tan^{-1}(W/2D)*120$$

Where a is the visual angle subtended in minutes of arc, W is the width of the stimulus in mm, and D is the distance from the stimulus in mm. Pattern elements were 32' or 10x10mm in size. The checkboard was 17.5"x17.75" approximating a visual angle of 25x25°. A small 2x2" white square was included offset to the side of the checkerboard in the subject's periphery as well to ensure proper stimulus timing via a photodiode circuit. PR stimuli checks consisted of 32x32 pixels at 100% contrast with a luminance of 130cd/m^2 (white) & 5cd/m^2(black). PR VEP stimuli can be seen in figure 12.

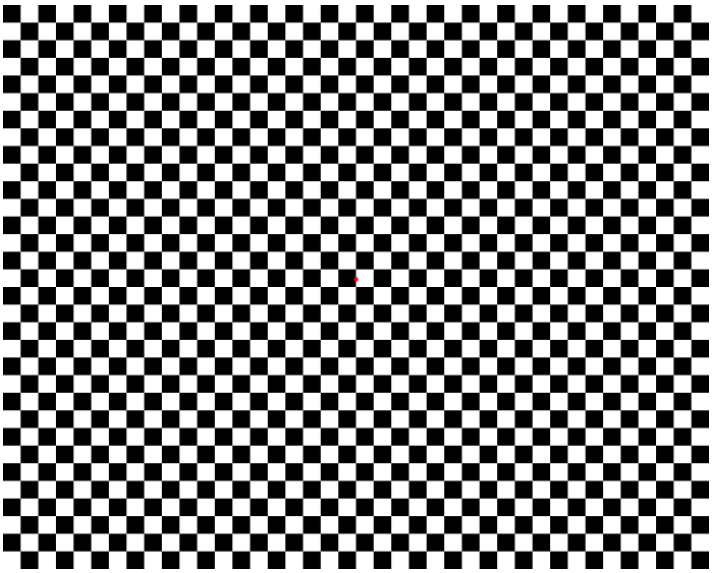

Figure 12: Example of the pattern reversal 32' checkerboard stimulus used for this paradigm, fixation target is the red dot in the center. A small 1 Hz blinking white check was located below the stimulus to ensure proper stimulus timing.

Unpatterned stimuli consisted of a diffuse white flash that encompassed the entire 25x25° at the same luminance level of 130 cd/m^2. All stimuli reversed at 1 Hz, (one full reversal in 1 sec) with unpatterned stimuli presented with 10:500ms (white to black) reversal rate. There was a minor 34 millisecond delay present in our recordings due to a delay in the speed of our projector after receiving the event (reversal) trigger from our presentation software. To account for this a small white square with an identical reversal rate of 1 Hz was added to the stimulus. This square was far from the checkerboard and partially occluded by a photodiode array made by the Psychology & Neuroscience Workshop at Dalhousie University. The photodiode was connected to the MEG via a coaxial cable and assigned to a miscellaneous channel. This allowed us to compare the stimulus trigger timing to the photodiode's change in current, which was consistently 34 ms after the event occurred.

3.4 Data Collection

3.4.1. Recordings:

Once the participant had undergone EEG/HPI coil placement preparation and head shape digitization, they were led into the MSR and seated in the MEG. EEG cap and HPI coils were connected the MEG and EEG channel impedance was checked through Neuromag's Acquisition software (Elekta Neuromag Oy, FL). When impedance was acceptable, the subject placed their head into the MEG helmet until the top of their head comfortably made contact with the inside surface of the helmet. Data was collected in randomized blocks determining which viewing condition the subject would begin with (binocular, monocular, filter). Within each block 6 recordings were performed, 3 PR VEP/VEF as well as 3 unpatterned flash recordings. The order of these recordings was assigned at random. Each unpatterned recording was approximately 55

seconds in length, with PR recordings being approximately 105 seconds. The total recording time for each block was approximately 10±2 mins, for a total of approximately 34 mins of total recording. Subjects were instructed to maintain fixation on the red fixation point for PR stimuli, and to blink as needed to avoid lapse in concentration or focus. During the monocular viewing block, an adhesive eye patch (Dynamic Diagnostics Inc. Plymouth MI, USA) was applied to the dominant eye for the duration of the recordings. During the asymmetric viewing block, an Optical Polymer Neutral Density Filter (Rangers, Shenzhen, China) measured to be 1.5 log unit in strength was held affixed to the top of the helmet using adhesive sticky tac in front of the dominant eye such that it did not impede on the visual field of the non-dominant eye. During the recording process the patient is enclosed in the magnetically shielded room, and monitored via video and audio by a camera positioned on the ceiling.

3.4.2 Data Processing

The Elekta magnetometer saved data in a .fif format that embedded a data section, as well as stimulus events, and sensor's localization parameters. The MNE environment (Gramfort et al. 2014) was used as the data analysis framework. The MNE environment relied on the Python 3.5.5 open-source programming language, which was deployed through the Terminal emulator included in macOS (version 10.14.2) or through the Spyder open-source cross-platform integrated development environment (IDE; version 3.3.1) under the control of the Anaconda Navigator package management system (version 1.9.6).

Within the MNE environment, the raw .fif data was initially preprocessed using Maxwell filtering, which used TSSS (Temporal Signal Space Separation) to analyze the

fundamental properties of bio magnetic fields and harmonic function expansions to separate the magnetic signals into three discrete components. These components are:

b_{in}: Brain signals originating inside the sensor array(S_{in}).
b_{out}: Noise signals originating outside the sensor array(S_{out}).
n: Noise/artefacts generated by the sensors located close to the sensors(S_T).

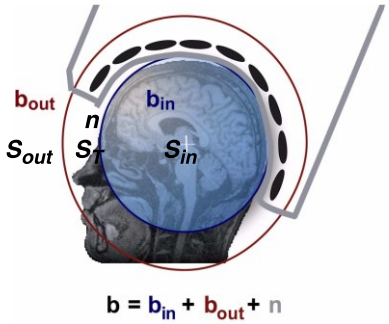

Figure 13: Geometrical representation of Maxwell filtering, separating brain signals within the helmet array from those emanating from the brain.

Magnetic interference is reduced by neglecting the b_{out} & n components as seen in Figure 13. This spatial filter allows for the suppression of external interference (radio waves, power lines, elevators etc.), and the addition of a temporal extension allows for suppression of internally located noise (metal objects, dental implants, stimulators etc.). Automatic bad channel detection is used following spatial filtering techniques to remove any channels by reconstructing the inside and outside signal and taking the difference between these, any channels exceeding the expected white noise generated by the SQUID sensors are automatically removed.

Following this, raw data channels were inspected manually to ensure no noisy/bad channels were missed by 'Autobad' removal software (Figure 14).

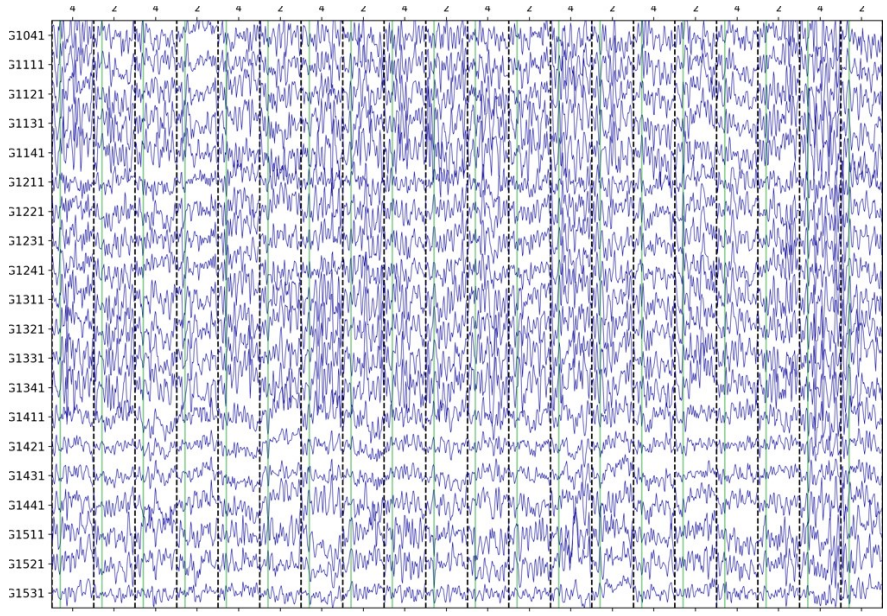

Figure 14. Example of continuous raw data (MEG signal, with stimulus events marked as vertical dashed lines) from one subject, after Maxwell bandwidth filtration and TSSS removal of artefacts related to extraneous sources such as eye movements and heart activity.

A Power Spectral Density spectrum plot (PSD) was produced to ensure that no uniform frequency present during the recording was interpreted as data. The data is then filtered using a 40 Hz low pass filter, and resampled from 1000 Hz to 250 Hz for ease of analysis.

Further artefact removal was done using ICA to remove eye movements, blinks and heartbeats from the signal to produce the final clean version of the raw data as seen in Figure 15.

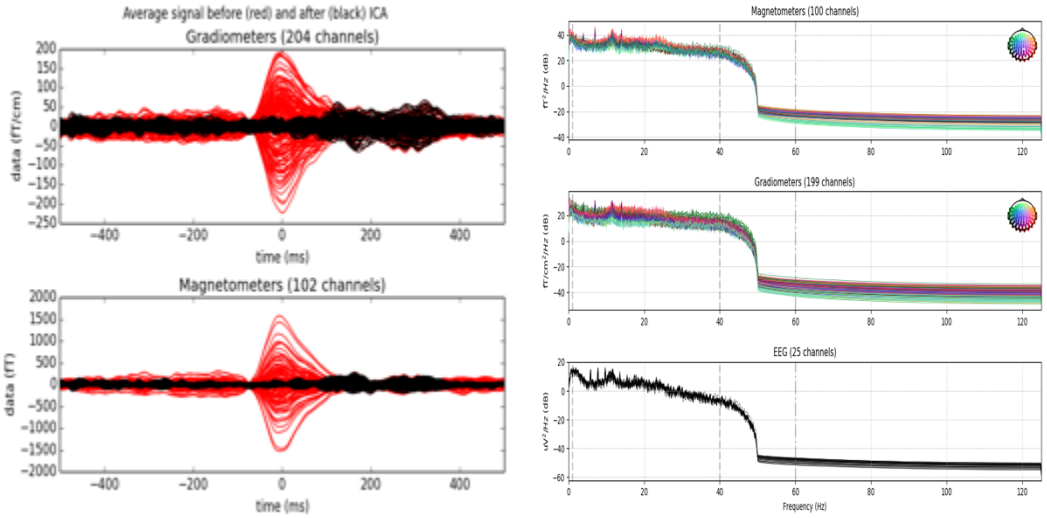

Figure 15: On the left is an example of noise reduction following ICA, with the original Max filtered data in red, and the remaining brain waves in black. On the right is a PSD curve demonstrating the distribution of activity at different frequencies in dB scale.

3.5 Data Analysis

Data analysis can be subdivided into 3 categories, sensor space MEG, source space MEG, & EEG data analysis. Sensor space data is that which is gathered directly from the recording after preprocessing and averaging. These waveforms represent the averaged amplitude in fT (femtoTesla, magnetic induction at the order of 10^{-15}) & fT/cm, with respect to time for the appropriate sensors. EEG data was similarly compared at the sensor level. Source level analysis was done using MNE-Python's built-in tools and is described in more detail below in Figure 16.

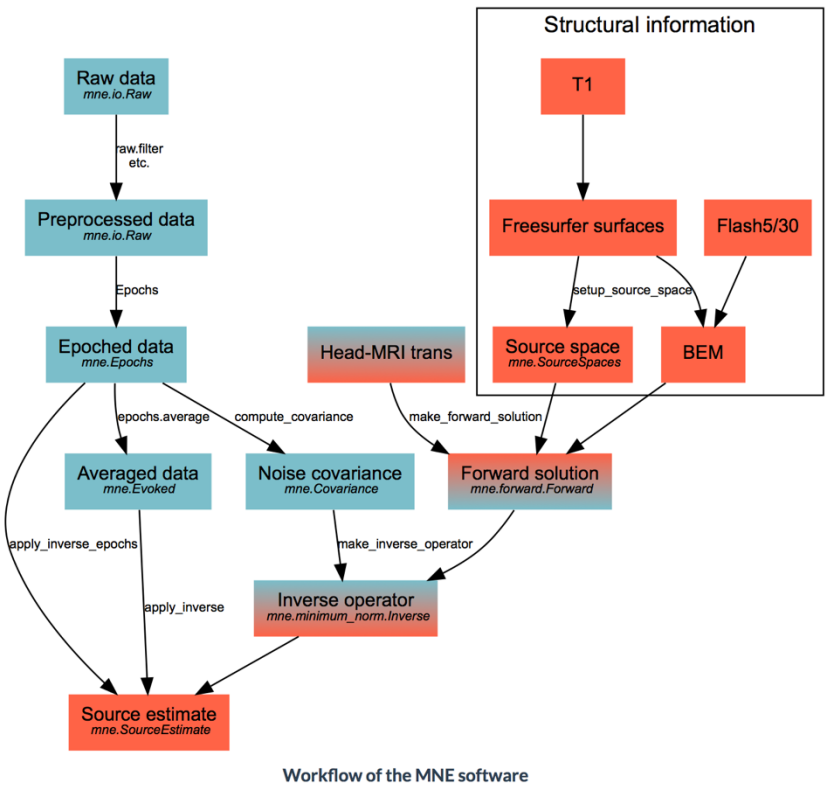

Figure 16: Typical MNE workflow for raw data processing & extracting structural information from MRI's to produce a source estimate (Adapted from Gramfort et al. 2014).

3.5.1 Sensor Space Analysis

Data was analyzed in typical visual evoked field fashion. Data was epoched between -0.100 to 0.400 s around stimulus onset. At the specified sampling rate, a data point is produced every 0.04 seconds. PR stimuli consisted of two events (1 per image) with flash stimuli consisting of one event (only flash) averaged at the specified epoch length to create an evoked response that represents the average of all 200 events (reversals).

EEG & MEG sensor data was analyzed in a conventional VEP fashion. The largest peak amplitude (μV for EEG, fT for MEG) was measured by producing a dataframe for each recording and taking the difference in amplitude between component peaks/troughs. For example, to measure the amplitude at P100 the following measurements were made: measured

the minimum amplitude at 70 msec (a), the maximum amplitude at 100 msec (b), the minimum amplitude at the 150 msec (c) component. The amplitude (μV) was then calculated using:

Condition component amplitude (μV) = (b-a)+(b-c)

$$Binocular\ Summation\ Ratio = \frac{Binocular\ component\ amplitude\ (\mu V)}{Monocular\ component\ amplitude\ (\mu V)}$$

$$Binocular\ Inhibition\ Ratio = \frac{Filter\ component\ amplitude\ (\mu V)}{Monocular\ component\ amplitude\ (\mu V)}$$

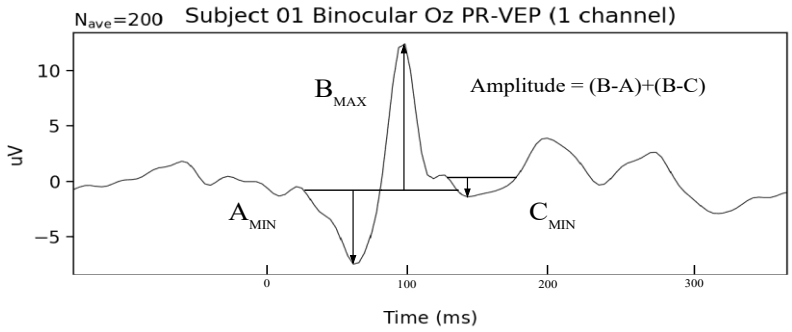

Figure 17: Example of how amplitude measurements were determined for components in EEG.

Binocular summation and inhibition ratios are used so that we can easily compare the relative amplitude of components between conditions to detect whether or not they are higher or lower than a ratio of 1, which represents the monocular level of activity. Component amplitudes were then averaged at each electrode position for each condition and a grand average was estimated over all subjects. Summation ratio's (binocular/monocular, filter/monocular) were then calculated at all electrode positions by division and grouped by location visual (midline/occipital sensors) and non-visual (frontal/central sensors).

For the analysis of MEG data at the sensor level, evoked gradiometer data was run through a similar pipeline. A grand average was calculated for each condition across all subjects, root mean square values of the two planar gradiometer data from these averaged data

files was used to produce summation ratio values for sensors grouped by location in both visual/ parietal areas and frontal/central areas for comparison.

Global Field Powers (GFP; spatial standard deviation that quantifies the amount of activity by time) were used to map out the general morphology of the VEF response for each area of the head and identify important activity peaks. MEG data was then concatenated and correlated to a reference EEG component (EEG058:Oz) to determine if any channels accurately mirrored the activity seen in EEG.

3.5.2 Statistical analysis

Data from EEG and MEGs and, for each modality, pattern and flash evoked data were analyzed independently. Amplitude of the main positivity around 100 ms post stimulus was computed for both EEG and MEG data, while in the former, computation was also made for the positivity around 200 ms post-stimulus. Binocular to monocular and filter to monocular ratio were then computed in Excel spreadsheets and then exported to Stata (version 12.1; StataCorp, Texas, USA) for statistical analysis. Data from individual electrodes were combined into occipital and central/frontal subsets, yielding a 2(EEG/MEG) x2 Pattern vs flash) x 2 (occipital vs central/frontal) comparison scheme. First and foremost, each component of this 2x2x2 database was compared to the unity (values significantly superior to 1 suggesting binocular facilitation, values lower than the unity being considered as evidence for binocular inhibition); this was performed by One-Sample Mean comparison. Differences between occipital and non-occipital sets of electrodes as investigated using paired t-test, for each of the components measured (N70, P100 and N150 and P200 for EEG; P70, P100 and P150 for MEG gradiometer responses), as well as differences for each of these components between pattern and flash

responses. Finally, whether all components were equally influenced by the viewing conditions was analyzed using a One-Way ANOVA. Because of the small sample size and the likelihood of non-conformity to normally distributed data, significance level for each parametric analysis was confirmed using non-parametric Sign-test for matched pairs and Wilcoxon rank-sum test. When appropriate, significance level was adjusted for multiple comparisons.

3.5.3 Source Space Analysis:

Data was then run through a source estimate pipeline that can be seen in Figure 18 below. In order to visualize a source estimate in the brain, a structural model must be co-registered with the participants Isotrak data so that both datasets exist in the same co-ordinate system. Some participants had an existing T1 MRI taken during other research opportunities that was used for this purpose. For those without an existing MRI, FSaverage – an averaged brain provided by FreeSurfer (Martinos Center, Mass. USA) was used in its place. Co-registration was done based on three primary fiducials, the left/right preauricular, and the nasion, as well as the additional landmarks produced by the scalp during digitization.

In order to calculate the forward solution & inverse operator, a noise covariance matrix was calculated and boundary element model (BEM) meshes produced to separate regions by conductivity. A dynamic statistical parametric mapping (dSPM: statistically reliable temporal activity maps) source estimate is then produced for each evoked data file. These source estimates are then averaged per subject for each condition and a grand average of each condition across subjects is produced. In order to compare coordinate-based activity in a grand average of all subjects using different co-registered models, the dSPM maps were then morphed onto the FSaverage brain.

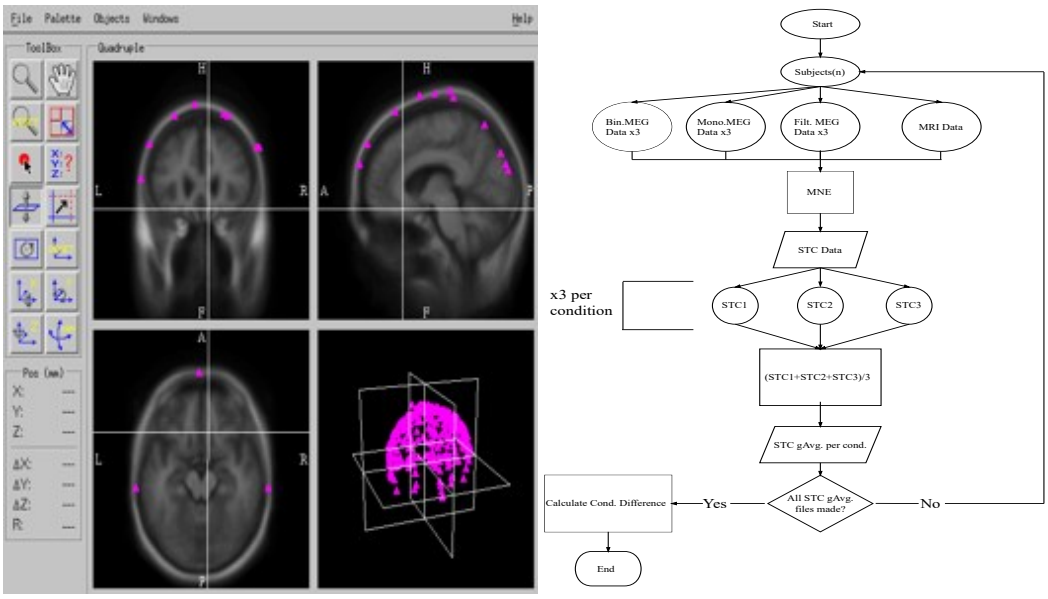

Figure 18: An example of MRI/MEG co-registration (left) and a source estimate processing pipeline (right).

Following this, grand average source estimates were compared at significant time points gathered from evoked waveforms and GFP's and the difference between conditions was determined by subtracting the binocular and filter source estimates from the monocular one rather than using the BM and FM ratio as in the statistical inference, as ratio based on non-adjusted time series could yield erroneous values. This latter analysis was performed for temporal visualization only; no statistical inference was performed at that level.

CHAPTER 4: Results:

4.1 EEG Data:

The data collected by the 306-channels Elekta Neuromag MEG system was in the form of continuous data acquisition; 25 EEG channels, 102 magnetometers and 204 planar gradiometers, 2 electrooculograms channels, one electrocardiogram, as well as one for the stimulus trigger generated by the Presenter system and one for the timeline (depending on the sampling frequency). The data presented in this thesis are all grand-average evoked data from the 8 normal subjects included in this study, unless otherwise stated. The grand-average data for the 25 EEG sensors are presented in Figure 19 in the evoked.joint-plot format generated by the MNE environment, for the three conditions tested (each consisting in concatenation of three randomly-presented acquisitions). The bottom part of each panel displays the individual evoked data around a stimulus change (t=0), with pattern-reversal on the left and flash stimulus on the right. The individual evoked responses are color-coded according to location, corresponding to the insert on the upper-left of the panel. On the top part of each panel are two-dimensional topographical maps corresponding to the strength (scale bar on the right side) of the activity for a specific time (or peak waveform) of the evoked data.

4.1.1 PR VEP Grand Averages

Evoked potential amplitudes are highest in the grand average of the binocular viewing condition, for all components. The channel with the largest amplitude is EEG channel 58 which corresponds to position Oz, which has an amplitude of 9.93 μv at 0.100 second. The monocular PR grand average had a maximum amplitude of 6.73 μv at 0.100 at Oz, while the Filter PR

condition produced an amplitude of 2.648 µv in Oz at 0.100 sec. The Filter PR VEP had its maximum amplitude slightly later in the time course at 4.05 µv at EEG channel 57 (O1) occurring at 0.118 sec. It is at this point that all channels appear to peak showing a increase in P100 component latency in the filter condition.

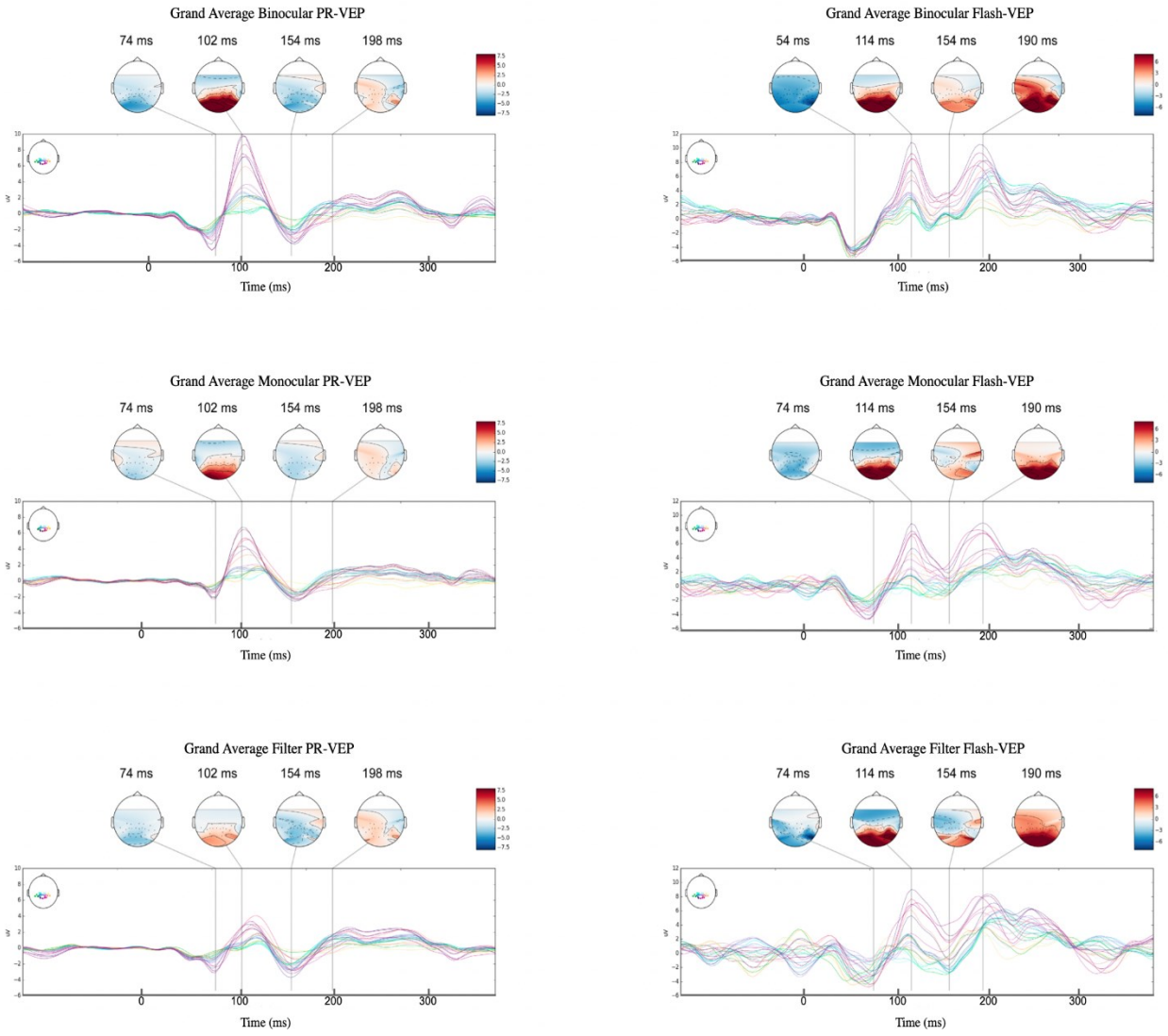

Figure 19: Grand average (n=8) of Pattern-evoked (left) and flash-evoked (right) EEG responses for the three testing conditions. Lower panels display location color-coded waveforms whilst the upper panels illustrate the topographical scalp distribution of the various peak components of the responses.

The two-dimensional topographical representations of the current dipole on the head reflect the activity seen in the waveform. Negative components N70 & N150 are strongest in channels nearest the occipital channels in the posterior. Similarly, positive components amplitudes are strongest in these same visual channels. At P200 the current dipole appears to dominate the left hemisphere in all conditions. This difference in surface distribution between N70 and P100 on one side and N150 and P200 on the other suggests they represent distinct cortical processing with dipole generators located in different region of the brain.

4.1.2 Flash VEP Grand Averages

Binocular flash responses produced the largest peak at 0.114 sec in Oz with an amplitude of 10.84 μv. The N70 component under binocular conditions had a maximum amplitude at an early latency of 0.054 sec. The monocular flash condition produced a maximum amplitude of 8.87 μv at Oz at 0.114 sec. The filter flash VEP produced a less uniform waveform on average, though components are conserved and identifiable. It produced a maximum amplitude of 9.02 μv at Oz at 0.114 sec. Unlike what was observed with the PR stimulus, a phase shift was not observed with the filter conditions.

Topographical maps for the flash stimuli show maximum activation in visually located posterior channels for each component, with a more diffuse distribution at P200, thus suggesting that the event happening at 0.200 sec with the flash stimulus does not correspond to the P200 obtained with the PR stimulus.

4.1.3 EEG binocular summation and inhibition.

In order to appreciate the respective contribution of binocular summation and binocular inhibition processes in the cortical integration of the evoked data, the amplitude ratio between components of the binocular and monocular conditions (BM) on one hand, and the filter and monocular conditions (FM) on the other hand, were computed for the first positive response (P100) and second positive response (P200) of the pattern-reversal stimuli, and the major positive response (P1) of the flash stimuli (Figure 20). On the left side are presented representative waveforms for the electrode positions referred to on the topographic maps (right hand-side); the top ones are from electrodes located on the midline in the anterior (non-visual, channel Pz) part of the brain, the bottom ones from a midline electrode from the occipital cortex (Oz). Binocular responses are in blue, monocular ones in orange and filtered ones in green. This convention will be kept consistent throughout all the figures.

The topographical maps display the results for the BM and the FM ratio. For the pattern-reversal P100 component, the BM ratio was uniformly superior to the unity, meaning that binocular summation was present in all of the electrode positions. For the FM ratio, binocular inhibition (ratio lower than unity) was concentrated at the occipital pole, while no difference between filter and monocular conditions could be observed in the more anterior electrode locations (ratio close to the unity). The filter condition, which is binocular, thus produced a P100 potential that was smaller in amplitude than the monocular one, corresponding to the definition of binocular inhibition. It is interesting to observe that the P200 component of the same evoked responses did not produce binocular inhibition and produced binocular summation that are of lesser amplitude.

For the flash stimulus responses, the binocular conditions produced a P1 component always larger than its monocular and filter counterparts, whilst the filter and monocular responses were generally of the same amplitude at the occipital cortex with the filter condition producing larger amplitude component in the more anterior part of the head. This qualitative interpretation of the data is supplemented by a more quantitative analysis found in section 4.3.

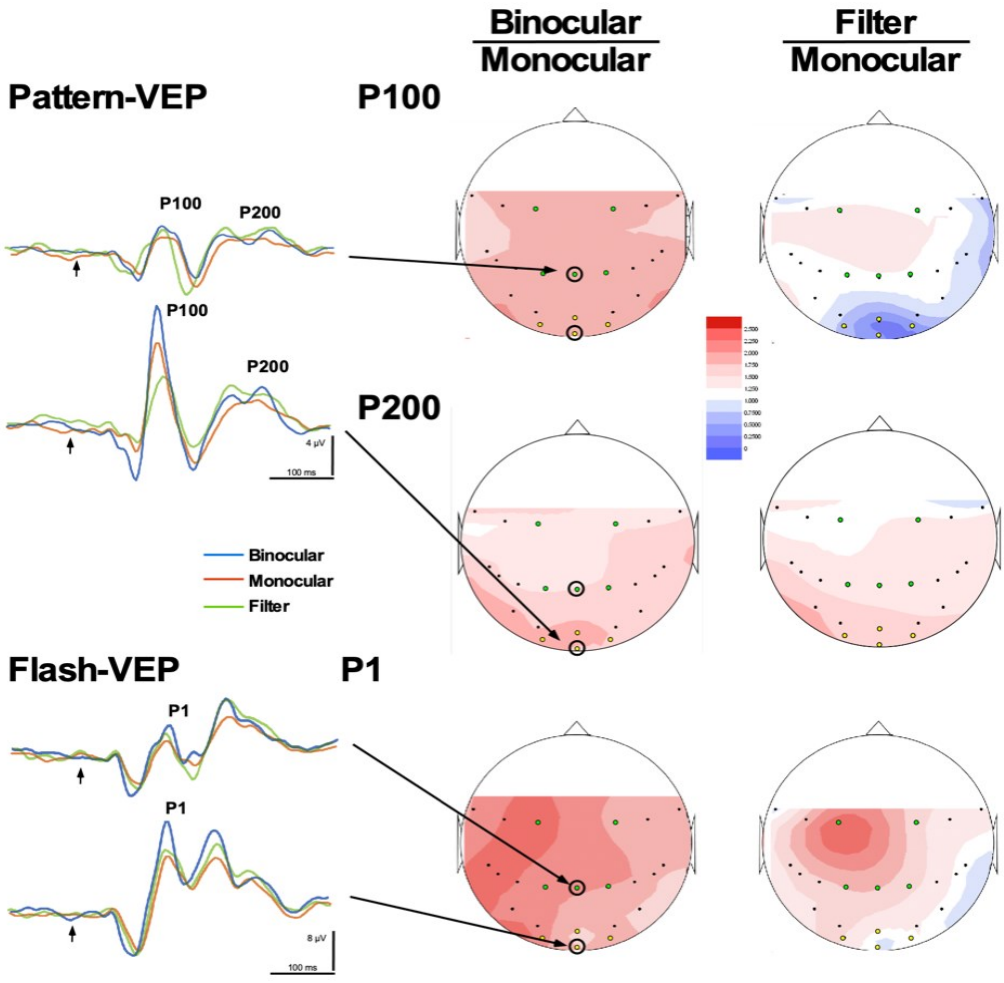

Figure 20. EEG data computation of the amplitude ratio between binocular and filter conditions versus monocular conditions for both pattern (P100 and P200) and flash (P1) responses.

4.2 MEG Data

Grand average MEG data can be seen for the pattern reversal and flash stimuli in Figure 21 & 22 respectively. The left side of each figure is presenting data from the gradiometers whilst the magnetometer responses can be found in the right hand-side. The presentation is the same as for Figure 19. By convention, the gradiometers lower panel is presenting all the planar responses (planar 1 and 2 being orthogonal) while the upper panel is presenting the square root of the summation of the square mean root of the two planar responses, yielding a topographical mapping with only positive components (scale is all red). The magnetometer responses are presented in the conventional way, with positive (red) and negative (blue) components.

4.2.1 PR VEF Grand Averages

Like for the EEG responses, gradiometer and magnetometer amplitudes do appear to differ substantially between conditions. Binocular recordings do appear to have the largest peaks at visual components in both the gradiometer and magnetometer data, with monocular conditions showing slightly reduced responses and filter amplitudes appearing with the smallest.

The two dimensional topographic representations of activity demonstrate a clear visual dipole at P100 in magnetometers that is strongest in binocular & monocular conditions and reduced in filter viewing conditions. Interestingly enough, this dipole seems to be weaker at the N150 but present again at P200. Gradiometer topographic maps also demonstrate a very strong visual response at P100 and P200, with activity mostly concentrated over the occipital lobe of the brain.

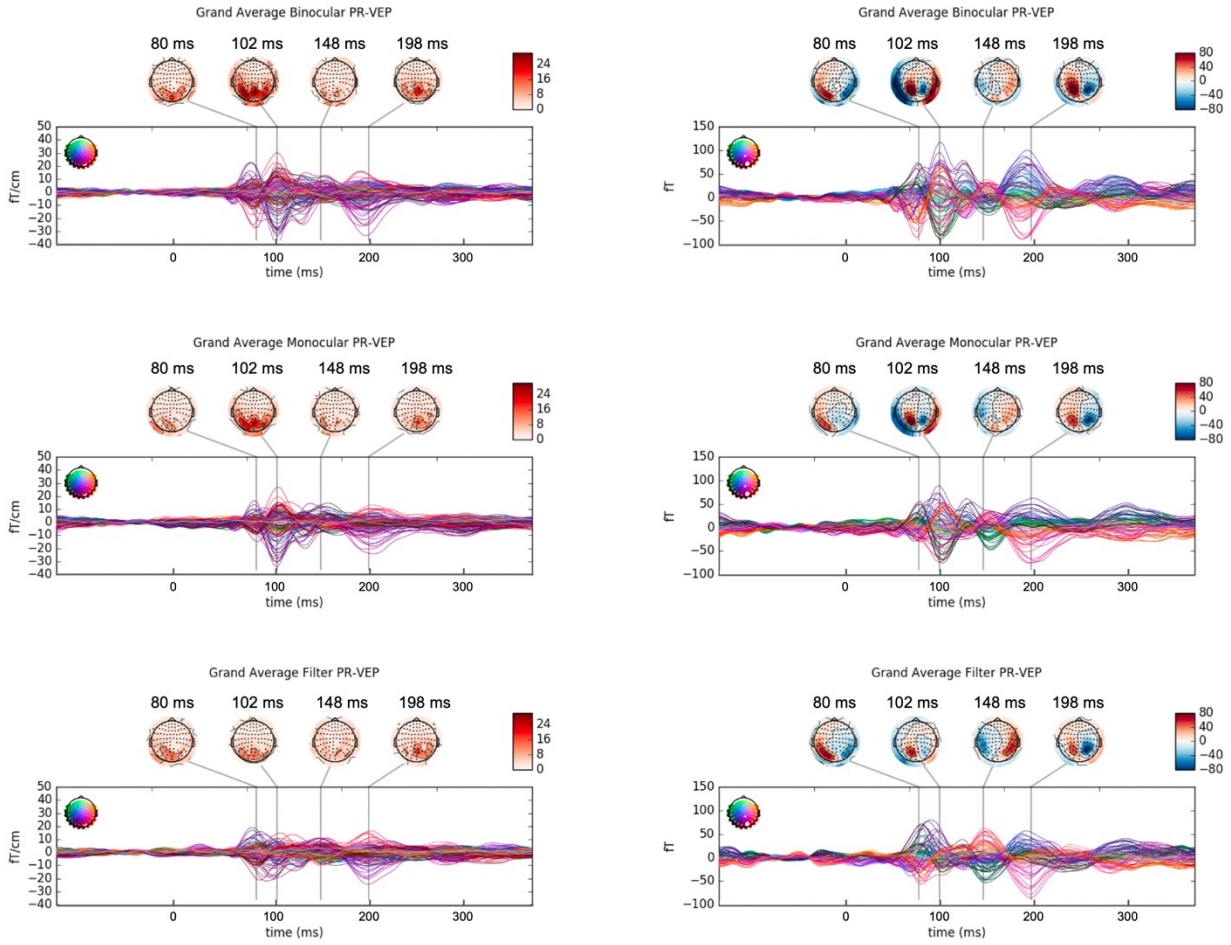

Figure 21: Grand average (n=8) of gradiometers (left) magnetometers (right) MEG responses for the pattern reversal stimuli, in the three testing conditions. Lower panels display location color-coded waveforms whilst the upper panels illustrate the topographical scalp distribution of the various peak components of the responses.

4.2.2 Flash VEF Grand Averages

Figure 22 illustrates the VEF produced from the flash stimuli. Morphology of these recordings appears to be remotely similar to morphology of the flash VEP waveforms. The difference between amplitude for each viewing condition is not immediately appreciable at a glance, with a few binocular channels exhibiting larger amplitudes but on average waveforms look similar between conditions within sensor types. Topographic plots do demonstrate some visually located activity at 115 & 170 ms time points.

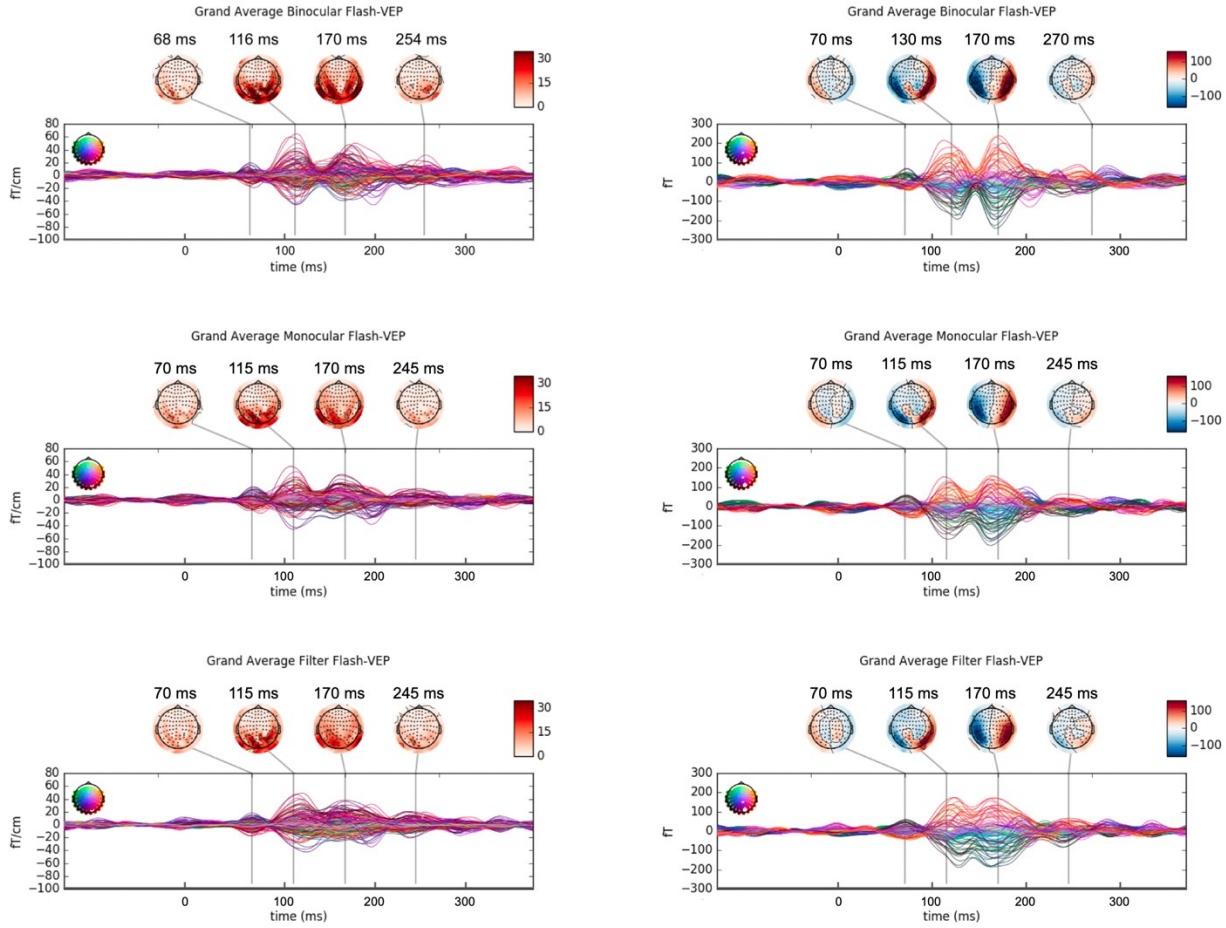

Figure 22: Grand average (n=8) of gradiometers (left) magnetometers (right) MEG responses for the flash stimuli, in the three testing conditions. Lower panels display location color-coded waveforms whilst the upper panels illustrate the topographical scalp distribution of the various peak components of the responses.

4.2.3 MEG Binocular Summation And Inhibition.

Following the same process elaborated for the EEG data, the MEG data (in the form of gradiometers) was analyzed in terms of amplitude ratio between binocular vs monocular (BM) and filter versus monocular (FM) conditions (Figure 23). The gradiometer waveforms (left hand-side) consist of positive only potential because they are the results from the root mean

square of the two set of the orthogonal planar responses. The main positive component ($P1_m$, from previous trough to peak) was computed and averaged for the 8 subjects to produce the topographic maps on the right hand-side. For the pattern-reversal $P1_m$ component, the BM ratio was in general superior to the unity, confirming the detection of binocular summation with the MEG data as well. The gradiometer data from the 102 sensors produce cortical gradients that are more variable than the EEG data, likely because of the small amplitude of the responses generated by the magnetic field and the insensitivity to the "low pass" characteristics of skull and skin structures. The FM computation revealed ratio inferior to the unity in the zone delimited by the occipital electrodes with ratios weakly superior to the unity in the more anterior regions. The variability in the ratio distribution makes the qualitative interpretation hazardous so more definitive conclusions might be achieved using quantitative analyses (section 4.3.3).

For the flash stimulus responses, the binocular conditions appear to produce larger amplitudes, resulting in BM ratio superior to unity in both occipital and frontal regions, and FM ratio showing larger responses with the filter conditions, again demonstrating the absence of binocular inhibition using unstructured stimuli.

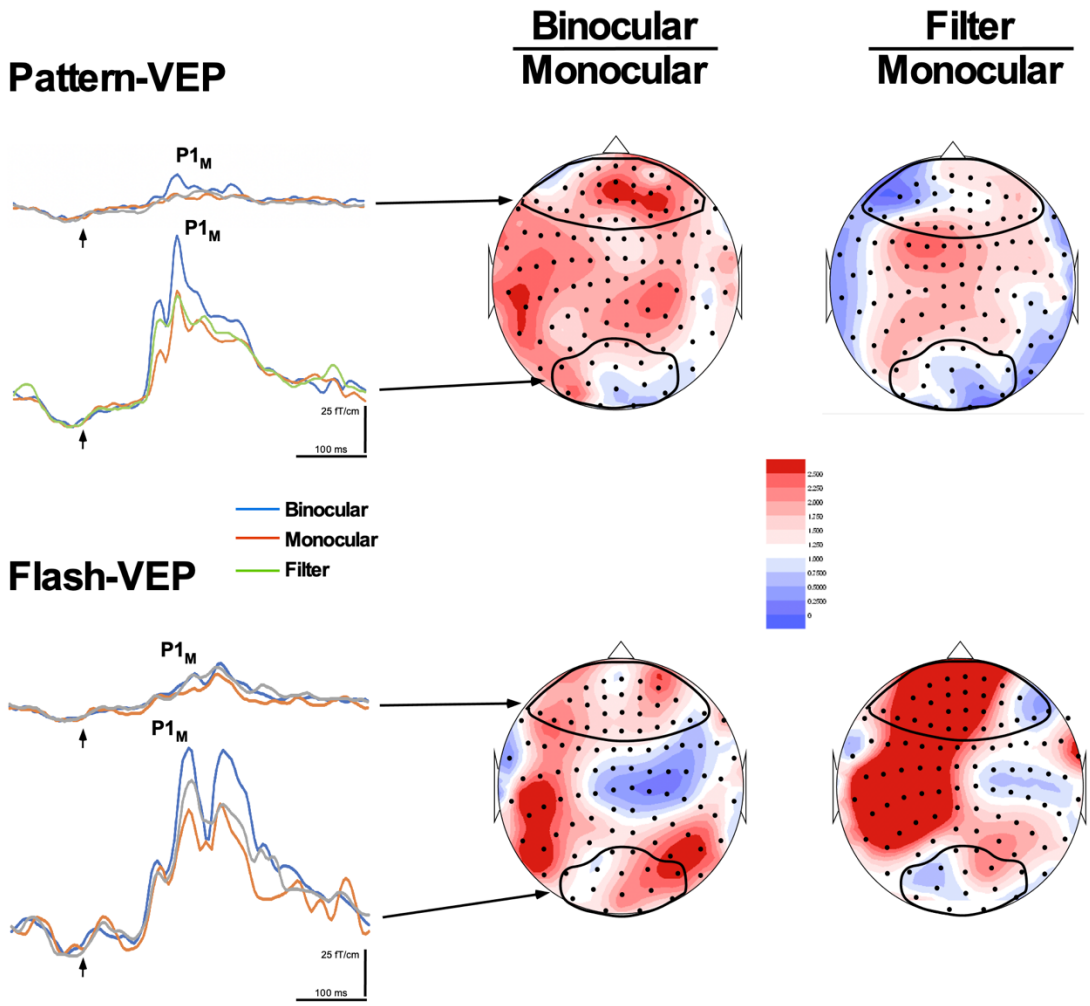

Figure 23. MEG data computation of the amplitude ratio between binocular and filter conditions versus monocular conditions for both pattern (P100 and P200) and flash (P1) responses. Representative waveforms resulting from the average responses of the occipital and frontal zone depicted in black lines on the topographical maps on the right that illustrate the variation in amplitude of the BM and FM ratio of the $P1_m$ component.

4.3 Quantitative Analysis PR-VEP

4.3.1 PR VEP

Figure 24 summarizes the statistical analyses performed on evoked EEG data in the presumed visual (top) and non-visual (bottom) areas, for the PR VEP (left) and Flash VEP (right). Data is regrouped according to waveform components (N70, P100, N150 and P200) for BM ratio (Blue) and FM ratio (Red).

4.3.1.1 PR VEP in presumed visually-driven areas

We first investigated whether the various components of cortical activity in the presumed visually-driven areas (Figure 24 top left) were differently affected in terms of occurrence of binocular summation and inhibition. A ratio significantly different from the unity suggests the impact of summation or inhibition. Thus, one-sample t-tests documented that binocular summation occurred for N70 ($p<0.004$), P100 ($p<0.001$), and N150 ($p<0.007$) but not for P200 and inhibition was present for P100 ($p<0.001$) and N150 ($p<0.03$) only.

Paired t-test for each component revealed significant differences between the two ratios for N70 ($P<0.05$), P100 ($p<0.001$), N150 ($p<0.001$) components with no significant difference between ratios at P200. The largest amount of BS occurred at N70 while the largest amount of BI occurred at P100; however, an ANOVA analysis calculated between components demonstrated significance only between N150 and P200 for BI ($P<0.05$) with all other differences between components demonstrating no significance. So, in summary, presence of BS demonstrated for N70, P100 and N150 and BI for P100 and N150 only. P200 is not affected by the binocularity.

4.3.1.2 PR VEP in presumed non-visually-driven areas

Figure 24 (bottom left) illustrates the statistical analyses for presumed non-visually-driven areas. Binocular summation was present for all the early components (one-sample t-test), whilst no inhibition could be documented. Paired t-test documented differences between summation and inhibition only for the P100 component while the one-way ANOVA is suggesting that BS is common between the early components (0.03 significance level between P100 and N150) and is not present in the later components. As for the inhibition, the one-way

ANOVA did not reveal any difference between components. So, for the presumed non-visual areas, BS is present but not BI.

4.3.1.3 PR VEP differences between presumed visual- and non-visually-driven areas

A series of two-group t-tests were performed to compare the strength of BS and BI for each component between presumed visually- and non-visually-driven areas. Essentially, the only significant difference is found for BI at P100 and N150.

4.3.2 Flash VEP

4.3.2.1 Flash VEP in presumed visually-driven areas

The same statistical approach as for the PR VEP analysis is being used (Figure 24 top right). It can be said that BS is present only for the P100 and N150 components, whilst no BI could be documented. The paired t-test documented differences between BS and BI for the P100 and N150 components, corroborating the one-sample analysis. Differences between components (one-way ANOVA) only revealed a distinctive N150 for BS but the high variability observed for that component make us hesitant in determining a particular status for that component. No difference could be detected for the BI.

4.3.2.2 Flash VEP in presumed non-visually-driven areas

In non-visually-driven areas, the flash VEPs do not appear to be influenced by either binocular condition. The only significance detected were some BS in the early components, that is sufficiently large for the N70 to produce a difference between BS and BI.

4.3.2.3 Flash VEP differences between presumed visual- and non-visually-driven areas

Essentially no statistically significant differences could be measured, suggesting that the BS and BI ratio of the Flash VEP responses are quite widespread and equally distributed amongst the various sensors, the only difference being the relative magnitude of the individual responses.

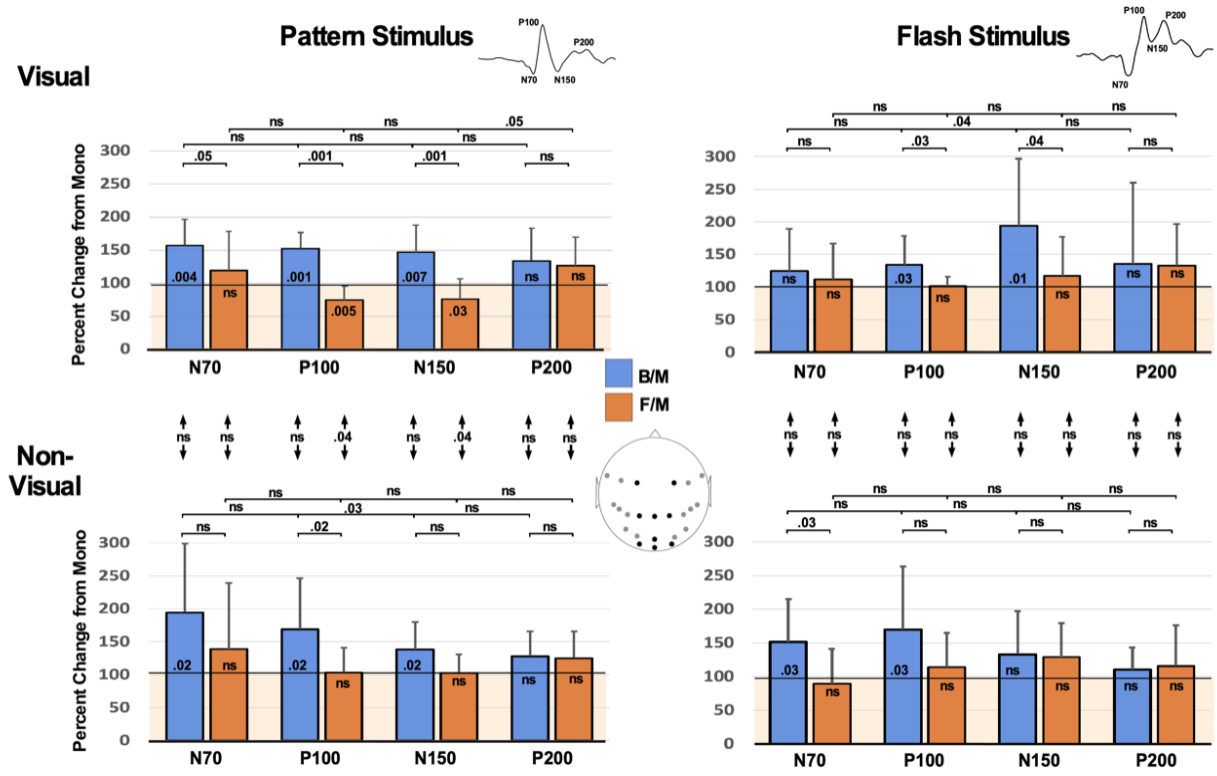

Figure 24: Statistical significance for SRs at each component and between components at visual and non-visual sensors for PR & Flash VEPs. BI present at P100 and N150 in PR stimuli visual sensors, this effect is absent in non-visual sensors, where Filter/Monocular ratio is much larger. Flash stimuli produced no BI.

4.3.3 PR VEF

The statistical analysis of the MEG sensor responses are summarized in Figure 25.

4.3.3.1 PR VEF in presumed visually-driven areas

PR VEF data gathered from gradiometers that are located around striate cortex demonstrated noticeable differences between BS and BI at P70 ($p<0.02$) and P100 ($p<0.005$) on t-test. Both of these components produced significant BS compared to monocular levels ($p<0.001$, $p<0.02$ respectively). BS was only significantly different between components P100 and P150 ($p<0.02$), whilst BI was only significantly induced at the P100 component ($p<0.05$), though it differed significantly between P70 and P100. While no BI was seen on average at P70, there was a significant difference between the average BI between P70 and P100 ($p<0.01$).

4.3.3.2 PR VEF in presumed non-visually-driven areas

Results from the non-visually-driven areas, selected sensor positions indicated no significant difference between BS and BI ratios at all components. Further, no significant differences were found when comparing BS/BI ratios across components. When comparing ratio values to unity, only BS at P100 was found to be significantly larger ($p<0.03$). No significant BI was produced in these channels.

4.3.3.3 *PR VEF differences between presumed visual- and non-visually-driven areas*

Confirming the results from the EEG data, the binocular inhibition in the gradiometer P100 responses are significantly different between visually- and non-visually-driven areas; these results are compatible with the proposition that BI is restricted to the occipital areas. Contrary to the EEG data, the responses at 150 ms did not reach significance here, likely due to a higher variability as the one-sample analysis suggests some BI in the visually-driven areas.

4.3.4 *Flash VEF*

The statistical analysis of the MEG sensor responses are summarized in Figure 25

4.3.4.1 *Flash VEF in presumed visually-driven areas*

Flash VEF data gathered from visually positioned sensors indicated no significant BS or BI at any component, between any component or when compared to population monocular values.

4.3.4.2 *Flash VEF in presumed non-visually-driven areas*

There was no significant difference found between SRs at any components for non-visual gradiometers. ANOVA demonstrated a significant difference between BS ($p<0.01$) and BI ($p<0.02$) between P70 and P100. Interestingly, SRs gathered for P70 were significantly smaller than monocular values ($p<0.04$, $p<0.05$); we have no explanation for that phenomenon that will need to be explored in future studies. Also very interesting is the fact the filter responses produced larger responses than the monocular one (BI significantly higher than the unity for P100), suggesting that for the flash stimulus, the presence of a filter did not preclude binocular summation; this effect was not found with the EEG data.

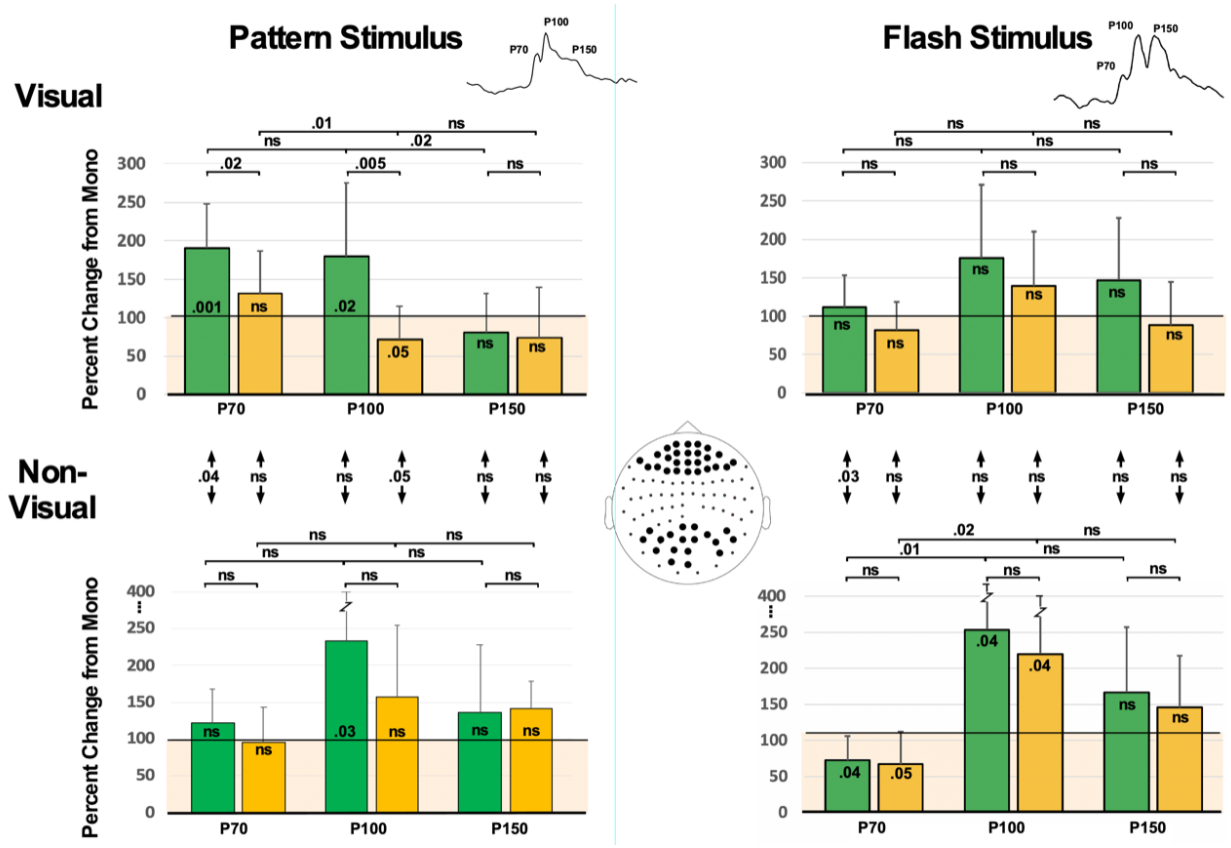

Figure 25: Statistical significance for SRs at each component and between components at visual and non-visual sensors for PR & Flash VEFs. BI present at P100 and N150 in PR stimuli visual sensors, this effect is absent in non-visual sensors. BS is produced at P70 and P100 but absent at P150 in visual sensors. Flash stimuli produced no BI or BS in visual sensors.

4.4 Model fitting including all sensors

While the statistical approach used in section 4.3 allows the detection of difference in the sensitivity of regrouped sensors in detecting BS and BI, it defeats the purpose of using a large array of sensors for improved localization of sources. Before performing source localization, a necessary step is to determine if taking into account the individual responses still allows detecting differences between BS and BI distribution in the various areas of the cortical surface. To that purpose, the amplitude (Figure 26, A-D) and BS & BI ratio (E-H) are presented in function of the antero-posterior (A-P) position of the sensors, for all the sensors (independently

of their lateral positioning) with a third-order polynomial function fitted to the data. For PR-VEP data (A), it is clear that the binocular responses are of larger amplitude for all A-P sensor positions (transparent blue area) whilst the filter responses are equal to the monocular responses in the anterior part of the head and smaller (BI; transparent green area) in the posterior part of the head, where the visually-driven occipital cortex is located. The same holds true for the PR-VEF responses, again demonstrating the interchangeability of EEG and MEG data when comes the time to analyze large scale phenomenon like BS and BI. When the BS and BI indexes are computed from the absolute amplitudes (E,G), the BS index is always superior to the unity (in terms of curve fitting), whilst the BI index is inferior to unity only in the posterior part of the head. The difference between BS and BI indexes (width of the transparent blue area) is larger in the posterior part of the head for the PR VEPs, but this could not be reproduced with the PR VEFs.

For the flash-induced responses, the binocular responses are still much larger with all sensor positions (B) but this time the filter condition does not yield any difference to the monocular responses, contrary to the conditions using the PR stimulus. For the Flash VEFs (D), the amplitude of the responses are slightly different in the posterior cortex, to converge to similar amplitude in the anterior part of the brain. Those observations are supported by the calculation of ratio for the Flash VEP responses but a high variability in the ratio computed for the Flash-VEF prevented any conclusion. This needs to be investigated further.

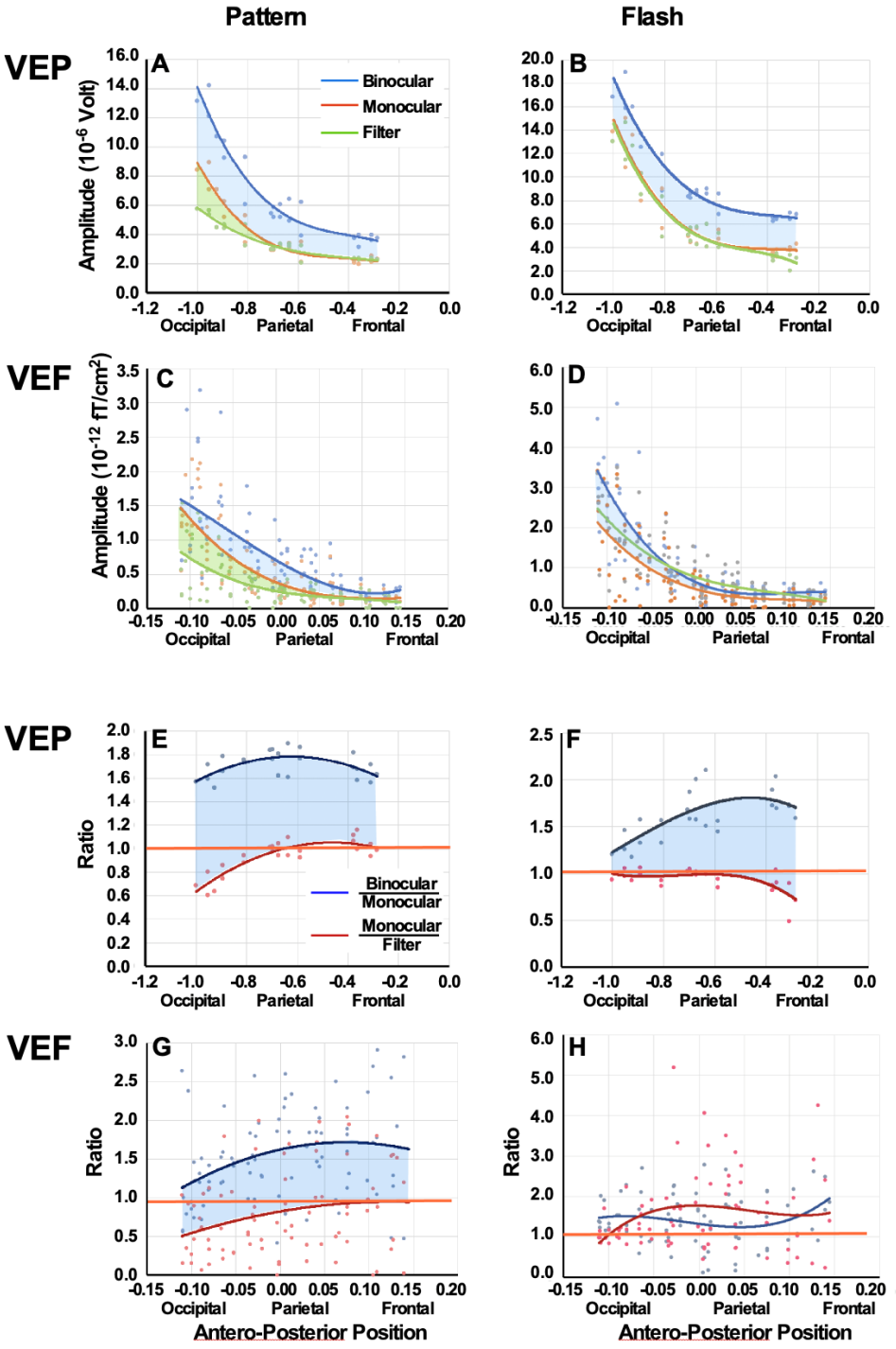

Figure 26: Graphical relationship between antero-posterior position of sensors and the overall amplitude of their responses in binocular, monocular and filter conditions (A-D) and BS and BI ratio (E-H).

4.5 Source Estimates

4.5.1 Grand Average PR VEF dSPM Maps

dSPM maps for VEF data can be seen in Figures 27-30. Figures 27-28 demonstrate statistically significant signals obtained through inverse solution calculations for each viewing condition for PR and flash stimuli. PR VEF in Figure 27 demonstrate widespread occipital cortex activation that is seen in all conditions. At N70 the binocular and filter conditions have the largest amounts of cortical activation. The strength of dipole activation at P100 appears to be strongest in binocular conditions with maximal activation on the left hemisphere. Monocular P100 strength does appear larger than the filter condition, and the activity distribution seems similar to binocular mapping. The filter condition has the least amount of activation at P100 with more reduction in left hemisphere activity than right. At N150 the three conditions appear very similar with minimal differences in strength of activity between binocular and monocular conditions. Once again the filter condition has slightly less activity overall.

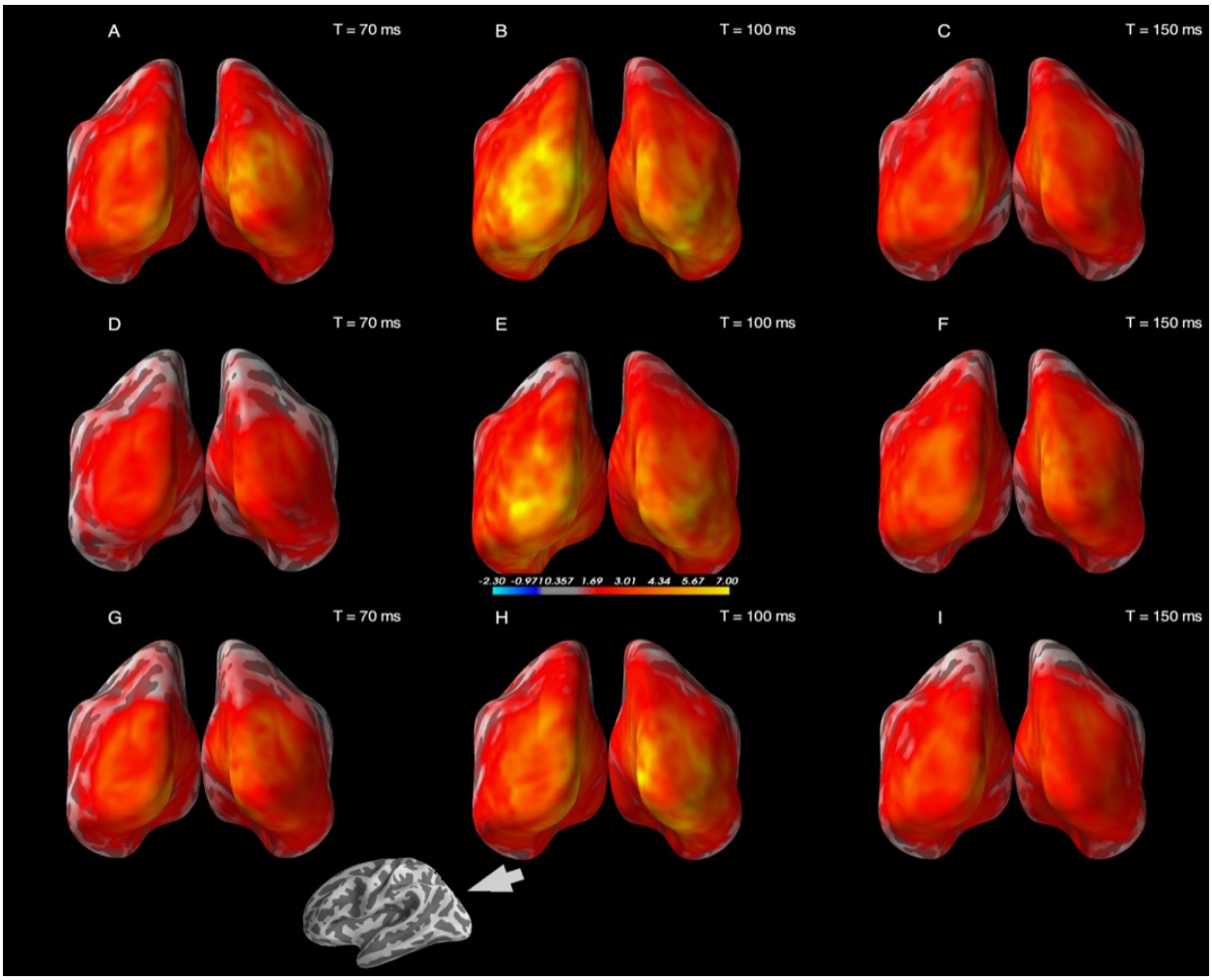

Figure 27: dSPM plots for Binocular (A-C), Monocular (D-F), and Filter (G-I) PR-VEF conditions.

4.5.2 Grand Average Flash VEF dSPM Maps

Source estimate maps produced for flash stimuli do not appear to vary substantially (Figure 28). All three viewing conditions at N70 have less activation in the visual cortices than their PR counterparts, and do not seem to differ between visual conditions. Similarly, at P100 and N150, condition does not seem to affect the strength of focality of activation. Binocular viewing seems to produce a small increase in the amount of activation at the striate cortex and

produces slightly more coverage in the extra striate cortices especially at N150, but otherwise there are no obvious differences.

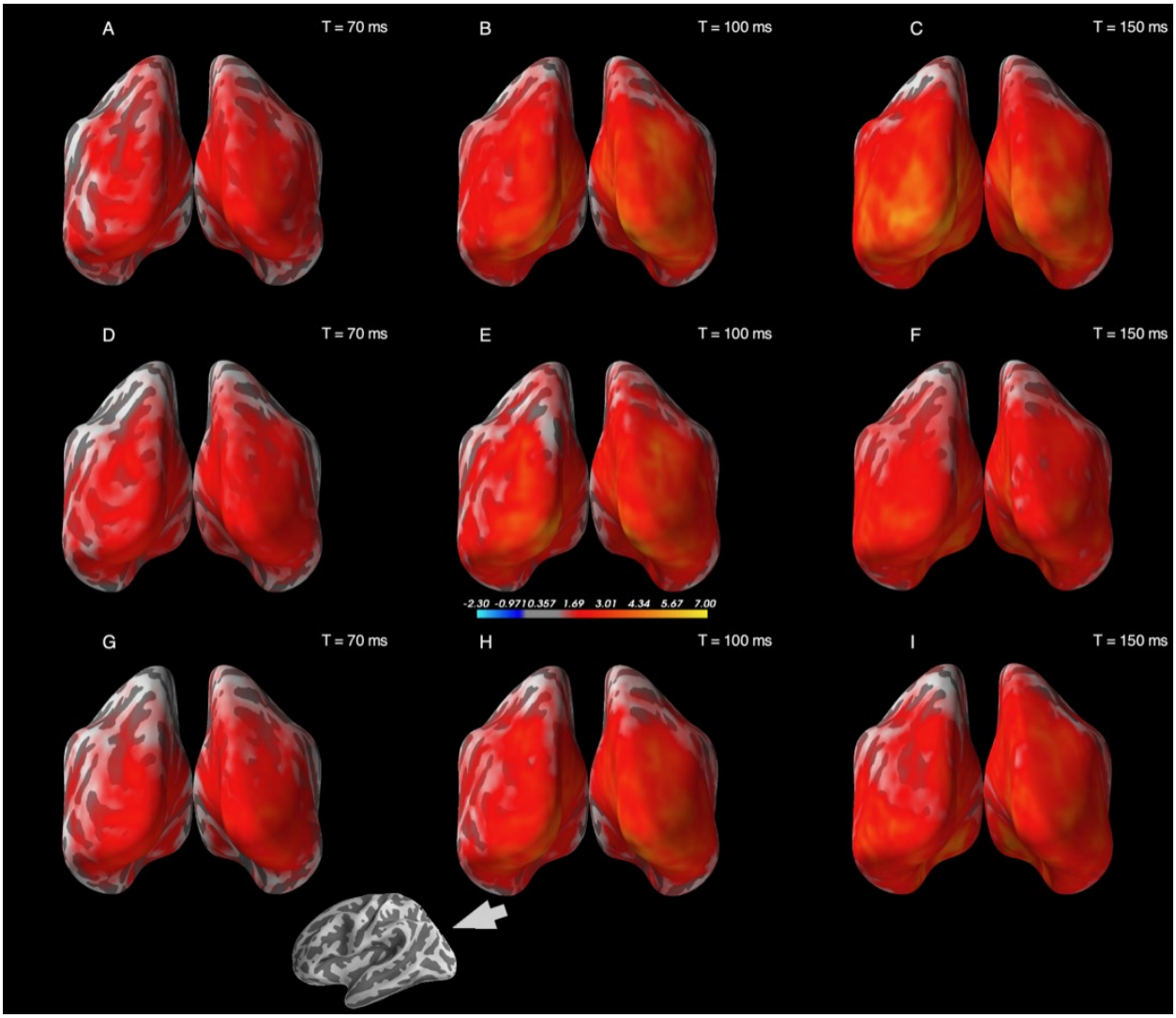

Figure 28: dSPM plots for Binocular (A-C), Monocular (D-F), and Filter (G-I) Flash-VEF conditions.

4.5.3 PR dPSM Differences

Figure 29 shows the differences between the binocular and monocular, and filter and monocular PR-VEF dSPM maps. The differences plotted for binocular and monocular demonstrate widespread BS at N70 that becomes reduced at P100 and predominantly smaller

than monocular activation at N150. For the differences between filter and monocular, a larger activation in filter conditions is seen at N70, but at P100 and N150, the monocular values exceed the filter throughout the majority of the occipital lobe with the largest difference occurring at the left striate cortex.

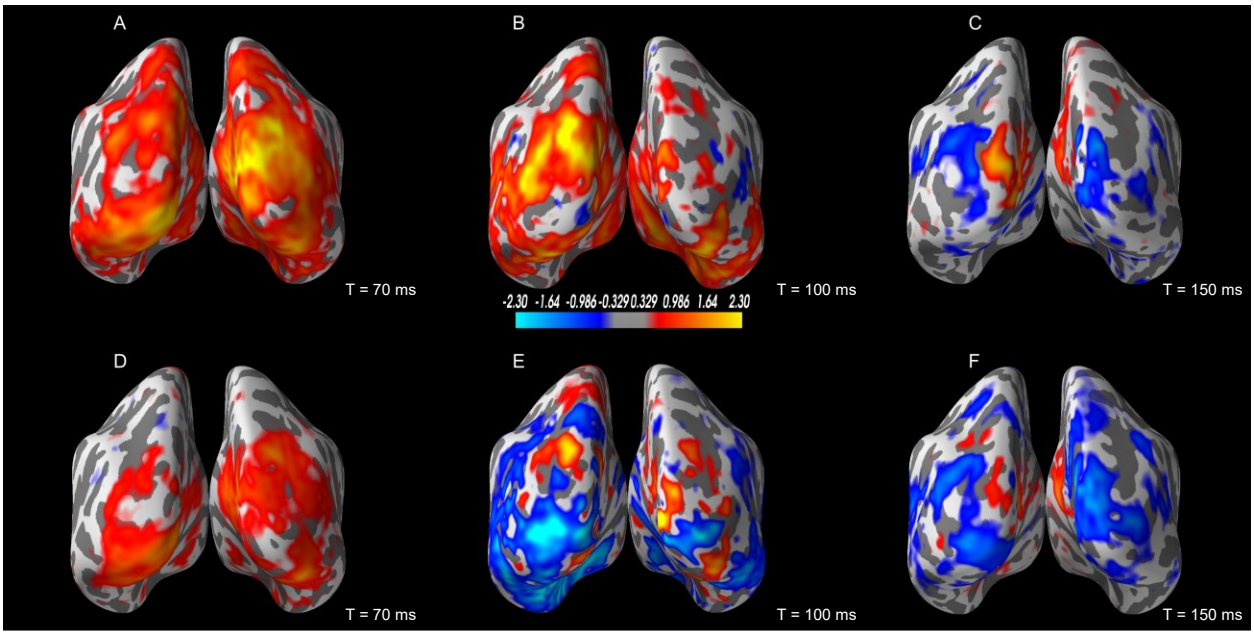

Figure 29: dSPM difference plots for Binocular-Monocular (A-C), Monocular-Filter (D-F) PR-VEF conditions.

4.5.4 Flash dSPM Differences

Activity differences with Flash stimuli are considerably smaller between conditions (Figure 30). BS appears moderately at N150 but there is minimal residual BS at P100. There is little BI seen in the filter-monocular dSPM mappings as well, with some negligible patches of inhibitory cortical activation at P100 and N150.

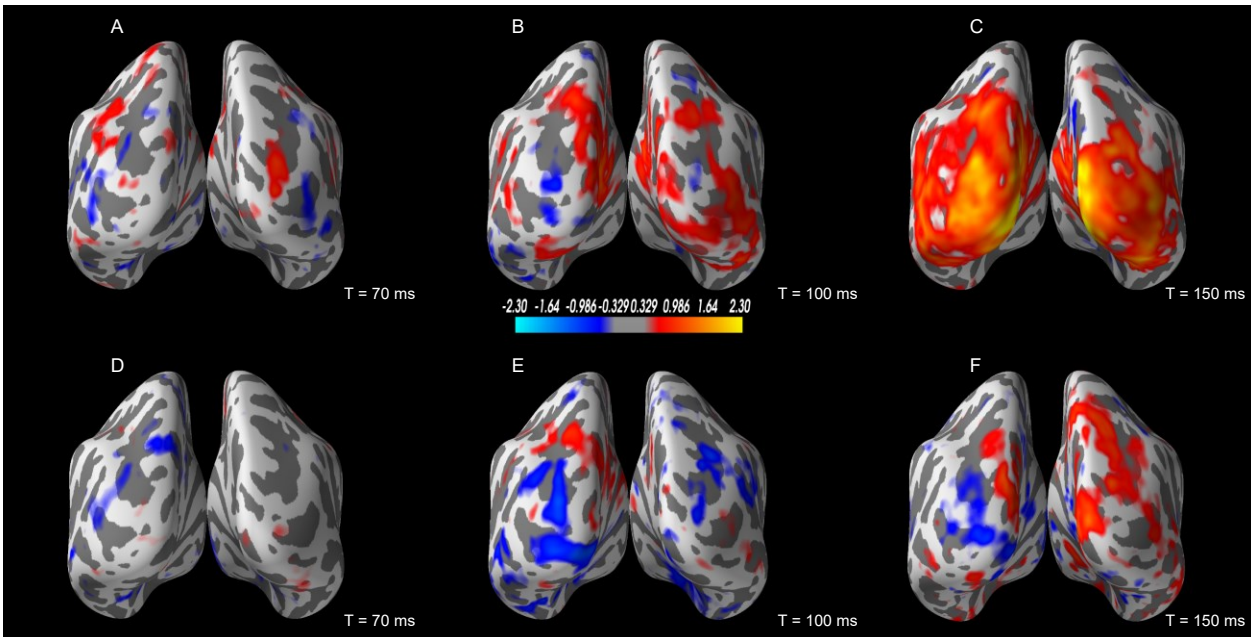

Figure 30: dSPM difference plots for Binocular-Monocular (A-C), Monocular-Filter(D-F) Flash-VEF conditions.

CHAPTER 5: DISCUSSION

5.1 Summary of findings

In this work, we have:

1) Confirmed previous work (Smith, 2013; Pardhan & Gilchrist, 1990) demonstrating that the reduction in visual potential of one eye produced brain activity that is lower than the one generated by the fellow eye alone
2) Confirmed that the nature of the stimulus presented is important for that effect to occur (Smith, 2013)
3) Demonstrated that binocular inhibition occurs only at the occipital pole whilst binocular summation is a more generalized phenomenon affecting all regions where visual activity could be evoked, thus suggesting that the binocular inhibition is a phenomenon inherently different than binocular summation and not only a particular case of binocular summation
4) Demonstrated that the cortical activity collected by the magnetoencephalography technique is also susceptible to the phenomenon of binocular inhibition
5) Demonstrated that the longer implicit time potentials within the same EEG recordings (P200, vs P100/135) were resistant to any binocular effects, thus suggesting they originate from different cortical processes.

5.2 Summation Ratio findings

5.2.1 Main Findings

It is apparent that the stimuli conditions used in this study were sufficient to produce significant BI and BS in EEG confirming previous studies (Katsumi et al 1988, Pardhan & Gilchrist 1990, Smith 2013). Figure 20 depicts the amplitude ratio for BS (Binocular/Monocular amplitude) and BI (Filter/Monocular amplitude) for components P100 and P200 as potential distributions across the scalp. P100 BS was seen to occur at all electrode positions in PR-VEPs for the Binocular/Monocular ratio. For the Filter/Monocular ratio, BI was not as uniformly produced and was primarily at the occipital pole (lowest amplitude) with some BI on the right parietal and temporal regions. Channels located at the central area of the head produced no inhibition demonstrating no difference between monocular and filter conditions in those waveforms. Pattern reversal amplitude ratios at P200 produced BS throughout all channels for both SRs, indicating no activity in the filter condition was reduced below monocular amplitudes.

Flash VEPs SR produced significant BS in all channels for the binocular/monocular comparison. The filter/monocular comparison however produced significant BS located more anterior and central, little BI was induced using this stimulus. These results confirm the findings of Smith (2013), in which BI was only found for one component and no significant difference was found between ND filter strength and the amount of BI induced. It has been speculated that homogenous areas of luminance elicit on positive activity even in the presence of IOD in luminance (Bolanowski, 1987, Grossberg & Kelly, 1999, Bourassa & Rule, 1994), and that the presence of contours is required to cause inhibitory activity (Leibowitz & Walker, 1956). Our findings are consistent with this.

The difference in location of the two SRs is interesting. BS in PR VEP stimuli is characterized by diffuse activation across all channels, with no dependency on channels being located near the visual cortex. BI in the PR-VEP on the other hand, was only seen primarily at the occipital pole in visually located channels, with non-visual channels producing no BI having amplitudes not significantly below those produced in monocular conditions. The Flash-VEPs produced less focal activity likely as a result of only demonstrating BS. This BS/BI distribution difference may indicate that these are discreetly different processes, especially considering the general distribution of BS between flash and PR-VEP is similar.

In our study, BI was demonstrated significantly at all components in the PR stimulus save the late P200 component. There is much debate around the origins of the PR VEP components. Researchers are in agreement that the N70 component arises from V1, but there is less of a consensus as to whether P100 originates in striate or extra-striate cortices (Di Russo et al. 2005, Onofrj et al. 1995, Noachtar et al. 1993). It is possible that due to the discrepancy between no measurable BI at P200 and significant BI at all earlier components that BI is a result of modified activity at the striate cortex. The controversy concerning P100 and N150 localization points to a potential involvement of V1. If BI occurs at this level, this is certainly supported by our findings, whereas P200 may arise from other extra-striate processes less susceptible to changes caused by BI.

Unfortunately, due to the limited number of electrodes we used, we cannot with any certainty calculate the source location due to the limited spatial sampling. Michel et al. (2014) demonstrated a significant change in P100 localization between 19-46 electrodes with distributions varying from occipital to whole head. They found that as they omitted frontal electrodes the P100 began to improperly localize towards the front of the head, whilst smaller

numbers of equally distributed electrodes conserved the occipital localization. As such we would recommend for any future inquiries into EEG source localization, at least 60 channel whole head EEG recordings would be required.

5.2.2 Clinical Implications

The obvious physiological advantage to binocular summation is supported by neural summation and the clinical findings of binocular vision, but there has yet to be any overt description of any advantage produced by a reduction in binocular performance below that of one eye in a normal healthy person. Clinical manifestations of inhibitory visual processing do however occur in a variety of pathologies most notably amblyopia. In cases of strabismic amblyopia occurring in childhood, the brain eliminates diplopia by developing suppression. Suppression in this case is defined as: "the active central inhibition of disparate and confusing images originating from the retina of the deviated eye" (Von Noorden & Campos, 1985). Suppression only occurs under binocular viewing conditions and while it is common in cases of childhood strabismus, it can occur in cases of normal binocular vision. Patients with monofixation syndrome may have minimal or no misalignment of their eyes and slightly reduced stereoacuity scores, and a central suppression scotoma. It has been postulated that the explanation for the development of suppression may involve the same neural processes involved in inhibitory interactions seen in binocular rivalry, which is a phenomenon seen in normal binocular patients. Binocular rivalry can be induced by presenting different images to each eye, often in the form of horizontal lines to one eye and vertical lines to the fellow eye. Because the images are dissimilar fusion does not occur, nor do the images appear superimposed. Instead, the images are perceived to alternate between the two, and are never seen together (Smith, Levi,

Manny, Harwerth, & White, 1985). Experiments have differentiated characteristics of these two forms of suppression. For example, increment threshold sensitivity functions during binocular rivalry of normal subjects produce wavelength specific losses during the suppression phase of rivalry. Esotropic patients with strabismic suppression and anomalous retinal correspondence did not produce this wavelength specific function under binocular rivalry conditions (Smith et al. 1985) and that led to the conclusion that under binocular rivalry conditions, the esotropes manifested a type of strabismic suppression and that there may be different mechanisms behind each form of suppression. However, it remains to determine whether or not binocular rivalry precedes strabismic suppression. It has been documented using PR stimuli that VEP amplitudes at P100 in strabismic amblyopic patients can be reduced for the amblyopic eye, and implicit times at P100 are increased for the amblyopic eye (Arden et al. 1974, Kubová et al. 1996). While the ND filter strength used in this study did not approach a high enough value to induce suppression, one must consider what modified process between normal binocular function and complete monocular suppression is producing such a reduced response. It could be that we are investigating a step that could lead to the development of suppression in the right context, and that the spectrum of these mechanisms share some similarities between adult and pediatric populations.

Previous research of SR in amblyopes has indicated that the amount of BI in amblyopes is directly related to the IOD in VA (Pardhan & Gilchrist, 1992), and that reduced BS on contrast sensitivity in strabismic amblyopes can be reversed if binocular stimulus strength was normalized between eyes using ND filters (Baker et al. 2007). Protocols similar to the ones used in the present study, if applied to amblyopes, could shed some light on the nature of these processes.

5.3 VEP & VEF differences

The current study was successful in replicating BI and BS using MEG in normal subjects, as proven by the results produced by EEG recordings. The task set out by research question 1 was to determine whether or not this brain activity would be captured in the same fashion using MEG. Our initial hope was to learn more about the location of sources during components between conditions to determine if any changes were due to contributions from other visual processing centers. As discussed in the introduction, MEG could provide a unique look at this phenomenon as magnetic fields have the advantage of ignoring the high resistivity of the skull and surrounding cranial tissues. It provided further benefits when compared to EEG such as its increased sensitivity to the detection of tangential brain activity, increased signal to noise ratio, and more accurate source localization. However, the variation we encountered at the sensor level to visual stimuli presented a significant problem in the identification of comparable components.

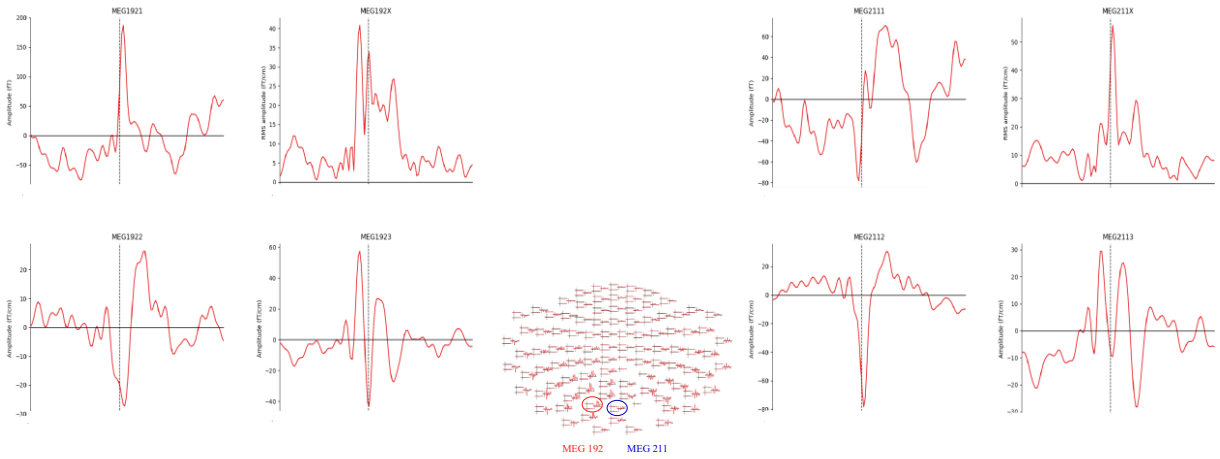

Figure 32 Gradiometer, magnetometer, and MSR grad data from two adjacent triplet sensors.

Figure 32 demonstrates this very clearly. These recordings are from adjacent sensors, and there is significant variation between magnetometers and gradiometers of the two positions. This variation also produced difficulties in identifying a P200 component which was not consistent between gradiometers or noticeable in combined RSM waveforms of the two opposing channels. Due to the fact that the planar gradiometers both measure the spatial derivative of the magnetic field in two orthogonal directions to create a gradient, the waveforms produced have the effect of mirroring one another. To overcome this change in polarity, the RSM of the planar data was used, which also allowed for 'ease' of component identification and then to produce SR's for each condition and stimulus type.

The variability in VEF's in comparison to their VEP counterparts could be due to differences in the selective sensitivity of sensor types. One of the original barriers to the development of MEG was determining whether or not MEG and EEG record independent information from the same brain source (Cohen, 1968, Malmivuo, 2012). If the measurements were fully independent then MEG would be able to derive new information from its biomagnetic data about the bioelectric sources produced by EEG. Since bipolar electric and magnetic lead fields in homogenous spherical volume conductors are orthogonal to one another, MEG and EEG are considered complimentary techniques, each capturing information that the other is not as sensitive too. While it is possible that source elements in the direction of either the electric or magnetic lead field in a volume conductor will only be measurable in the direction of said lead, this is an unlikely explanation for the variability of VEF activity captured in this study. Only in very rare circumstances are source elements oriented in such a way that they are not collected by both methods, as source activity almost always has components in the direction of both magnetic and electric lead fields (Malmivuo, 2012). An alternative explanation would be the fact that

MEG is sensitive primarily to tangentially oriented sources and less sensitive to radial brain sources. If the coherence of the VEP signal is due to one or a combination of radial sources then this could possibly explain the discrepancy between VEF and VEP morphological differences. Previous research comparing orientation sensitivity in MEG & EEG using forward modeling demonstrated that the MEG did have a source orientation that would produce very little MEG data in most locations of the cortex, more specifically laterally located superficial regions of the cortex (Ahlfors, Han, & Belliveau, 2010). Whereas EEG has good sensitivity across the entire brain with a reduction at the orbitofrontal and temporal pole regions. As such, an issue with source orientation is not conclusive, as both modalities have very good resolvability with respect to the visual cortices, and it is unlikely for the activity we see on BS & BI to have the exact orientation of the lowest sensitivity. It is possible that the depth of the activity is a limiting factor, as MEG is less sensitive to deeper brain sources but previous visual studies in MEG using different visual stimuli have not encountered such an obstacle.

5.4 Source Localization

The cortical activation produced in the dSPM source maps were fairly consistent with the statistically significant differences we found with PR & Flash VEF's. The PR VEF maps in particular demonstrate a descending level of activity (binocular largest, filter smallest) at P100 very clearly, where SRs were largest for BS and BI. The flash maps also demonstrated little difference between conditions outside a slight increase in binocular activity. Difference plots are an easy way to illustrate the summation and inhibitory effect seen throughout the cortex at large. While useful to glimpse the general activity at a glance, future directions for paradigms following this study would be advised to produce more focal activity maps. It was our original

hope to disclose a coordinate difference in components between conditions in the context of equivalent dipole modeling, however attempts to produce consistent dipole positioning proved unreliable even within condition blocks for the same subject. One can postulate that the size of the visual stimulus used in this study may have been too large to produce a more focal source estimation. Our stimulus size was chosen to replicate the conditions that best facilitated BI based off of previous literature for reproducibility's sake. Standard VEF paradigms (Brenner, Williamson & Kaufman, 1975; Ahlfors et al. 1992; Nakamura et al. 1997; Chen et al. 2005; Hagler et al. 2009) tend to use smaller stimuli, organized in quadrants or hemifields, an often altitudinal in nature (above/below fixation). This change along with retinotopically constrained dipole inverse methods that fit dipole projections along anatomically distinct visual areas, is thought to help to avoid cross talk from simultaneously active associative visual areas (Hagler et al. 2009). Despite this, there is still difficulty with widespread activation of extracortical areas producing maps with identical time courses across the visual system but varying amplitudes, much like we have seen in our own dSPM data. It could be that the activation of multiple sources causes the superimposition of overlapping signals of opposite polarity. This would cause a decrease in signal to noise ratio which would result in a more difficult source estimation. This occurrence is more frequent when the cortical activity extends into the walls of a sulcus or gyrus. Sources at V1 is a well-known example of this, as visual stimuli that cross the horizontal meridian produce sources that cancel across the calcarine fissure (Ahlfors, Han, & Lin, 2010). In the case of our data, the widespread activation related to the full field stimuli would be a result of retinotopic activation at V1. Such widespread activity would be expected to involve a larger amount of cancellation as opposite sides of gyri and sulci walls would be involved. This widespread activation coupled with the spatial extension of interconnected associative visual

cortices could explain some of the patchy activation peaks in our dSPM maps. Cancelled signals are often arising from tangential sources in the brain, leaving more radial sources untouched which may further compound the localization issue. Again, the difference in source orientation may provide an answer to the differences we are seeing, as a similar discrepancy was seen in cognitive P300 evoked responses. On EEG these P300 responses are robust and large in amplitude, but MEG sensors in the same position produce small amplitude deflections (Halgren, Marinkovic, & Chauvel, 1998). Only by looking at other nearby sensors can the full amplitude of this component be identified, similar to the highly correlated temporal MEG channels in our study.

5.5 Limitations Of The Study

This study was certainly hampered by the limited number of subjects that could be studied within the limits of the budget of the small IWK grant obtained for this project through a competitive grant contest. This number was deemed adequate to provide sufficient power to an EEG study (calculation was based on Smith, 2013, who used EEG technology only). The variability obtained with the MEG gradiometer data precluded an analysis per sensor and we had to regroup sensors by regions of the brain, which defeats the purpose of accurate localization. In order to counteract that variability, more subjects could be one route but also modification of the stimulus presentation (smaller field coverage to stimulate smaller zones, more rapid rate of reversal to allow more averaging) could also be considered. This study was also limited by the quality of the initial digitalization of the electrode positions and the fact not all subjects had an MRI available prior to the study. All those factors prevented us from performing adequate inverse solution for our data.

5.6 Future Studies

With the current data, it would be interesting to use the parcellation strategy (Destrieux et al. 2010) to further investigate the source localization behind the BS and BI processes. For future investigations, a reduction in the stimulus size may help improve source localization. Investigating subjects with various forms of amblyopia who demonstrate suppressive scotoma may also help shed light on the mechanisms and purpose of BI. Up to now, all BI investigations have used neutral density filters to reduce vision in one eye; it might be interesting to see if other factors affecting vision, such as visual acuity, could also produce BI.

5.7 Conclusion

The results of this study indicate that BI & BS may arise from different cortical generators. We were able to affirm that BI is sensitive to contour based stimuli (PR), and insensitive to interocular difference in Flash stimuli. Differences in potential distribution of BI/BS ratios produced by PR-VEP indicate that BS and BI are discreetly different processes. These distributions may suggest that BI could originate primarily from V1, while BS may involve extra-striate areas. Use of MEG demonstrated a similar selectivity to BI/BS to pattern reversal stimuli. MEG was able to detect BI at the sensor level in visual areas during PR-VEF stimuli and also showed no significant BI using Flash stimuli.

REFERENCES

Adachi, E., & Chiba, J. (1979). Visual resolution at the central retina detected with human visually evoked cortical potentials (author's transl). *Nippon Ganka Gakkai Zasshi, 83*(7), 1036-1042.

Ahlfors, S. P., Han, J., Belliveau, J. W., & Hämäläinen, M. S. (2010). Sensitivity of MEG and EEG to source orientation. *Brain Topography, 23*(3), 227-232.

Ahlfors, S. P., Han, J., Lin, F., Witzel, T., Belliveau, J. W., Hämäläinen, M. S., et al. (2010). Cancellation of EEG and MEG signals generated by extended and distributed sources. *Human Brain Mapping, 31*(1), 140-149.

Ahlfors, S. P., Ilmoniemi, R., & Hämäläinen, M. (1992). Estimates of visually evoked cortical currents. *Electroencephalography and Clinical Neurophysiology, 82*(3), 225-236.

Anderson, S. J., Holliday, I. E., & Harding, G. F. A. (1999). Assessment of cortical dysfunction in human strabismic amblyopia using magnetoencephalography (MEG). *Vision Research, 39*(9), 1723-1738. doi:10.1016/S0042-6989(98)00259-4

Anderson, S. J., & Swettenham, J. B. (2006). Neuroimaging in human amblyopia. *Strabismus, 14*(1), 21-35. doi:10.1080/09273970500538082

Apkarian, P. A., Nakayama, K., & Tyler, C. W. (1981). Binocularity in the human visual evoked potential: Facilitation, summation and suppression. *Clinical Neurophysiology, 51*(1), 32-48.

Arden, G., Barnard, W., & Mushin, A. (1974). Visually evoked responses in amblyopia. *The British Journal of Ophthalmology, 58*(3), 183.

Avidan, G., Harel, M., Hendler, T., Ben-Bashat, D., Zohary, E., & Malach, R. (2002). In Avidan G. (Ed.), *Contrast sensitivity in human visual areas and its relationship to object recognition* doi:10.1152/jn.2002.87.6.3102

Baker, D. H., Meese, T. S., Mansouri, B., & Hess, R. F. (2007). In Baker D. H. (Ed.), *Binocular summation of contrast remains intact in strabismic amblyopia* doi:10.1167/iovs.07-0194

Bardouille, T., Picton, T., & Ross, B. (2006). Correlates of eye blinking as determined by synthetic aperture magnetometry. *Clinical Neurophysiology, 117*(5), 952-958.

Blake, R., & Fox, R. (1973). The psychophysical inquiry into binocular summation. *Perception & Psychophysics, 14*(1), 161-185.

Blake, R., & Wilson, H. (2011). Binocular vision. *Vision Research, 51*(7), 754-770. doi:10.1016/j.visres.2010.10.009

Bolanowski Jr, S. J. (1987). Contourless stimuli produce binocular brightness summation. *Vision Research, 27*(11), 1943-1951.

Bourassa, C. M., & Rule, S. J. (1994). Binocular brightness: A suppression-summation trade off. *Canadian Journal of Experimental Psychology/Revue Canadienne De Psychologie Expérimentale, 48*(3), 418.

Brenner, D., Williamson, S. J., & Kaufman, L. (1975). Visually evoked magnetic fields of the human brain. *Science, 190*(4213), 480-482. doi:10.1126/science.170683

Brookes, M. J., Gibson, A. M., Hall, S. D., Furlong, P. L., Barnes, G. R., Hillebrand, A., et al. (2004). A general linear model for MEG beamformer imaging. *NeuroImage, 23*(3), 936-946. doi:10.1016/j.neuroimage.2004.06.031

Burian, H. M., & Von Noorden, G. K. (1985). *Burian-von noorden's binocular vision and ocular motility: Theory and management of strabismus* CV Mosby.

Caton, R. (1875). Electrical currents of the brain. *The Journal of Nervous and Mental Disease, 2*(4), 610.

Celesia, G. G., Bodis-Wollner, I., Chatrian, G. E., Harding, G. F., Sokol, S., & Spekreijse, H. (1993). Recommended standards for electroretinograms and visual evoked potentials. report of an IFCN committee. *Electroencephalography and Clinical Neurophysiology, 87*(6), 421-436.

Chen, W., Ko, Y., Liao, K., Hsieh, J., Yeh, T., Wu, Z., et al. (2005). Optimal check size and reversal rate to elicit pattern-reversal MEG responses. *Canadian Journal of Neurological Sciences, 32*(2), 218-224.

Cohen, D., Schläpfer, U., Ahlfors, S., Hämäläinen, M., & Halgren, E. (2002). New six-layer magnetically-shielded room for MEG. Paper presented at the *Proceedings of the 13th International Conference on Biomagnetism. Jena, Germany: VDE Verlag,* pp. 919-921.

Cohen, D. (1968). Magnetoencephalography: Evidence of magnetic fields produced by alpha-rhythm currents. *Science, 161*(3843), 784-786. doi:10.1126/science.161.3843.784

Cohen, D., & Cuffin, B. N. *Demonstration of useful differences between magnetoencephalogram and electroencephalogram* doi://doi.org/10.1016/0013-4694(83)90005-6

Collins, D. W., Carroll, W. M., Black, J. L., & Walsh, M. (1979). Effect of refractive error on the visual evoked response. *British Medical Journal, 1*(6158), 231-232.

Compston, A. (2010). The berger rhythm: Potential changes from the occipital lobes in man, by E.D. adrian and B.H.C. matthews (from the physiological laboratory, cambridge). brain 1934: 57; 355-385. *Brain, 133*(1), 3-6. doi:10.1093/brain/awp324

Cortese, F., Wong, A., Goltz, H., Cheyne, D., & Wong, A. (2009). Neural interactions of pattern perception in human amblyopia: An MEG study. *NeuroImage,* (47), S86.

Cuffin, B. N. (1993). Effects of local variations in skull and scalp thickness on EEG's and MEG's. *Biomedical Engineering, IEEE Transactions On, 40*(1), 42-48. doi:10.1109/10.204770

Cutolo, F., & Ferrari, V. (2018). The role of camera convergence in stereoscopic video see-through augmented reality displays. *World, 2*, 3.

Dale, A. M., Liu, A. K., Fischl, B. R., Buckner, R. L., Belliveau, J. W., Lewine, J. D., et al. (2000). Dynamic statistical parametric mapping: Combining fMRI and MEG for high-resolution imaging of cortical activity: Combining fMRI and MEG for high-resolution imaging of cortical activity. *Neuron, 26*(1), 55-67. doi:10.1016/S0896-6273(00)81138-1

Denison, R. N., Vu, A. T., Yacoub, E., Feinberg, D. A., & Silver, M. A. (2014). Functional mapping of the magnocellular and parvocellular subdivisions of human LGN. *NeuroImage, 102*(2), 358-369. doi:10.1016/j.neuroimage.2014.07.019

Destrieux, C., Fischl, B., Dale, A., & Halgren, E. (2010). Automatic parcellation of human cortical gyri and sulci using standard anatomical nomenclature. *NeuroImage, 53*(1), 1-15. doi:10.1016/j.neuroimage.2010.06.010

Di Russo, F., Pitzalis, S., Spitoni, G., Aprile, T., Patria, F., Spinelli, D., et al. (2005). Identification of the neural sources of the pattern-reversal VEP. *NeuroImage, 24*(3), 874-886. doi:10.1016/j.neuroimage.2004.09.029

Di Summa, A., Polo, A., Tinazzi, M., Zanette, G., Bertolasi, L., Bongiovanni, L., et al. (1997). Binocular interaction in normal vision studied by pattern-reversal visual evoked potentials (PR-VEPS). *The Italian Journal of Neurological Sciences, 18*(2), 81-86.

Donzis, P. B., Rappazzo, J. A., Burde, R. M., & Gordon, M. (1983). In Donzis P. B. (Ed.), *Effect of binocular variations of snellen's visual acuity on titmus stereoacuity* doi:10.1001/archopht.1983.01040010930016

Fatima, Z., Quraan, M. A., Kovacevic, N., & McIntosh, A. R. (2013). ICA-based artifact correction improves spatial localization of adaptive spatial filters in MEG. *NeuroImage, 78*, 284-294.

Fischl, B., Van Der Kouwe, A., Destrieux, C., Halgren, E., Ségonne, F., Salat, D. H., et al. (2004). Automatically parcellating the human cerebral cortex. *Cerebral Cortex, 14*(1), 11-22.

Garcés, P., López-Sanz, D., Maestú, F., & Pereda, E. (2017). Choice of magnetometers and gradiometers after signal space separation. *Sensors, 17*(12), 2926.

Gençer, N. G., & Acar, C. E. (2004). Sensitivity of EEG and MEG measurements to tissue conductivity. *Physics in Medicine & Biology, 49*(5), 701.

Gramfort, A., Luessi, M., Larson, E., Engemann, D. A., Strohmeier, D., Brodbeck, C., et al. (2014). MNE software for processing MEG and EEG data. *NeuroImage, 86*, 446-460.

Grossberg, S., & Kelly, F. (1999). Neural dynamics of binocular brightness perception. *Vision Research, 39*(22), 3796-3816.

Hagler, D. J., Riecke, L., & Sereno, M. I. (2007). Parietal and superior frontal visuospatial maps activated by pointing and saccades. *NeuroImage, 35*(4), 1562-1577. doi:10.1016/j.neuroimage.2007.01.033

Hagler, D. J., Halgren, E., Martinez, A., Huang, M., Hillyard, S. A., & Dale, A. M. (2009). Source estimates for MEG/EEG visual evoked responses constrained by multiple, retinotopically-mapped stimulus locations. *Human Brain Mapping, 30*(4), 1290-1309. doi:10.1002/hbm.20597

Halgren, E., Marinkovic, K., & Chauvel, P. (1998). Generators of the late cognitive potentials in auditory and visual oddball tasks. *Electroencephalography and Clinical Neurophysiology, 106*(2), 156-164.

Hall, S. D., Holliday, I. E., Hillebrand, A., Furlong, P. L., Singh, K. D., & Barnes, G. R. (2005). Distinct contrast response functions in striate and extra-striate regions of visual cortex revealed with magnetoencephalography (MEG). *Clinical Neurophysiology, 116*(7), 1716-1722. doi:10.1016/j.clinph.2005.02.027

Halliday, A. M., Mcdonald, W. I., & Mushin, J. (1973). Visual evoked response in diagnosis of multiple sclerosis. *British Medical Journal, 4*(5893), 661. doi:10.1136/bmj.4.5893.661

Hämäläinen, M., Hari, R., Ilmoniemi, R. J., Knuutila, J., & Lounasmaa, O. V. (1993). Magnetoencephalography—theory, instrumentation, and applications to noninvasive studies of the working human brain. *Reviews of Modern Physics, 65*(2), 413.

Hansen, P., Kringelbach, M., & Salmelin, R. (2010). *MEG: An introduction to methods* Oxford university press.

Heng, S., & Dutton, G. (2011). The pulfrich effect in the clinic. *Graefe's Archive for Clinical and Experimental Ophthalmology, 249*(6), 801-808. doi:10.1007/s00417-011-1689-6

Holliday, I., Anderson, S., & Harding, G. (1996). Magnetoencephalographic (MEG) investigation of cortical dysfunction in human amblyopia. *NeuroImage, 3*(3), S278.

Horton, J. C., & Hocking, D. R. (1997). Timing of the critical period for plasticity of ocular dominance columns in macaque striate cortex. *The Journal of Neuroscience : The Official Journal of the Society for Neuroscience, 17*(10), 3684-3709.

Hubel, D. H., & Wiesel, T. N. (1959). In HUBEL D. H. (Ed.), *Receptive fields of single neurones in the cat's striate cortex*

Jeffreys, D., & Axford, J. (1972). Source locations of pattern-specific components of human visual evoked potentials. II. component of extrastriate cortical origin. *Experimental Brain Research, 16*(1), 22-40. doi:10.1007/BF00233372

Katsumi, O., Hirose, T., & Taninol, T. (1988). Objective evaluation of binocular function with pattern reversal VER. *Acta Ophthalmologica, 66*(2), 194-200. doi:10.1111/j.1755-3768.1988.tb04011.x

Katsumi, O., Tanino, T., & Hirose, T. (1985). Objective evaluation of binocular function with pattern reversal VER. *Acta Ophthalmologica, 63*(6), 706-711. doi:10.1111/j.1755-3768.1985.tb01586.x

Katsumi, O., Tanino, T., & Hirose, T. (1986a). Objective evaluation of binocular function using the pattern reversal visual evoked response. II. effect of mean luminosity. *Acta Ophthalmologica, 64*(2), 199-205. doi:10.1111/j.1755-3768.1986.tb06900.x

Katsumi, O., Tanino, T., & Hirose, T. (1986b). Objective evaluation of binocular function with pattern reversal VER. *Acta Ophthalmologica, 64*(6), 691-697. doi:10.1111/j.1755-3768.1986.tb00687.x

Kothari, R., Bokariya, P., Singh, S., & Singh, R. (2016). A comprehensive review on methodologies employed for visual evoked potentials. *Scientifica, 2016* doi:10.1155/2016/9852194

Kubová, Z., Kuba, M., Juran, J., & Blakemore, C. (1996). Is the motion system relatively spared in amblyopia? evidence from cortical evoked responses. *Vision Research, 36*(1), 181-190. doi:10.1016/0042-6989(95)00055-5

Leibowitz, H., & Walker, L. (1956). Effect of field size and luminance on the binocular summation of suprathreshold stimuli. *Josa, 46*(3), 171-172.

Levi, D. M., Knill, D. C., & Bavelier, D. (2015). Stereopsis and amblyopia: A mini-review. *Vision Research, 114*, 17-30. doi:10.1016/j.visres.2015.01.002

Macmillan, E. S., Gray, L. S., & Heron, G. (2007). Visual adaptation to interocular brightness differences induced by neutral-density filters. *Investigative Ophthalmology & Visual Science, 48*(2), 935. doi:10.1167/iovs.06-0958

Malmivuo, J. (2012). Comparison of the properties of EEG and MEG in detecting the electric activity of the brain. *Brain Topography, 25*(1), 1-19.

Matsumoto, R., Ikeda, A., Nagamine, T., Matsuhashi, M., Ohara, S., Yamamoto, J., et al. (2004). Subregions of human MT complex revealed by comparative MEG and direct electrocorticographic recordings. *Clinical Neurophysiology, 115*(9), 2056-2065. doi:10.1016/j.clinph.2004.03.030

Millett, D. (2001). Hans berger: From psychic energy to the EEG. *Perspectives in Biology and Medicine, 44*(4), 522-542. doi:10.1353/pbm.2001.0070

Nakamura, A., Kakigi, R., Hoshiyama, M., Koyama, S., Kitamura, Y., & Shimojo, M. (1997). Visual evoked cortical magnetic fields to pattern reversal stimulation. *Cognitive Brain Research, 6*(1), 9-22. doi:10.1016/S0926-6410(97)00013-X

Noachtar, S., Hashimoto, T., & Lüders, H. (1993). Pattern visual evoked potentials recorded from human occipital cortex with chronic subdural electrodes. *Electroencephalography and Clinical Neurophysiology/Evoked Potentials Section, 88*(6), 435-446.

Olmsted, J. M. D. (1955). *A translation of luigi galvani's de viribus electricitatis in motu musculari commentarius. commentary on the effect of electricity on muscular motion (book review)*

Onofrj, M., Fulgente, T., Thomas, A., Curatola, L., Peresson, M., Lopez, L., et al. (1995). Visual evoked potentials generator model derived from different spatial frequency stimuli of visual field regions and magnetic resonance imaging coordinates of V1, V2, V3 areas in man. *International Journal of Neuroscience, 83*(3-4), 213-239.

Onofrj, M., Fulgente, T., Thomas, A., Malatesta, G., Peresson, M., Locatelli, T., et al. (1995). Source model and scalp topography of pattern reversal visual evoked potentials to altitudinal stimuli suggest that infoldings of calcarine fissure are not part of VEP generators. *Brain Topography, 7*(3), 217-231. doi:10.1007/BF01202381

Osinga, E., van Oosten, B., de Vries-Knoppert, W., & Petzold, A. (2017). Time is vision in recurrent optic neuritis. *Brain Research, 1673*, 95-101. doi:10.1016/j.brainres.2017.08.012

Oy, E. N. (2017). No title. *The MEG Signal Processor (Graph) Users Guide and Reference Manual,*

Pardhan, S., & Gilchrist, J. (1991). The importance of measuring binocular contrast sensitivity in unilateral cataract. *Eye (London, England), 5 (Pt 1)*, 31.

Pardhan, S. (1997). A comparison of binocular summation in the peripheral visual field in young and older patients. *Current Eye Research, 16*(3), 252-255. doi:10.1076/ceyr.16.3.252.15407

Pardhan, S., & Gilchrist, J. (1992). Binocular contrast summation and inhibition in amblyopia. *Documenta Ophthalmologica, 82*(3), 239-248.

Pardhan, S., Gilchrist, J., Douthwaite, W., & Yap, M. (1990). Binocular inhibition: Psychophysical and electrophysiological evidence. *Optometry and Vision Science, 67*(9), 688-691. doi:10.1097/00006324-199009000-00006

Pineles, S. L., Velez, F. G., Isenberg, S. J., Fenoglio, Z., Birch, E., Nusinowitz, S., et al. (2013). Functional burden of strabismus: Decreased binocular summation and binocular inhibition. *JAMA Ophthalmology, 131*(11), 1413-1419.

Pirenne, M. H. (1943). Binocular and uniocular threshold of vision. *Nature,*

Purves, D. E., Augustine, G. J., Fitzpatrick, D. E., & Katz, L. C. (1997). Neuroscience.

Remington, L. A., & Goodwin, D. (2011). *Clinical anatomy and physiology of the visual system* Elsevier Health Sciences.

Ryhänen, T., Seppä, H., Ilmoniemi, R., & Knuutila, J. (1989). SQUID magnetometers for low-frequency applications. *Journal of Low Temperature Physics, 76*(5-6), 287-386.

Sadun, A. A., Bassi, C. J., & Lessell, S. (1990). Why cataracts do not produce afferent pupillary defects. *American Journal of Ophthalmology, 110*(6), 712-714. doi:S0002-9394(14)77079-5 [pii]

Shigeto, H., Tobimatsu, S., Yamamoto, T., Kobayashi, T., & Kato, M. (1998). Visual evoked cortical magnetic responses to checkerboard pattern reversal stimulation: A study on the neural generators of N75, P100 and N145. *Journal of the Neurological Sciences, 156*(2), 186-194. doi:10.1016/S0022-510X(98)00026-4

Simpson, W. A., Manahilov, V., & Shahani, U. (2009). Two eyes: 2 better than one? *Acta Psychologica, 131*(2), 93-98.

Singh, S. (2014). *Magnetoencephalography: Basic principles*. Mumbai: doi:10.4103/0972-2327.128676

Smith, E., Levi, D., Manny, R., Harwerth, R., & White, J. (1985). The relationship between binocular rivalry and strabismic suppression. *Investigative Ophthalmology & Visual Science, 26*(1), 80-87.

Smith, K. (2013). In Department of Clinical Vision Science, et al (Ed.), *How binocular visual performance is changed when one eye has lower vision: Characterization of inhibitory binocular interactions*

Sokol, S. (1980). Pattern visual evoked potentials: Their use in pediatric ophthalmology. *International Ophthalmology Clinics, 20*(1), V. doi:10.1097/00004397-198002010-00012

Sokol, S., & Moskowitz, A. (1981). Effect of retinal blur on the peak latency of the pattern evoked potential. *Vision Research, 21*(8), 1279-1286.

Steinbach, M. (1981). Alternating exotropia: Temporal course of the switch in suppression. *Investigative Ophthalmology & Visual Science, 20*(1), 129-133.

Steinman, S. B., Garzia, R. P., & Steinman, B. A. (2000). *Foundations of binocular vision: A clinical perspective* McGraw-Hill New York.

Suzuki, M., Nagae, M., Nagata, Y., Kumagai, N., Inui, K., & Kakigi, R. (2015). In Suzuki M. (Ed.), *Effects of refractive errors on visual evoked magnetic fields* doi:10.1186/s12886-015-0152-6

Taulu, S., & Hari, R. (2009). Removal of magnetoencephalographic artifacts with temporal signal-space separation: Demonstration with single-trial auditory-evoked responses. *Human Brain Mapping, 30*(5), 1524-1534.

Tsao, D. Y., Conway, B. R., & Livingstone, M. S. (2003). Receptive fields of disparity-tuned simple cells in macaque V1. *Neuron, 38*(1), 103-114. doi:10.1016/S0896-6273(03)00150-8

van den Broek, Sebastianus Petrus, Reinders, F., Donderwinkel, M., & Peters, M. (1998). Volume conduction effects in EEG and MEG. *Electroencephalography and Clinical Neurophysiology, 106*(6), 522-534.

Van Drongelen, W., Yuchtman, M., Van Veen, B., & Van Huffelen, A. (1996). A spatial filtering technique to detect and localize multiple sources in the brain. *Brain Topography, 9*(1), 39-49.

Van Veen, B. D., Van Drongelen, W., Yuchtman, M., & Suzuki, A. (1997). Localization of brain electrical activity via linearly constrained minimum variance spatial filtering. *Biomedical Engineering, IEEE Transactions On, 44*(9), 867-880. doi:10.1109/10.623056

Vrba, J., & Robinson, S. E. (2001). Signal processing in magnetoencephalography. *Methods, 25*(2), 249-271.

APPENDIX A : PARTICIPANT ASSESSMENT FORM

Interocular inhibition: An opportunity to determine how binocular integration is taking place within various visual areas of the occipital cortex

Patient assessment form

Patient ID: _____

Age: _____

Sex: _____

	RE	LE	BEO
VA:	_____	_____	_____
Ocular dominance:	_____	_____	
Frisby:			_____
Titmus:			_____
Phoria:	_____	_____	_____
Refractive error:	_____	_____	_____

Date: _____

Time: _____

APPENDIX B: SAMPLE CONSENT FORM

Visual Electrodiagnostic Lab
F. Tremblay (902) 470-8326
ftrembla@dal.ca

MagnetoEncephalography Lab
T. Bardouille (902) 470-3936
tim.bardouille@Dal.Ca

Research Services
5850/5980 University Avenue
P.O. Box 9700, Halifax
Nova Scotia B3K 6R8 Canada
Tel: 902-470-8037
www.iwk.nshealth.ca

INFORMATION AND CONSENT FORM

Interocular inhibition: An opportunity to determine how binocular integration is taking place within various visual areas of the occipital cortex

Investigators

Principle Investigators:
Francois Tremblay, PhD. Professor in the Department of Ophthalmology, Physiology & Biophysics, and the Clinical Vision Science Program, Dalhousie University

Timothy Bardouille, PhD. Research Scientist, BIOTIC, IWK Health Ctr, Adjunct Professor in School of Physiotherapy, Faculty of Computer Science and Department of Psychology and Neuroscience, Faculty of Sciences

Co-Investigator:
Mike Craig, BSc. Clinical Vision Science Program, Dalhousie University

Funding

Funding for this study has been provided by the IWK Health Centre.

Introduction

You have been invited to take part in the research study entitled "*Interocular inhibition: An opportunity to determine how binocular integration is taking place within various visual areas of the occipital cortex*". This form provides information about the study. Before you decide if you would like to take part, it is important that you understand the purpose of the study, the risks and benefits and what you will be asked to do. You do not have to take part in this study. Taking part is entirely voluntary (your choice). Informed consent starts with the initial contact about the study and continues until the end of the study. A member of the research team will

be available to answer your questions. You may decide not to take part or you may withdraw at any time. Withdrawing will not affect care that you may receive at the IWK Health Centre.

Purpose

The MEG (MagnetoEncephaloGraphy) is a new and very powerful technique to investigate the brain activity. It has the advantage of being much easier on the patient as, contrary to the traditional EEG (ElectroEncephaloGraphy) technique, the brain activity can be recorded without having to install electrodes on the scalp; the MEG recording is obtained without contact to the subject. This makes the MEG technique particularly interesting for diagnostics in children, who can sometimes be fussy about having electrodes installed on their scalp. The MEG technique being relatively new, we still do not know if it provides the same information as the traditional EEG technique. In this project, we want to determine if the results of a very specific test we developed using EEG can be reproduced using the MEG technique. To that purpose, we need normal adult volunteers.

How will the researchers do the study?

The previous testing procedure we developed with EEG was investigating the brain activity in conditions where one eye, the two eyes, or the two eyes with one covered with sunglasses, were used to look at a pattern presented on a computer monitor. The sunglasses were used to mimic an eye disease. This test proved to provide useful information on the level of binocular vision (the ability to use the two eyes together) and is now used as a diagnostic test in the Visual Electrodiagnostic Laboratory at the IWK.

We have developed the same experiment but this time using the MEG technique, which offers the advantage of using non-contact electrodes that covers the whole brain, not only one location as with the previous technique. Once data is collected from several adults with normal vision (like yourself), we will compare the results with the ones obtained in the previous study to determine what are the advantages / disadvantages of using the MEG technique in clinical investigations.

What will I be asked to do?

You have joined this study because you are between 18 and 60 years of age and you have good vision. After contacting us to get more information on the study, you have been given this appointment. The first thing we will do is to make sure you have normal binocular vision. This is done by measuring visual acuity in each eye; you have to look at a wall chart with letters on it and read the letters until you cannot see them anymore because they are too small. A second test will consist in pointing with one finger at an object, with both eyes open, then closing one eye and telling us if your finger is still pointing at the object. Finally, you will have to look at plates with engraved triangles and tell us if you see them in 3D. These tests will confirm your ability to use both eyes together. Once confirmed, we will ask a few very general questions about your current health and history of eye disease or treatment, to confirm your admissibility. If you are not admissible, we will give you a voucher worth of $10 for your trouble. If admissible, you will be asked to come in the lab and perform the test, which will

take approximately one hour to complete. You will have to sit in a chair, facing a computer monitor. A few skin electrodes will be placed on each side of your eyes and at the back of your head. Then a large module will be moved down to wrap around your head but without touching it. You will then be asked to pay attention to various patterns that will be presented repetitively for about one minute each on the computer monitor. During this time, we will ask you to view the patterns under two additional conditions. We will ask you to perform a proportion of the test while wearing an eye patch over one eye, as well as a separate part of the test where we will ask you to view the patterns while one eye has a tinted lens placed in front of it. We will have to present about 30 patterns, but breaks will be given so you will never have to look at the monitors for more than one minute at the time. If you become tired during the testing, you will be able to take a rest break. Once all the tests are completed, we will take away the large module and remove the skin electrodes. After the test is complete the module will be moved away from your head and the skin electrodes will be removed. Both the module and the skin electrodes should not leave any visible marks on your body, however there is a chance that your skin may be slightly irritated. You will get a $25 voucher to help pay for your expenses and trouble.

What are the burdens, harms and potential harms?

EEG and MEG tests are frequently performed at the IWK and are not usually harmful in any ways. Some fatigue may result from prolonged viewing of the computer monitor. Rarely, a slight skin irritation may occur at the location of the electrodes or around the eye that is not being tested due to the eye patch.

If complications arise at any time or if you have concerns about your vision, an IWK Eye Doctor will be contacted by the investigators. After discussion of the concern, the Eye Doctor will determine the need for further assessment or follow-up appointments. If you choose, a notice of the findings will be sent to your family physician or ophthalmic/optometric practitioner.

What are the possible benefits?

This study is not designed to provide a benefit for you. We hope to improve our understanding of the EEG and MEG tests to assist us in using these techniques more efficiently for our patients in the future. However, in the case that the visual assessment done prior to the study reveals something abnormal regarding your binocular vision, such information will be shared with you. Furthermore, you may be referred to an Eye Doctor at the IWK Health Centre.

Can I withdraw from the study?

Participation in this study is entirely voluntary (your choice). You may decide not to participate or you may withdraw at any time. If you decide to withdraw, you may choose to have your data removed from the study or remain part of it. Withdrawal will not affect your care at the IWK Health Centre in any way. If the study is changed in a way that may affect your willingness to participate, we will ask you again for your consent.

Will the study cost me anything and if so, how will I be reimbursed?

There are no direct costs related to this study but you may incur indirect expenses related to your time commitment, travel, or parking expenses. Some reimbursement is available. If during

the brief initial examination that includes questions and vision tests, if you are found to be not eligible for the study, you will be reimbursed $10 for this 15-minute visit. Participants who continue on for the MEG tests will be reimbursed a total of $25.

Are there any conflicts of interest?

Mike Craig, the investigator responsible for the testing, is a graduate student and this project is related to his school work; this could be perceived as a conflict of interest. Drs Tremblay and Bardouille, who are supervising the student's work, have no conflict of interest and will not obtained any benefice from that study. The study has been scientifically evaluated by the Research Committee at the IWK Health Centre and is financially supported by the IWK Health Centre.

What is the possible profit from commercialization of the study results?

This study is not aimed at developing commercial devices. The researchers will not receive any profit from the study results other than publication of the results in scientific journals.

How will my privacy be protected?

Any information that is learned about you will be kept private. Only research study staff will have access to identified records. All data collected from the study will be de-identified (your name replaced by a code). It is possible that the study data may be examined by the IWK Health Centre Research Services or by the regulatory authorities in Canada who assure proper conduct of research but this process remains confidential. If the results of the study are published in the medical literature, the publication will not contain any information that could identify you. Study records will be kept in a locked area for 5 years after the research study is published, after which they will be destroyed. The confidentiality of your research records will be protected to the full extent provided by law.

What if I have study questions or problems?

If you have any questions or concerns about the study, you may contact:
Mike Craig by email: mc994830@dal.ca
Francois Tremblay: Phone: (902) 470-8326; email: ftrembla@dal.ca
Timothy Bardouille: Phone: (902) 473-5315; email: tim.bardouille@iwk.nshealth.ca

In the event that participation in this study has led to any serious events such as sudden double vision, or a skin irritation that will not resolve please contact Francois Tremblay as soon as possible. He will review the situation with you and arrange appropriate medical care.

What are my research rights?

Your signature on this form will show that you have understood to your satisfaction the information about the research study. If you become ill or injured as a result of participating in this study, necessary medical treatment will be available at no additional cost to you.

By signing this document, you are not waiving any of your legal rights, nor are you releasing the investigator(s) and institution(s) from their legal and professional responsibilities.

If you have questions at any time during or after the study about research in general, and you would like an independent opinion, you may contact the Research Office of the IWK Health Centre at 470-8765, Monday to Friday between 9am and 5pm.

CONSENT FORM

Interocular inhibition: An opportunity to determine how binocular integration is taking place within various visual areas of the occipital cortex

Participant ID: _____

Participant INITIALS: _____

PARTICIPANT CONSENT

I have read or it had read to me the information and consent form for the above-mentioned research project and have had the chance to ask questions that have been answered to my satisfaction before signing my name. I understand the nature of the study and I understand the potential risks. I understand that I have the right to withdraw from the study at any time without affecting my care in any way. I have received a copy of the Information and Consent Form for future reference. I freely agree to participate in this research study.

Name of Participant:(print) _____

Participant Signature: _____

Date: _____ Time: _____
(day/month/year)

STATEMENT BY PERSON PROVIDING INFORMATION ON THE STUDY

I have explained the nature and demands of the research study and judge that the participant named above understands the nature and demands of the study.

Name (print) _____

Signature: _____ Position:_____

Date:_____Time: _____
(day/month/year)

STATEMENT BY PERSON OBTAINING CONSENT

I have explained the nature of the consent process to the person authorized and judge that they understand that participation is voluntary and that they may withdraw at any time.

Name (print) _____

Signature: _____ Position:_____

Date:_____Time: _____
(day/month/year)

Will I be informed of study results?

The general research results will be made available to you at the completion of the study. If you wish to have a copy of the results, indicate your address below and a summary will be mailed to you or discussed orally, if you prefer.

Would you like to receive a summary of the study results? Yes_____ No _____

If yes, provide your preferred contact information:

Phone:_____

Email:_____

Postal address: _____
_____
_____

Future use of study data

May we keep your test results gathered during this study for use in future studies similar to this one?

Yes ____ No ____

May we use your test results at some time in the future for purposes other than research (e.g. teaching)?

Yes ____ No ____

Future contact

May we contact you about participating in future studies similar to this one?

Yes ____ No ____

Participant Initials _____

APPENDIX C: SAMPLE RECRUITMENT POSTER

New Research Study!

IWK Health Centre

Interocular inhibition: An opportunity to determine how binocular integration is taking place within various visual areas of the cortex.

Help us determine how your brain puts information from your two eyes together!

The purpose of this study is to investigate how our two eyes are working together to provide information about depth perception, using a new MEG technique (MagnetoEncephaloGraphy) that allows us to collect brain activity.

We are seeking the participation of adults between the age of 18 and 65 years with good vision and no history of eye diseases (glasses are fine). The study will involve one visit that will take about 1 1/2 hour. It will take place in the IWK Health Center, in the MEG unit located in the basement level of the Goldbloom Pavillon. First we will have you view a few basic tests (looking at charts) to assess how well your eyes are working together. In the case that your results on the tests are inadequate for the purposes of our study we will stop here and you will be compensated for your time. If the results of these tests are normal, then we will continue by placing some skin electrodes around your eyes and at the back of your head. You will then sit in a special device (the MEG apparatus, see picture) and be asked to look at various sets of changing patterns presented on a screen with rest periods in between. A stipend of $25 will be provided to cover your expenses and commitment.

This research study has been approved by the IWK Research Ethics Board and is supported by an IWK scientific grant. It is part of a Master of Science degree in the Clinical Vision Science Program.

For more information, please make an initial contact by email to:
Mike Craig, BSc. Clinical Vision Science Program, Dalhousie University
mc994830@dal.ca
Mike will contact you back to provide more information and set an appointment time

More information can also be obtained by contacting the two main investigators:

Francois Tremblay, PhD. Professor in the Department of Ophthalmology, Physiology & Biophysics, and the Clinical Vision Science Program, Dalhousie University
ftrembla@dal.ca

Timothy Bardouille, PhD. Research Scientist, BIOTIC, IWK Health Ctr, Adjunct Professor in School of Physiotherapy, Faculty of Computer Science and Department of Psychology and Neuroscience, Faculty of Sciences
tim.bardouille@iwk.nshealth.ca